Appendix B

Borehole Logs

Appendix B-1

Graphic Core Logs for W205 & W208
are included in the attached map tube.

Appendix B-2

Interpretive Graphic Core Logs for W201 through W208
are included in the attached map tube.

Appendix C

Borehole Image Processing System (BIPS)
Images for W201 through W208
are included in the attached map tube.

Appendix D

Geophysical & Composite Logs

Appendix D-1

Montage Plots for W205 & W208

Description of Tracks Presented on the Montages for Coreholes W205CH1 and W208CH2

Track 1:

Bit size — Size of borehole as reported to logging engineer in the field.

Caliper — Borehole diameter as measured during a logging run. The final montages use the HCAL array measured by the Platform express. It is a single arm measurement that is based on the extension of the powered caliper of the density tool. This reports a borehole diameter every 2 inches.

Washout — Area fill between bit size and caliper. Provides a visual representation of the amount of hole missing due to sloughing and fractures. It provides a good visual representation of potential problem areas where log measurements are suspect. The measurements most affected by washout are: CMR, density, and neutron (basically all of the porosity tools). The least affected are passive gamma ray devices. Note that the bit size may have been adjusted to match the caliper. If the entire hole had a consistent washout, then an adjustment was made.

Gamma Ray — Gross measurement of gamma ray activity. The GR responds to the activities of potassium, uranium family, and thorium family radionuclide. In general, a high GR is suggestive of increased clay content. Conversely, low GR activity is a sand-rich and clay poor zone. The vertical resolution of this tool is around 1 foot and a measurement is recorded every 6 inches. The average mean free path of a gamma ray in typical rocks is around 9 inches.

This track is commonly used for correlation. This passive system is included in every logging run. Using this tool, every logging run (except the FMI) was depth shifted to ensure that all comparisons were depth consistent throughout the entire borehole. The average depth shift was less than 6 inches.

High Res GR — Same as GR except the measurements are made every 2 inches. Provides better vertical resolution at the expense of measurement precision.

SP — Spontaneous potential. The SP is the electrical potential produced through interactions between formation water, borehole water, and shale. The SP typically records a baseline measurement through shaley sections. It departs in permeable zones. The magnitude of departure depends on the salinity contrast between formation waters and borehole water. The position of the baseline provides no useful information.

The SP measurements in 205 and 208 are included for completeness. They are essentially featureless reflecting little salinity contrast between formation and borehole waters and the lack of permeable zones. Note that there maybe slight deflections to the left in especially sandy zones.

Dip — Orientation of borehole as measured by GPIT sonde of FMI. The tadpole presents the magnitude of dip from 0 to 5°. The long tadpole tail shows the dip azimuth, the short tadpole tail shows the azimuth of pad 1 of the FMI tool.

Track 2: Resistivity

This track presents the results of the Array Induction Tool. The tool simultaneously measure formation resistivity at depths of 10, 20, 30, 60, and 90 inches. The vertical resolution for each measurement is 1 foot. In addition the tool measures the resistivity of the borehole liquid, labeled mud resistivity. All are shown on a linear scale to accentuate variances between the curves which should assist when correlating with these curves.

The results indicate that formation resistivity increases with depth of investigation and there is no appreciable difference between the values measured at 60 and 90 inches. Also, the mud resistivity is less than practically all of the formation measurements. It is likely that the trend towards lower resistivity near the borehole wall is a result of a slight amount of invasion or diffusion of borehole water into the formation. Those zones where the resistivities coincide are always at the low end of the spectrum near the mud resistivity. These zones may be slightly more permeable or fractured, thus permitting the invasion of borehole waters.

This track also includes the RXO8, a microresistivity device measured on the same pad as the density too. This measurement is a cyndrically focused with a vertical resolution of 1 inch. The depth of investigation of 3 inches. This measurement is made during the nuclear pass, so it doesn't have the upper depth constraints of the AIT.

Track 3: Porosity Tools

This tracks presents the results from the various porosity tools: density, neutron, sonic, and CMR. Each tool measures porosity primarily with a secondary response from matrix effects. For these wells, the matrix effects are strongest with the neutron and sonic tools. The purpose of this track is to show each of the porosity curves from which lithology and other geologic properties can be estimated. A calculated porosity is provided in the hydrology section of the montage. Each of porosity results are

labeled as phi in this track to reduce confusion between these measurements and the calculated porosity provided elsewhere.

The neutron phi curve depicts a porosity measurement that is much higher than what should be expected. The neutron system measures the hydrogen index of the formation, regardless of whether it is water in a pore space or a hydroxyl ion in a clay mineral lattice. The elevated phi measurements indicate that there is a considerable quantity of hydrogen in the formation, much of it is probably in hydrous minerals—probably clay minerals.

The sonic phi curve estimates porosity from the Delta t compressional slowness. The porosity was estimated using the Wylie equation:

$$\phi = \frac{\Delta t_{\log} - \Delta t_{matrix}}{\Delta t_{water} - \Delta t_{matrix}}$$

where $\Delta t_{\log}$ is measured with the logging tool, Δt_{matrix} was estimated to be 55.8 µsec/ft, the typical value for quartz, and Δt_{water} is 189 µsec/ft. The elevated porosity is caused by too small a value for the Δt_{matrix} because the other values are invariant. The Δt_{matrix} for montmorillonite and illite are poorly defined. They are a function of clay compaction, but typical values are around 80 µsec/ft or greater. In order to get the sonic porosity plot to overlie the CMR log requires a Δt_{matrix} of around 68 µsec/ft. This provides further evidence that there is a significant clay content in the formation.

The density phi curve is calculated from the bulk density measured by the nuclear tool string. The porosity is estimated from the following equation:

$$\phi = \frac{\rho_{matrix} - \rho_{\log}}{\rho_{matrix} - \rho_{lwater}}$$

where $\rho_{\log}$ is measured by the density log and ρ_{matrix} was adjusted to match the core porosity values plotted on this track. The resulting ρ_{matrix} is 2.71 g/cm^3, identical to the average matrix density reported for these core analyses. The close agreement between the core porosity values and the density phi curve indicates that the core porosity is measured through a granulometric procedure that uses the same equation as that provided above.

The CMR provides a porosity measurement that is least affected by matrix effects. The CMR makes continuous pulse-echo Nuclear Magnetic Resonant measurements of the subsurface formation. These measurements are sensitive to the hydrogen nuclei (protons) contained in the pore space of the formation and contain information relating to both pore volume and pore size. The pore size information can be used to partition the formation porosity into bound and free fluid volumes. This information can, in turn, be used to estimate formation permeability. The pore size information is unique to NMR logging devices.

Permanent magnets in the CMR skid set up a powerful magnetic force that aligns the hydrogen protons in the formation. A pulse is transmitted from the antenna, causing the protons to tip 90° and precess. This precessional motion creates a signal that the antenna detects between pulses. The time constant of the energy decay rate of these signals is called the transverse relaxation time (T_2) and is a function of the pore size distribution in the formation. The sensed volume is 1 inch from the surface of the CMR skid. The measurement aperture is 6 inch.

The CMR transverse relaxation time, or T_2, measurement, which is equivalent to the brightness of the CMR quality curve (far right track of hydrology section), is directly proportional to porosity, and the decay rate relates to pore size. Short T_2 times indicate small pores and low permeability, while longer times indicate larger pores with generally higher permeabilities. I used a 33 msec cut off time to separate total and effective porosity. This is the typical value used for sandstones.

Two CMR curves are shown on this track: 1) total porosity and 2) effective porosity (T2 > 33 ms). The difference is capillary bound water and is shown by the blue shading.

The CMR measurement is very shallow and the volume of investigation is small; thus, the tool reports high values of porosity in zones with open fractures or other rugose zones.

Track 4: **Bulk Density measurements**

This track presents the results from the density tool. It includes bulk density and photoelectric effect.

The bulk density is calculated through the measurement of the Compton scattering of gamma rays by the formation. The tool has a collimated gamma ray source (Cs-137) and two detectors that measure the number of gamma rays that traverse the formation. The ratio of counts is proportional to the density of electrons within the formation. The resulting measurement is very well behaved. The depth of investigation is around 2 inches, the vertical resolution is around 4 inches.

A high resolution density curve is also presented. It is recorded at 2 inch resolution. The actual measurement is similar to that recorded in the typical density just collected more often.

Bulk density values from core are plotted above the log bulk density. The two data sets coincide once the core density is adjusted upwards by 0.1 or 0.05 g/cm^{3}This may be due to drying of the core sample prior to measurement which would reduce the bulk density of the core sample.

The photoelectric (Pe) measurement is also provided by the density tool. Gamma rays interact with matter in three manners:

1. pair production
2. Compton scattering
3. photoelectric absorption

The method of interaction is dependent on the energy of the gamma ray and the average atomic number (Z) of the matter that the gamma ray traverses. Photoelectric absorption becomes much more prevalent at low gamma ray energies where it becomes primarily dependent upon the formation Z. The relationship between Pe and Z is

$$Pe = \left(\frac{Z}{10}\right)^{3.6}$$

Pe is measured by counting the number of low energy gamma rays at the density detectors. The more low-energy gamma rays, the lower the formation Pe because fewer of the gamma rays have been photoelectrically absorbed.

Track 5: **Spectral Gamma Ray**

Naturally occurring gamma rays come from the following radionuclides:

- potassium-40
- thorium family
- uranium family

Uranium and thorium decay through a complex series of daughters until they transmutate to lead. Several of the daughter products produce gamma rays. Fortunately, the gamma rays produced by the daughter products of thorium and uranium and those produced by potassium-40 are at different energies. The spectral gamma ray logging tool measures the energies and intensities of gamma rays and divides the signal into the activity of each of these radionuclides.

Potassium is common in the crust and occurs in K-feldspar, micas, and certain clay minerals. Thorium is quite rare in the crust. It is insoluble and is typically found in clay minerals with a high cation exchange coefficient. The thorium crystallized in specific igneous minerals that were subsequently transformed to clay. The thorium remained within the clay lattice because it is too insoluble to migrate. Uranium is also rare in the crust. Its solubility and mobility is a function of the redox potential of the subsurface environment. Uranium is soluble in oxidizing environments and precipitates as salts in reducing environments. A common ca for reducing conditions is the presence of organic materials.

Thorium and potassium measurements made with the spectral gamma ray log in the NC wells was very useful in determining clay content and discriminating between the two common clay minerals—illite and montmorillonite. There was little variation in uranium content indicating that there is little variation in organic material within the formation.

Tracks 6 and 7: ELAN

Elemental analysis (ELAN) is a computational method used to calculate the mineralogy and fluid content of the formation through the use of log data. Two ELAN plots are provided. Both use CMR, neutron, density, spectral gamma, and sonic tools to calculate the plotted results. The ELAN plot on the left also includes Elemental Capture Sonde (ECS) results.

ELAN applies a series of linear or non-linear equations to convert the log results to mineralogy and fluid contents. The user picks the expected mineralogy, equations, and uncertainties to be used to calculate the ELAN. The mineralogy picked for the North Carolina wells was based on core descriptions. The minerals used for the ECS ELAN were:

1. illite
2. montmorillonite
3. clay-bound water

4. quartz

5. albite (An20)

6. muscovite

7. hematite (labeled Special Mineral 1)

8. calcite

9. water-filled porosity

The non ECS ELAN did not include calcite and muscovite.

In order to have a determined system, ELAN requires at least as many equations as there are unknowns. The equations used were:

1. neutron phi

2. bulk density

3. cmr porosity

4. U

5. potassium

6. thorium

7. calcium (ECS)

8. iron (ECS)

9. silicon (ECS)

10. delta T compressional

An internal database assigns parameters to every equation that are specific to each mineral. For example, quartz has a silicon content of 0.457. A primary concern in using ELAN with the North Carolina mineralogy is that many of these parameters are poorly defined for the clay minerals. Clays have variable geochemistry and their physical properties can vary significantly based on compaction

and diagenesis. Total clay content is typically a robust determination because these minerals are distinctly different from the Q-F-M and calcite part of the formation. However, differentiating the Q-F-M fraction is sensitive to the clay parameters.

ELAN assigns a precision to each equation (log measurement) based on well defined log responses. In addition, an uncertainty is assigned that weights the value of each equation in determining the mineralogy. The uncertainties are commonly adjusted to compensate for uncertainties in some of the parameters.

ELAN calculates a mineralogy for each depth interval (6 inches). A synthetic log curve for each equation, based on the equations and parameters input into ELAN, are subsequently calculated. The synthetic log curves are overplotted on the actual log curves and residual differences are plotted. A good ELAN should have very small residuals. However, it is very important to realize that ELAN does not provide an unique solution and one with a small residual may not be correct. Core data are necessary to ensure that the ELAN results represent reality, at least as expressed by core analyses.

Core XRD results are overplotted on the ECS-developed ELAN. The circle shows the total XRD Clay content, the square is the clay + quartz content. The triangle is the clay + quartz+feldspar content. XRD results do not report muscovite or lithic fragments, large contributors to the rock according to the thin section point counts. Note that the core results are reported in dry weight percent and ELAN results are reported in wet volume fraction. The core results were converted to wet volume fraction prior to plotting on the ELAN display.

ECS is a geochemical logging tool that uses a chemical neutron source to identify and quantify the amount of Si, Fe, Ca, Ti, S, Gd, and H in the formation. The measurements are based on neutron capture where thermal neutrons are captured by nuclei that emit gamma rays of specific energies dependent on the capture nucleus.

ECS data were invaluable in discriminating between the quartz-feldspar-mica portion of the formation. Core results indicate that the predominant feldspar is andesine (An_{20}). Andesine has the same density, neutron porosity, delta T Compressional slowness, and spectral gamma signal as quartz. These two minerals, however, can be readily distinguished by their differing Si content (the Si content of quartz is much higher).

ECS was also very valuable in determining the amount of hematite and calcite in the formation. The direct measure of Fe provided the best discriminator for hematite; the direct measure of Ca was the

best measure for calcite. The latter, however, was also affected by varying Ca content in the clay minerals so it also relied on other log information.

The S and Ti data were not very useful because neither occurred in significant quantity within the formation.

The ELAN calculated without ECS provides a robust measure of total clay content, but is incapable of discriminating the Q-F-M fraction. As stated earlier, there is too little difference between the quartz and An_{20} and too little difference between muscovite and clay minerals. The feldspar in this ELAN was calculated by honoring (with significant uncertainties) the ratio between quartz and feldspar reported in the core analyses.

Track 8: **FMI Image**

A normalized FMI image is provided in order to see a compressed electrical image of the borehole. Its primary use is to look at gross features of the stratigraphy and several of the larger fractures.

Track 9: **Bed Orientation**

Two sets of dip azimuth and dip magnitude are presented. The black are considered to be "bed boundaries." These are slightly dipping boundaries between groups of fining-upwards sequences. The contacts are typically sharp with conductive units (shales?) overlain by resistive units (sands?). Commonly this contact is not absolutely planar, indicating that was some slight amount of downcutting that occurred during the deposition of the overlying unit.

The red tadpoles show the orientation of bedding and laminae within each sedimentary sequence.

The lack of significant channeling suggests rapid deposition in a subsiding basin

Note that the bedding sequences are commonly better illustrated in a non-normalized FMI image

Track 10: **Fracture Orientation**

Tadpoles for all fractures identified in the FMI images are included. All fractures were conductive, filled with a material more conductive than the surrounding formation. This typically indicates either a clay or an open fracture filled with water. Bedding plane fractures are very difficult to map from FMI images. The FMI provides a surficial image of the borehole. Thus it can only detect those fractures that intersect the borehole.

Track 11: **Fracture Aperture**

A scaled FMI image was used to calculate the aperture (open gap) of each fracture. The FMI image is scaled to an AIT induction log so that an accurate value of formation conductivity can be assigned to the image.

An aperture and a map of the aperture trace for each fracture is generated in GeoFrame. Unfortunately, the current release of GeoFrame Playback will not permit the plotting of this information onto a montage. Rather a 50 foot average of aperture was plotted. Note that the average aperture does not vary much throughout the wells.

Track 12: **Stoneley Reflection Coefficients**

Attenuation of direct Stoneley waves (essentially a tube wave that is transmitted along the borehole interface) is due to fluid flow into the permeable fracture, a mechanism that also produces reflected Stoneley waves.

The amplitude of a Stoneley wave is reduced as it crosses a fluid-filled gap (open fracture). A reflected Stoneley wave is generated at the gap. When the direct Stoneley wave encounters the gap, a wave is generated within the gap that propagates radially away from the borehole. Thus, a Stoneley wave processed to look for reflections generated within the borehole can be used to identify fractures. The Stoneley wave has a depth of investigation up to 30 feet; however, the vertical resolution is only around 4 feet.

The magnitude of a Stoneley anomaly can be quantified by calculating a reflection coefficient. A reflection coefficient is the ratio of the amplitude of a reflected wave to the amplitude of the incident sonic wave. The larger the reflection coefficient, the greater the Stoneley anomaly (larger the fracture).

Reflection coefficients are calculated and displayed for Stoneley waves that are generated and transmitted both uphole and downhole. The location of potential fractures are defined by their location. The magnitude of the fracture is proportional to the reflection coefficient.

Track 13: **Stoneley Processed Waveform**

The processed waveform displays down-going reflected arrival waveforms in the time domain. This plot is made by separating the reflected Stoneley waves from the total sonic signal. For most fractured rocks, the Stoneley-mode slowness is dominated by the bulk modulus of the borehole fluid. This bulk

modulus is assumed to not change; thus, the arrival time of the direct Stoneley wave should not vary significantly over a small section of borehole. For reflected Stoneley waves (emanating from fluid-filled fractures), all waveforms in the sonic array are stacked along a line corresponding to the inverse of the Stoneley wave. This enhances the reflected Stoneley, and rejects most undesired components such as remnants of compressional or shear arrivals.

The resulting plot highlights down-going reflectors that are generated from fractures or hole washouts. The presence of up-going reflectors are a good indication of a significant Stoneley -wave anomaly.

Track 14: Porosity

A series of porosity logs are plotted on Track 3. Each curve is affected by matrix affects; the magnitude is dependent upon formation conditions and the type of porosity measurement. The purpose of this track is to plot a computed porosity that is believed to represent true formation porosity.

The computed and edited CMR porosity is believed to be the best representation of formation porosity. A total CMR and effective CMR porosity curve is plotted. Core porosity is also plotted. It is evident that the CMR porosity closely matches point count results from core. It does not, however, closely match the granulometric results from core.

An ELAN-computed apparent porosity is also presented. This curve does not use the CMR results, so is much more affected by the rock matrix. In general, the ELAN phi closely matches the CMR porosity except for the upper part of each borehole.

The deviation in the upper part of each borehole indicates that there is a difference in the rock matrix within these zones, probably due to weathering. The ELAN phi is calculated primarily from sonic, neutron, and density measurements. Close inspection of these logs suggests that the primary contributor to the increased shallow ELAN phi is the sonic and neutron logs. The CMR log is usually not effected.

The base of the weathered zone is usually very apparent in the logs. The delta T compressional coherence [sonic STC plot (last track)] almost always degrades at this point. The caliper increases and the density correction increases. These phenomena suggest that the hole washes out at the bottom of the weathered zone due probably to a physical change in the formation.

The ELAN phi likely reflects an alteration of the formation where mechanical changes (due to unloading?) are causing a change in the formation. The highly compacted shales are probably micro-

fracturing and expanding and authigenic minerals are forming. The authigenic minerals have not been compacted by 3 km of burial so they have a lower density and greater sonic slowness.

Any porous zones that are real (confirmed by CMR) appear to have a much higher permeability that those found in the unaltered part of the boreholes. This is may be a result of the difference in cementation between these zones.

Track 15: Permeability

Perhaps the most important feature of NMR logging is the ability to record a real-time permeability log. Permeability is derived from empirical relationships between NMR porosity and mean values of T_2 relaxation times. These relationships were developed from brine permeability measurements and NMR measurements made in the laboratory on hundreds of different core samples. The following formula is commonly used:

$$k_{NMR} = C(\phi_{NMR})^4 (T_{2,\log})^2$$

where k_{NMR} is the estimated permeability, ϕ_{NMR} is CMR porosity, $T_{2,\log}$ is the logarithmic mean of the T_2 distribution and C is a constant, typically 4 for sandstones and 0.1 for carbonates.

CMR permeability is plotted on this track. Core permeability is overplotted. In general , the two agree well and no change was made to C. Most of the core permeability was below 0.1 mD and was not plotted. In well 208 one permeable zone is plotted that was not confirmed by log. This sample, however, is from a fractured shale and the core results warn that it may be affected by these fractures.

Permeable zones are rare in 205 and none appear to exist in 208. Note that there was no CMR log for 208; permeability was estimated from the ELAN geochemistry. The most permeable zone in 205 had very similar core and CMR results. The zone at 156' had core perm above 0.1 mD. The log did recognize a permeable zone but the peak perm was well below 0.1 mD.

Track 16: Hydraulic Conductivity

The perm curve of Track 15 is converted to hydraulic conductivity (cm/s) using a conversion algorithm provided in Freeze and Cherry.

The results of the hydrophysical logging is also plotted in logarithmic scale. The highest flow rate coincided with the permeable zone measured with the CMR.

Track 17: **CMR Quality**

This track provides a 2-D contour map of the CMR waveforms. Any lighter zones indicate porosity. Those zones to the left of the red line are bound water and those to the right indicate effective porosity. The logarithmic mean of T2 (used to calculated perm) is also plotted. For most of the log (non-porous zones) the curve is just recording noise in a non-signal.

The CMR log is adversely affected by standoff. Some of the most porous zones directly coincided with washouts recorded with the caliper log. The resulting porosity and permeability were edited out of the previous tracks. Lighter representations of the unedited results are also presented.

Track 18: **Sonic Slowness**

The slowness for shear, compressional, and Stoneley waveforms are presented. The shear and compressional values are overplotted at a ratio of 1:1.8.

Track 19: **Dynamic Elastic Moduli**

Elastic moduli are calculated from the shear, compressional, and density logs. These values are dynamic, calculated from sonic waves with frequencies greater than 1 kHz; therefore, they should not be compared directly to typical uniaxial and triaxial core results. These curves can be used to get an qualitative measure in changes in the mechanical properties of the formation.

Track 20: **Sonic STC Plot**

The Slowness-Time Coherence plot presents a 2-D representation of the data used to label each of the three sonic waveforms. A tight and bright zone indicates good coherence and a confident sonic slowness. The shear slowness can be seen to be weak in several intervals and one should use shear data from those intervals with caution.

Appendix D-2

FMI Logs

FMI Interpretation Summary Report

Processing

Wells W201AR1A, W202AR1, W203AR1, W204AR1, W206AR1, and W207AR1 were examined on the Schlumberger GeoFrame software for structural and stratigraphic features. Prior to interpretation, the following corrections were made to the FMI (Formation Micro Imager): bad buttons were detected and corrected, image arrays were equalized on a button–to-button basis, EMEX correction applied to the buttons, and depth errors caused by the differences in tool and cable velocities were applied to image arrays and associated curves. The images were normalized using a 2-ft. running window to enhance the displayed data (these normalized data are displayed on the left in each of the playbacks). The final step in processing scales the FMI button response to a calibrated shallow resistivity curve (AHT20 in each well except W201 where RX08 was used). This scaling process allows fracture apertures to be computed, and is displayed in each of the playbacks in the fourth track next to the aperture calculation.

Interpretation Method

The images were evaluated for the following data sets: bedding, internal sands, scour, cross bedding, fractures (also called Fracture B on the plots), healed fractures, faults, and drilling induced fractures. Bedding is picked in shale, estimating present-day overall structural dip of the well. Internal sands are bedding planes within sands showing more high energy events. These give information as to the source area of the sand. Scours are downcutting events, usually of greater energy than internal sands, giving clues to the depositional environment along with source area. Cross-bedding is picked as a series of either planar or trough layers which can be of variable thickness. Cross-bedding gives information on flow direction and depositional environment. "Fractures" (also called Fracture B on some plots) are open or partially open natural fractures. A best fit sine wave is assigned to each fracture. An aperture trace is calculated off of the scaled image in order to calculate a thickness of the open portion of the fracture. An average apparent hydraulic aperture is assigned to each fracture. Note that because bedding planes cannot be distinguished between bedding plane fractures on the FMI images, horizontal fractures are not picked in this interpretation. A fault is picked where there is evidence of movement, and a dip and azimuth is assigned to the fault plane. A drilling-induced fracture is seen as a very vertical fracture. These occur in very brittle rocks where there is a strong principal stress field in the area.

Explanation of Log Display

For each well, a 1"=10' vertical scale display is provided. In the far left track is the depth in feet along with the gamma ray log from the FMI tool string, and the 2 perpendicular caliper curves (C1 and C2) calculated from the FMI. In the second tract, the dynamic normalized image is displayed on a 0-360 degree scale. Overlying this are the sinusoid dips for each of the stratigraphic and structural events observed. In the third track are the "tadpoles" associated with each

event. The head of the tadpole gives the magnitude of the dip read on a 0-90 degree scale, and the tail points to the direction of dip, North being at the top of the plot and East to the right. The fourth track shows a scaled image; therefore showing an image of true resistivity of the formation (dark being conductive, the light colors being resistive). In the fifth track are the fracture traces of open natural fractures. The scale at the top indicates the openness of the trace along the fracture. The black or blue dot in this track is the average mean hydraulic aperture for each trace, given in inches. The last track is a note track with observations made while interpreting the images documented.

Following each log plot is a series of stereonets. The first is a stereonet with structural features including natural "Fractures" (blue dots), healed fractures (pink dots), and drilling-induced fractures (pink pentagons). The data are shown first as a Wulff projection giving dip magnitude and azimuth of each feature. Following this is a Strike Rosette diagram showing overall strike direction of the cluster. Next the stratigraphic features are displayed on the stereonet including scour bedding (green circles), scour (light blue circles), cross-bedding (red circles), and internal sands (yellow circles). The stratigraphic data are first displayed as an upper Hemisphere Wulff projection showing again the dip direction and magnitude of each feature, and then as an azimuthal rosette diagram showing the overall dip direction of the cluster.

Facies Interpretation

The overall data quality is good and the holes are in gauge. There are signs of drill bit scars frequently on the images: very regular diagonal striping on the images. Also at the top of some wells the images become very light on the scaled image, yet details are still seen in the normalized images. This is likely an affect of the fluids in the top of the hole displaced during logging.

Average bedding trends East in wells 201, 202, 203, and 204: however the trend wells in 206 and 207 is more ENE. Bedding dip is relatively high in wells 201-204 (roughly 19 degrees), however less steep in wells 206 and 207 (roughly 9 degrees). Although scour cuts are present, there are rarely large clasts at the base of the scours. Cross-bedding is not commonly seen in this data, although locally present. Internal sand bed deposition, along with bedding, is interpreted to be more stable in wells 201-204, yet more dispersed in wells 206-207. Sorting within the conglomerates is typically very poor. In addition, clasts appear poorly rounded on the FMI, reflecting a short distance of transport. Fossils are not noted, however there is some evidence of local bioturbation. Local caliche horizons are seen in wells 203-207. All of these features indicate a setting where deposition is very rapid and subsidence is keeping up with deposition.

W201

Well 201 contains occasional conglomerates mixed with horizontally layered sand and shale. Average bedding dips to the east at 17.83 degrees. Fractures are steeply dipping (average 70.5 degrees) and strike N-S.

Average Dip Set Attributes

	True Dip	True Azimuth	Apparent Dip	Apparent Azimuth
Bedding	17.83	61.79	19.07	60.8
Internal Sand	15.02	91.19	15.97	88.18
Scour	23.16	122.93	23.56	120.31
Deformation	19.73	99.39	20.64	96.76
Fracture	70.48	269.47	69.58	269.71

W202

Well 202 contains some rare channel sands and typical fining upward sequences. Soft sediment deformation is common. Average bedding dips to the east at 18.42 degrees. Fractures are again high angle (63 degrees) and strike N-S. Some possible drilling-induced fractures are picked which strike NW-SE. A single fault has been picked in this well with a dip of 40.82 and azimuth of 104.77.

Average Dip Set Attributes

	True Dip	True Azimuth	Apparent Dip	Apparent Azimuth
Bedding	18.42	85.83	17.13	86.61
Internal Sand	21.76	75.24	19.58	74.29
Scour	21.47	121.76	20.1	122.53
Cross-bed	15.86	110.08	13.41	116.2
Deformation	44.83	119.71	43.6	119.82
Fracture	63.18	253.36	64.37	253.35
Healed Fracture	67.5	338.08	68.22	336.94
Fault	40.82	104.77	39.52	105.76

W203

Well 203 shows more thick sands with fining upward sequences. Average bedding for the well is 21.88 at an 86.27 degree azimuth. The fracture pattern in this hole is more widely dispersed, when viewing the entire well. Within a particular zone however, the fracture patterns appear more regular.

Average Dip Set Attributes

	True Dip	True Azimuth	Apparent Dip	Apparent Azimuth
Bedding	21.88	86.27	19.4	93.48
Internal Sand	20.8	85	18.83	89.39
Scour	26.63	81.94	24.53	84.32
Cross-bed	21.8	132.45	21.57	139.1
Deformation	37.69	91.45	35.31	95.45
Fracture	64.24	269.99	65.45	269.28
Healed Fracture	51.67	18.98	50.43	17.86

W204

Well 204 contains fluvial and debris flow deposits. A large permeable zone is interpreted from 90-97 feet based on the low gamma-ray. However, resistive colors (dark) are seen on the scaled image. Internally this feature is a channel sand with a fining upward sequence. Bedding dips due East with an average dip of 22.39 degrees. Fractures are high angle and strike either N-S or E-W.

Average Dip Set Attributes

	True Dip	True Azimuth	Apparent Dip	Apparent Azimuth
Bedding	22.39	89.08	21.09	89.17
Internal Sand	22.38	86.16	21.47	85.73
Scour	29.83	98.21	29.11	98.07
Cross-bed	22.28	72.41	21.16	71.91
Deformation	32.65	138.64	32.22	138.63
Fracture	59.56	235.66	59.56	235.89

W206

Interpreted sheetflood conglomerates are common in well 206. Internal sand deposits are more random in direction than in previous wells. Bedding dip is much lower than seen in wells 201-204, and the bedding dips to the ENE. Fractures are again random, but strike dominantly W-E. A few microfaults are noted with an average dip of 62 degrees and strike WNW-ESE.

Average Dip Set Attributes

	True Dip	True Azimuth	Apparent Dip	Apparent Azimuth
Bedding	9.16	104.89	9.33	117.11
Internal Sand	14.17	102.25	13.06	112.29
Scour	21.33	78.17	20.62	84.87
Cross-bed	19.8	23.54	17.51	27.12
Deformation	47.17	186.46	47.34	186.65
Fracture	66.07	165.57	65.26	165.84
Healed Fracture	56.64	324.64	52.34	322.01
Micro Fault	61.8	138.36	62.2	138.44
Drilling-Induced Breakout	84.48	351.83	81.3	351.8
Drilling-Induced Fracture	79.4	229.6	82.7	229.07

W207

Well 207 contains fining upward conglomerates along with sheetflood deposits. A couple of large clasts are noted, indicating episodic massive deposition. Average bedding is 10 degrees to the ENE. Fractures are very random, as seen by the stereonet logs.

Average Dip Set Attributes

	True Dip	True Azimuth	Apparent Dip	Apparent Azimuth
Bedding	10.11	54.98	9.44	55.06
Internal Sand	14.47	83.57	14.89	88.03
Scour	17.2	54.94	16.47	54.93
Cross-bed	32.21	47.57	31.75	47.07
Deformation	31.64	117.6	31.63	117.83
Fracture	59.03	207.63	59.41	207.82
Drilling Ind. Fracture	80.41	159.42	80.53	159.57

Appendix D-3

Panel Diagrams
are included in the attached map tube.

Descriptions of Tracks Shown on Panel Diagrams Track 1:

Hole size was measured using a 3-arm caliper by COLOG. Also shown is HCAL, the hole diameter obtained from the extension of the backing arm used to eccenter the PEX logging sonde. The 3-arm caliper is much more sensitive to hole enlargements associated with fractures. This serves two purposes. First, it provides information on fracture severity, and second, it identifies sections in which the other logs are affected by hole enlargement.

Track 2:

U is the product of logged density (RHO) and photoelectric factor (PEF). U8 is the product of PEF8 and RHO8, the high resolution curves, and U is the product of RHOZ and PEFZ, the standard resolution data. U8 has slightly greater vertical resolution and, therefore, provides better bed boundary definition, but is more sensitive to hole size changes associated with fractures. Because both grain density and atomic number are higher in clays, micas, and mafic minerals than for quartz and feldspar, U is an excellent "clay indicator".

Track 3:

Reprocessed sonic data are shown in this track, with slowness increasing linearly from right to left (velocities increasing to the right). 1.9*DTCO is plotted to allow visual estimation of the shear to compressional velocity ratio, which has an approximate mean value overall of 1.9. Values to the left of DTSM indicate lower Vp/Vs; values to the right indicate higher Vp/Vs. DTSM (shear slowness) and DTST (Stoneley-wave slowness) are plotted without rescaling. Lighter colors and thinner lines are plotted where coherence is lower. The coherence cutoffs are 0.9 for Stoneley, 0.7 for compressional, and 0.4 for shear wave data. The data were smoothed prior to release by Schlumberger.

Track 4:

This track shows a number of curves which are related to various measures of porosity. Density porosity (DPHZ, normal resolution and DPH8< shaded>, high resolution) is computed from bulk density assuming a grain density of 2.71 gm/cm^3. Porosity from the CMR sonde (CMRP) is also plotted and shaded in this track. It has not been edited to remove intervals where washouts cause erroneously large values. Neutron porosity curves with high (HNPO) and normal (NPHI) resolution displayed in this track respond mainly to hydrogen associated with clays and mineral surfaces. Lower values of density porosity than neutron porosity are associated with higher clay content, largely because or this effect.

Track 5:

Photoelectric factor is measured by the PEX tool. This value is related to the mean atomic number of elements in the formation. PEFZ (normal resolution) and PEF8 (high resolution) are generally similar except for the greater vertical

resolution of PEF8, and within zones of hole enlargement where PEF8 values are too low. Quartz has a lower PEF than other minerals, so lower values of PEF are generally found in "sands".

Track 6:

Resistivity measurements were obtained by the AIT and by the PEX tool. Two AIT curves are plotted here along with RXOZ, the normal resolution "flushed zone" resistivity. If there is no variation in resistivity with distance from the borehole and if the curves are not affected by hole size, all three curves should be identical. The primary conductive elements in these rocks are pore fluids and clays. Because pore fluids here have low conductance, more clay-rich and finer-grained intervals generally have lower resistivity than "sands".

Track 7:

Density obtained from the PEX tool is plotted here. High (RHO8) and normal (RHOZ) resolution data are shown. As with the other PEX measurements, higher resolution data is better for bed definition but is more sensitive to hole enlargements associated with fractures. Density in these rocks is primarily controlled by porosity, which makes the density tool the best overall single-log measure of porosity. Even better precision can be obtained by combining the density log with the CMR porosity.

Track 8

Although NGT records a number of additional data, only SGR (standard gamma ray) and CGR (computed gamma ray, the intensity of radiation associated with potassium and thorium decay series) are displayed here. High gamma activity is generally associated with clays. CGR is considered to be a better indicator of clay mineral volume than SGR because it does not respond to uranium. These curves are insensitive to hole size or roughness.

Track 9

Seismic travel time displayed in this track was computed by integrating the reprocessed DTCO data. It corresponds to the relative time at which a reflection from a given depth would appear in a seismic section.

Track 10

Stoneley-wave reflectivity calculated by Schlumberger increases in intervals of hole enlargement or increased wall roughness and where permeable features intersect the borehole. The data plotted here has not been edited to remove reflections associated with hole size increases, so large values can at best be only qualitatively related to permeable fractures.

Track 11

Porosity computed using ELAN and permeability determined from CMR data are plotted in this track. Where two ELAN passes were made, two porosity curves are presented. CMR permeability, plotted on a linear scale increasing from right to left, has not been edited to remove intervals where washouts affect the data.

Track 12

Log-derived lithology was obtained from ELAN without the use of the ECS data (**see Appendix D-1**). The width of each shaded interval corresponds to the volume associated with the given mineral. The unshaded portion at the right-hand edge is the porosity which was replotted in Track 11. Because the logs used in this analysis are not sensitive to the difference between quartz and the predominant feldspar, this ratio was fixed for purposes of display.

Track 12a

Log-derived lithology in this track was determined with ELAN using ECS results in addition to the other logs (see **Appendix D-1**).

Track 13

This track is a lithologic column prepared using the BIPS data to detect bed boundaries and identify geologic attributes. Gamma and FMI data was used to further refine the results. The process is described in more detail in Section 4-2.

Track 14

The BIPS data is presented in this track at a greatly reduced scale relative to its resolving power, as an unwrapped (N-E-S-W-N) image of the inside of the borehole. The dark band which winds around the borehole is a shadow cast by the light source.

Track 15

Orientations of fractures detected in the BIPS data are displayed here using a "tadpole" plot. Dip angle is plotted using a linear scale from zero to ninety degrees; dip azimuth is drawn as a "tail" which projects in the down dip direction measured clockwise from north defined as up in the plot, from the "head" of the tadpole. Each fracture is plotted at its midpoint depth.

Track 16

Lines are plotted in this track every foot whose length is proportional to the number of fractures in the one-foot interval surrounding the plotted depth.

Track 17

The length of the lines in this track is proportional to the sum of the apertures of fractures within the one-foot interval as measured on the BIPS images.

Track 18

Temperature log recorded with the downgoing ambient FEC log obtained during HpL™ data collection.

Track 19

FEC (fluid electrical conductivity) recorded at the start of HpL™ logging and prior to replacement of the fluid in the borehole with deionized water. Because these wells have been drilled and evacuated, sometimes several times, the FEC profile does not necessarily represent the profile of pore fluid conductivity in the rock surrounding the well.

Track 20

Summary of the results of HpL™ logging includes a selection of the FEC profiles conducted during the active pumping phase of the test, and bars which represent on a log scale the interval specific hydraulic conductivities obtained by COLOG from a forward model for the response of the well to pumping.

Track 21

Transmissivities displayed in this track were computed over the intervals isolated using packers during long-term fluid drawdown tests. In some cases models of the response allowed determination of the transmissivities of both an inner and an outer zone around the borehole.

Appendix E

Fracture Analysis

Fracture Analysis Comparison

Three different methods were used to acquire fracture data during the GM-1 pilot study. These included analysis of recovered core and the analysis of both optical and electrical wellbore image data. There are important differences in these techniques that are outlined in sections 3.3.4, 3.4.2.2 and 3.4.2.7 of this report. There are also differences in the analysis and interpretations procedures used to detect and measure fractures using these methods. Further, these three types of data analyses were completed independently for the GM-1 study to provide unbiased data for a comparative study of the methods.

Examples of the orientation and classification of fracture populations measured in drillhole W205CH1 from electrical, optical and core analysis are presented in the Fracture Analysis Comparison Figure. This figure compares the different fracture detection and analysis techniques used in the GM-1 pilot program over the intervals 130 to 145 feet, 275 to 290 feet, and 630 to 640 feet which represent typical data from the analysis of planar features in this study. Column (a) shows intervals of W205CH1 where stratigraphic dips were measured from electrical image data. The red tadpole symbols indicate the orientation of internal bedding fabric whereas black represents bed boundaries. Column (b) shows the corresponding interval of fracture planes picked from the electrical image data. Both bedding parallel and non-bedding parallel fractures measured in the optical image data are shown in column (c). The depth offset in the measured fractures is due to a known 1.5 feet depth mismatch between the electrical and optical image logging runs. It is recommended for follow-on studies that such depth discrepancies be identified and corrected before the start of the data analysis.

The open tadpoles in column (c) represent fractures that appear to be open in the optical image data. The "open" classification is interpretive and not an indication of the hydrologic importance of these fractures. The hydrologic importance of planar features observed in any wellbore image data can only be evaluated by hydrologic testing.

Comparison of columns (a) and (c) shows that the population of bedding parallel features detected in the optical image data is represented by the population of the bedding fabric and bed contacts measured in the electrical image data. Low angle features are more poorly oriented in image data because it is more difficult to uniquely measure the orientation of shallow dipping fractures, and thus the dip direction and magnitude are not identical. Higher angle fractures detected in the electrical image data generally correspond well with higher angle fractures measured in the optical image data (e.g. columns (b) and (c)).

Column (d) shows fractures detected in core over the intervals 130 to 145 feet and 275 to 280 feet. The red and black symbols indicate mineralized and non-mineralized fractures respectively. The red tadpole symbols in column (c) represent fractures that appear to be mineralized in the optical image data; these generally correspond to the mineralized fractures detected in core. These data segments also show that electrical imaging resolved most

mineralized fractures detected in the optical image data and core but somewhat fewer of the fractures that were interpreted as open in the optical image data.

From this comparison it is apparent that each method used to detect and measure fractures produces somewhat different results. However, the overall structural trends of the fractures and strata are quite similar for both imaging methods. Many of the differences between the methods are due to differences in the display and analysis tools used to interpret the data. Differences in the classification of planar features may also be the result of different interpretations of these features by the analysts.

W205CH1 — Fracture Analysis Comparison

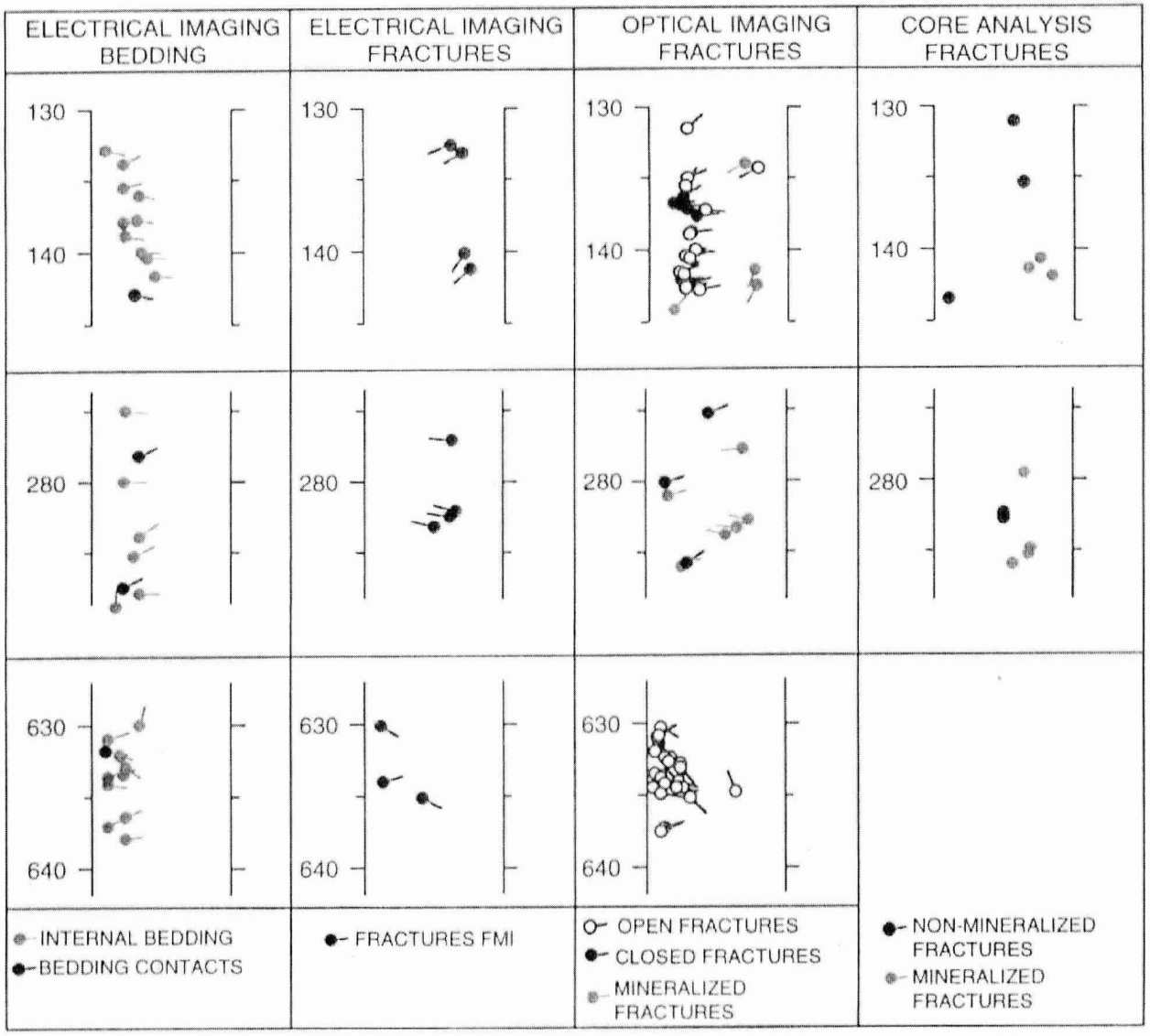

(a) (b) (c) (d)

Trench Fracture Data Analysis NCLLRWDF Site: Trench GM-1 East

All Fractures Interpreted from Trench Data

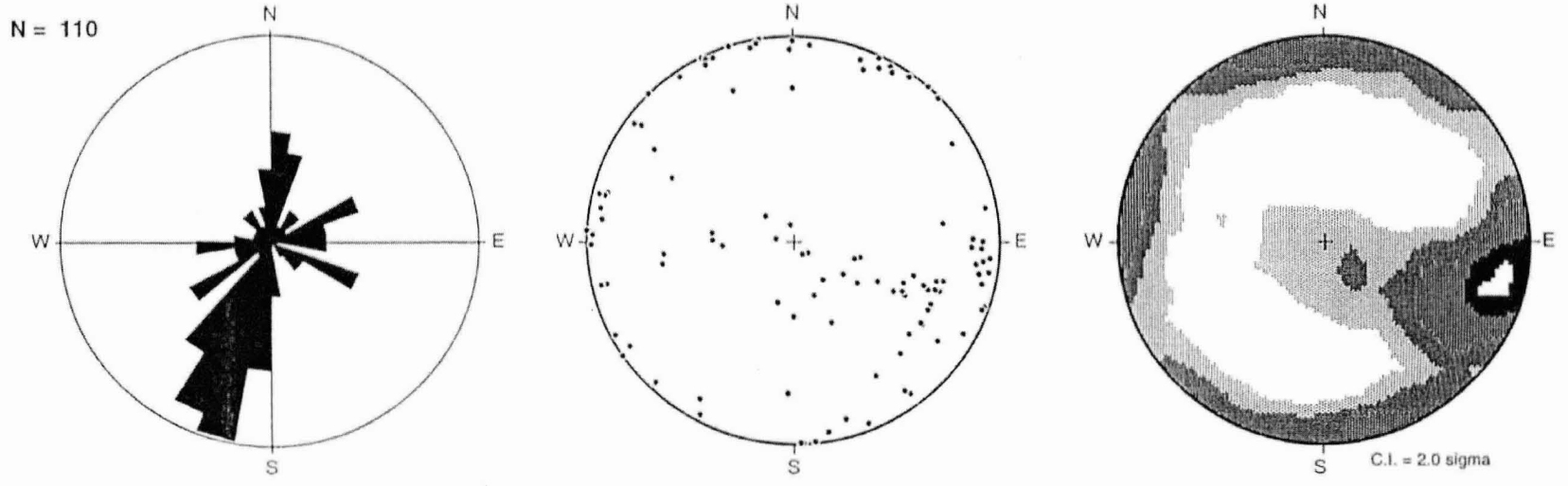

Trench Fracture Data Analysis NCLLRWDF Site: Trench GM-1 West

All Fractures Interpreted from Trench Data

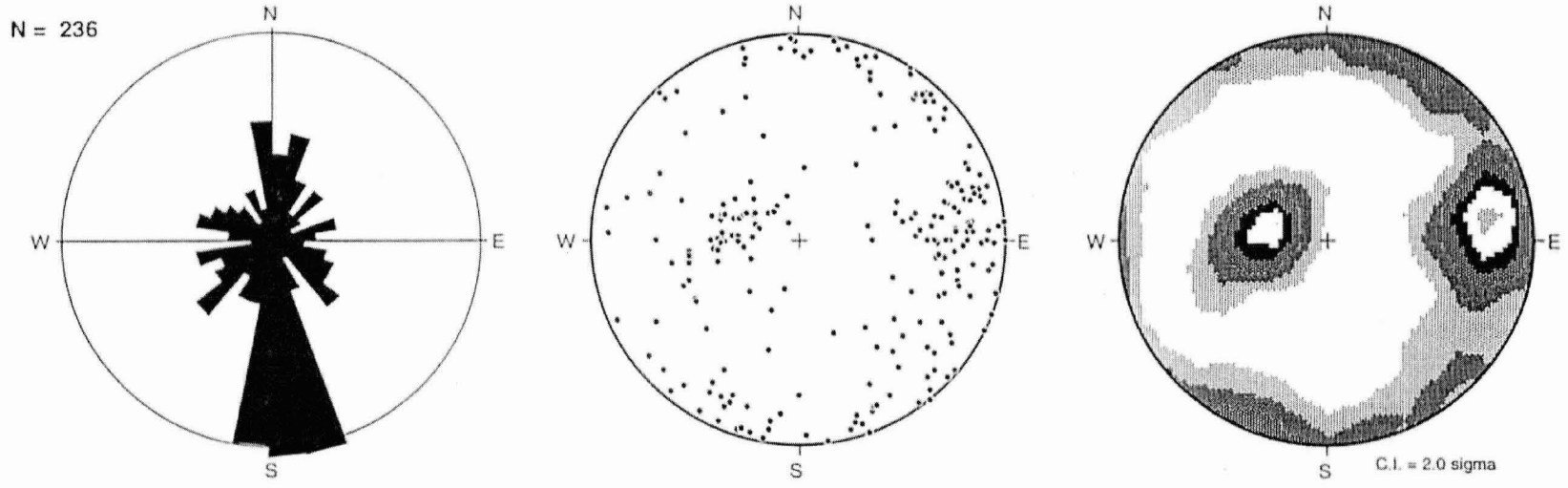

Trench Fracture Data Analysis NCLLRWDF Site: Trench GM2

All Fractures Interpreted from Trench Data

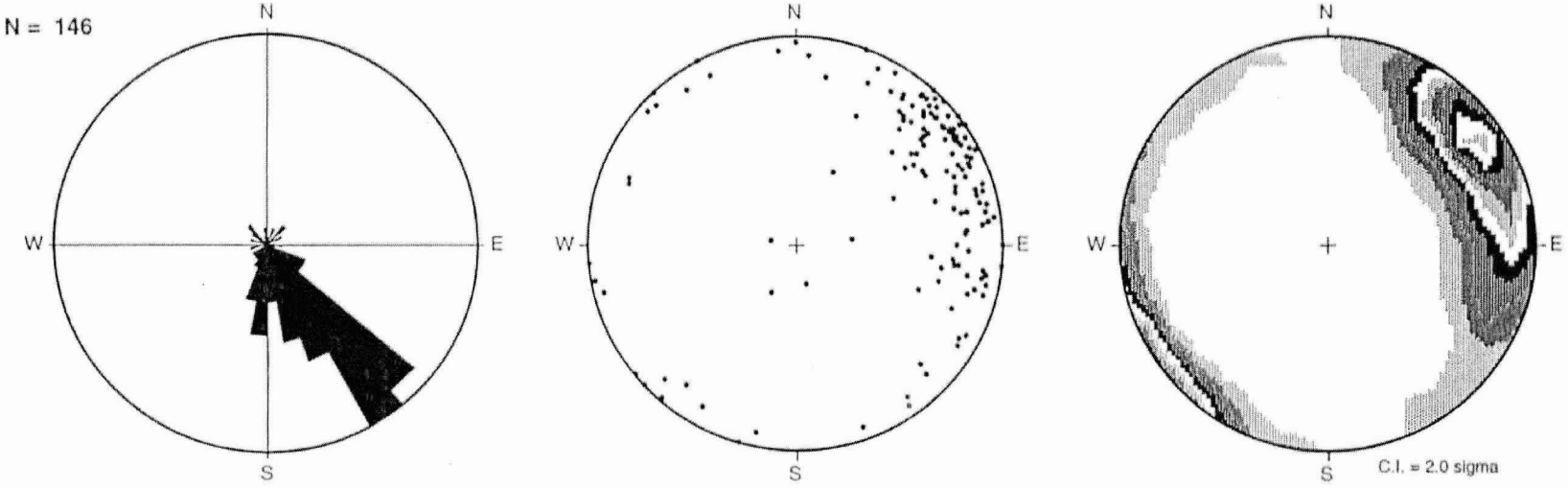

Open Fractures Interpreted from Trench Data

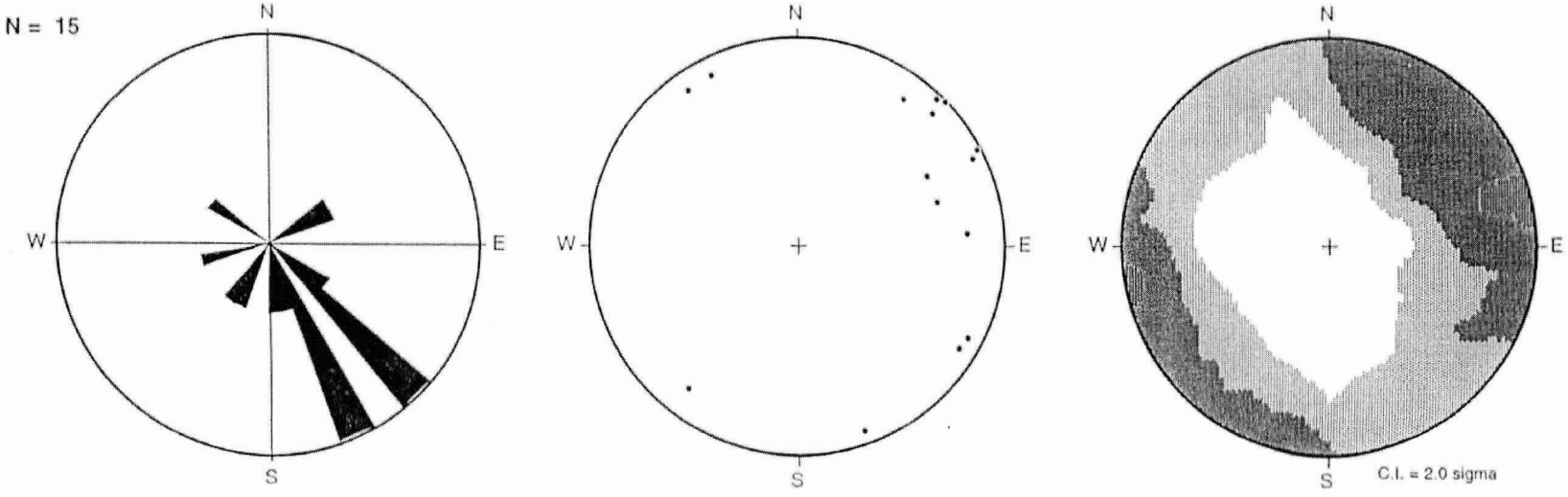

Trench Fracture Data Analysis NCLLRWDF Site: Trench GM3

All Fractures Interpreted from Trench Data

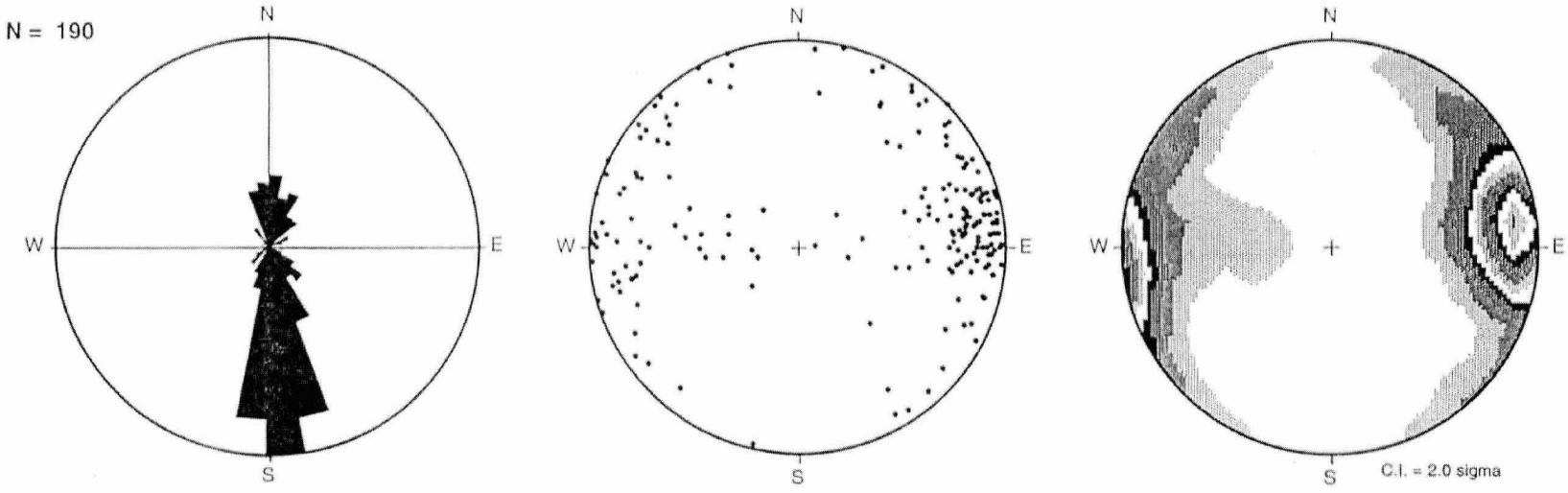

Open Fractures Interpreted from Trench Data

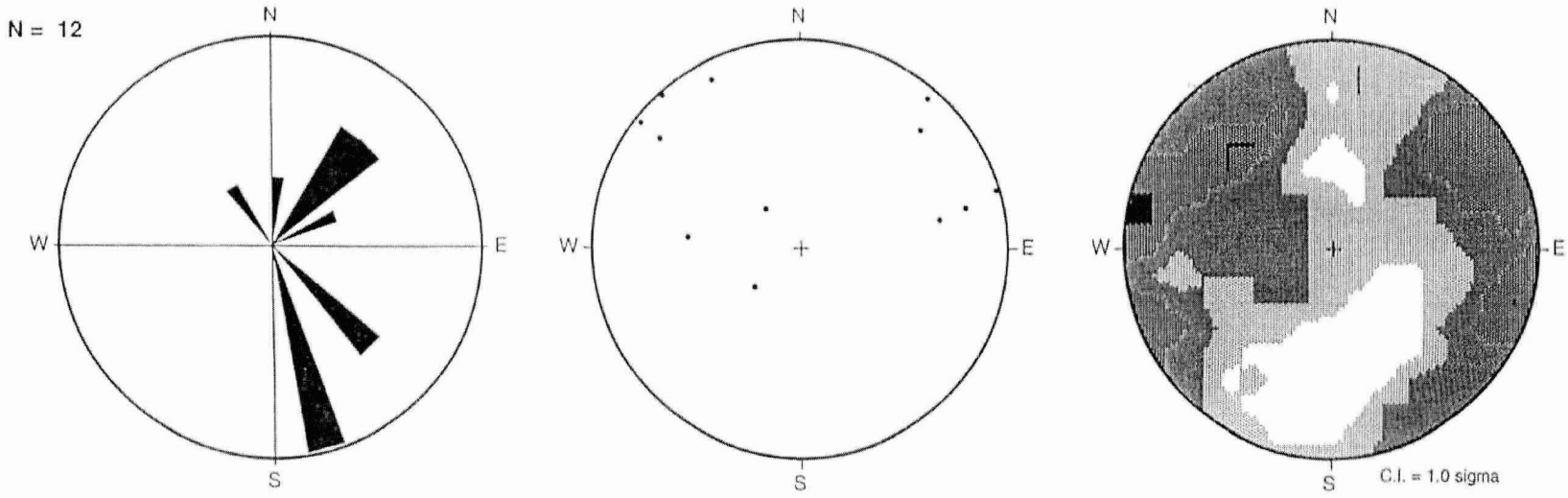

Trench Fracture Data Analysis NCLLRWDF Site: Trench GM4

All Fractures Interpreted from Trench Data

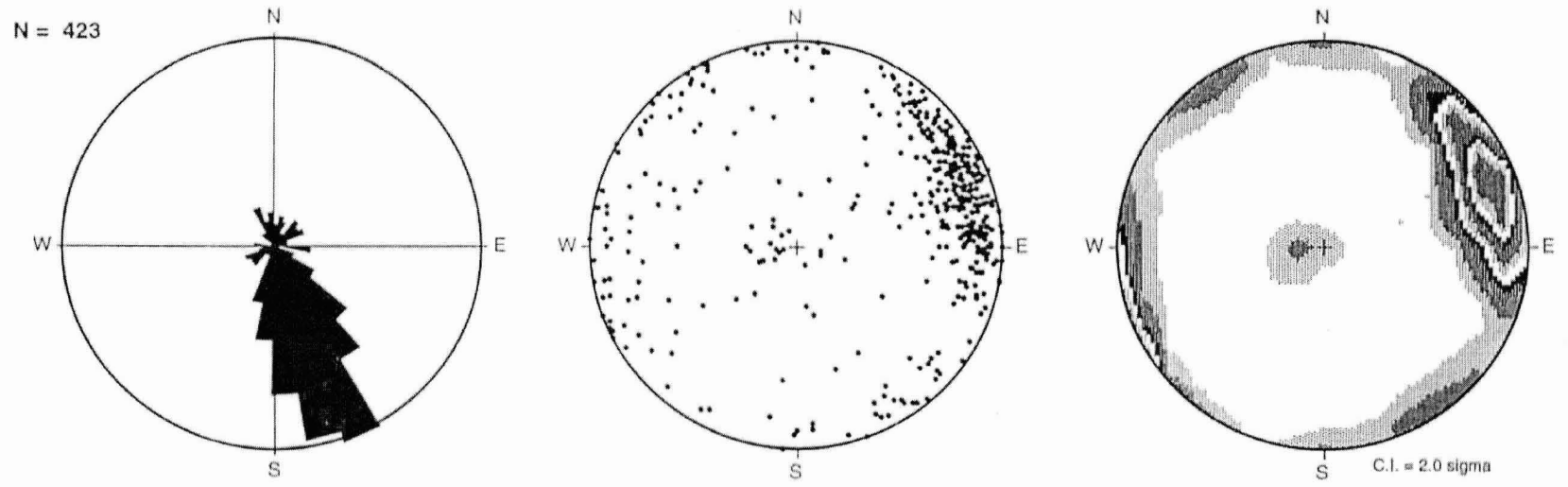

Open Fractures Interpreted from Trench Data

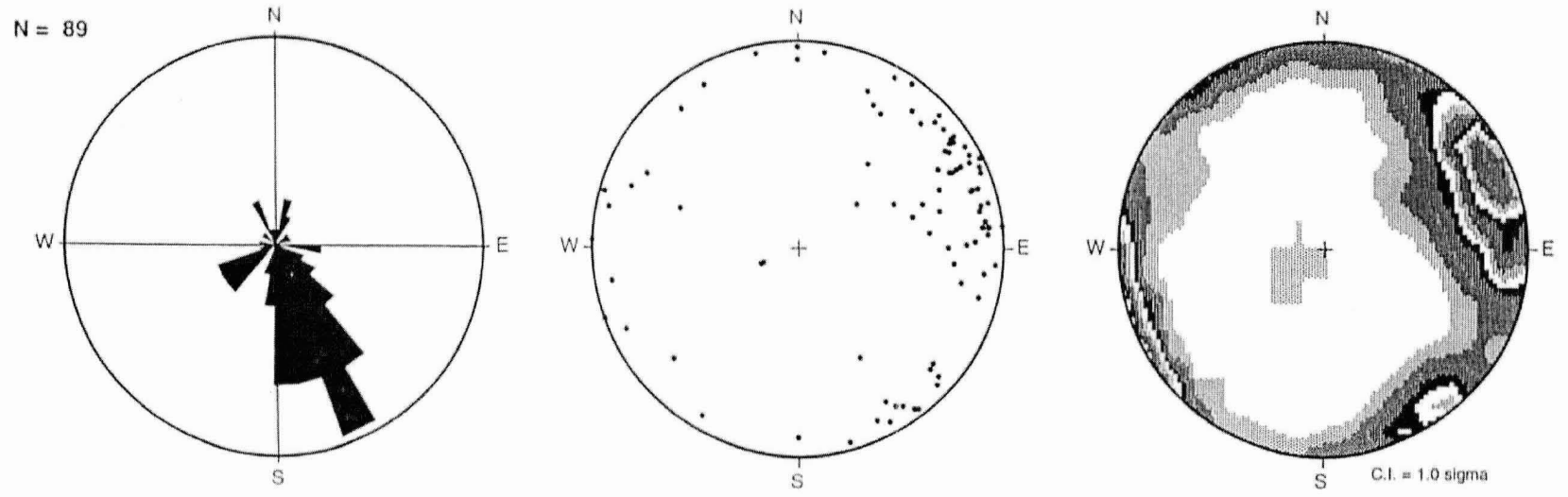

BIPS and FMI Fracture Analysis NCLLRWDF Site: Well W201

All Fractures Interpreted from BIPS Image Data ***Depth Interval 34–115 ft***

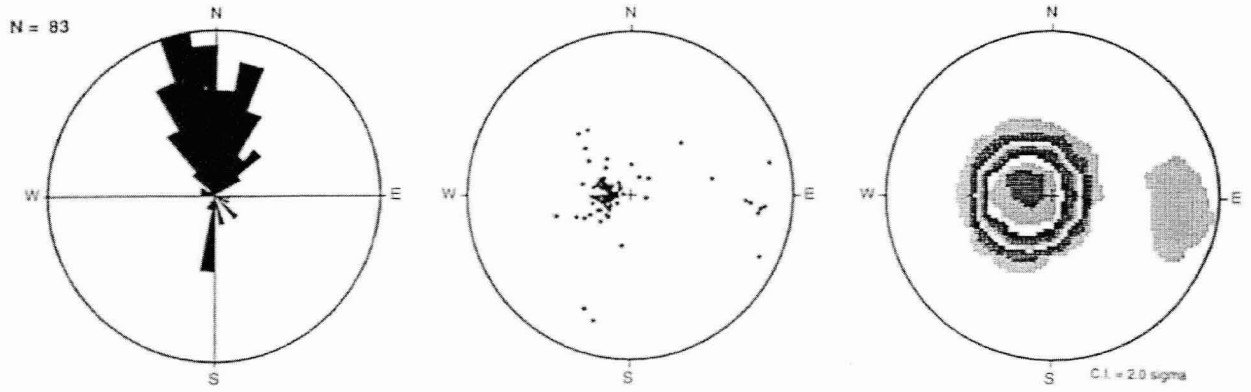

Open Fractures Interpreted from BIPS Image Data ***Depth Interval 34–115 ft***

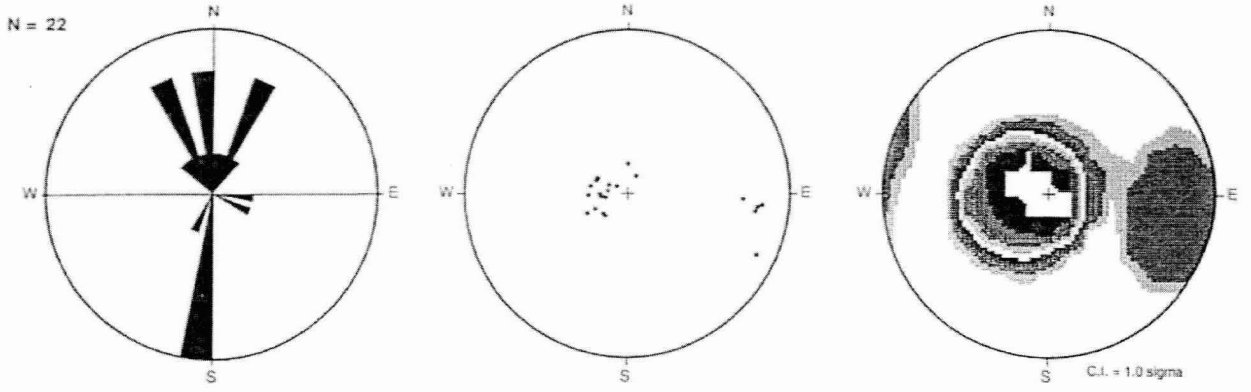

All Fractures Interpreted from FMI Image Data ***Depth Interval 37–112 ft***

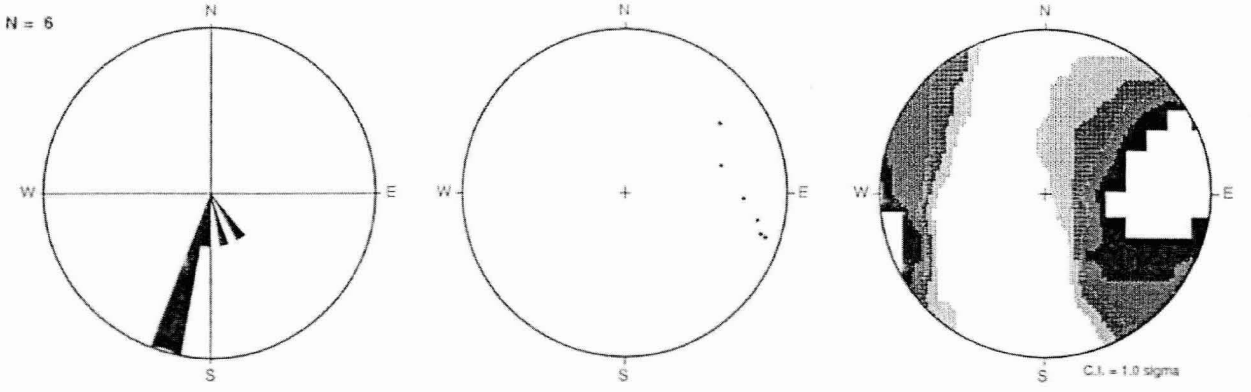

BIPS and FMI Fracture Analysis NCLLRWDF Site: Well W202

All Fractures Interpreted from BIPS Image Data *Depth Interval 31–215 ft*

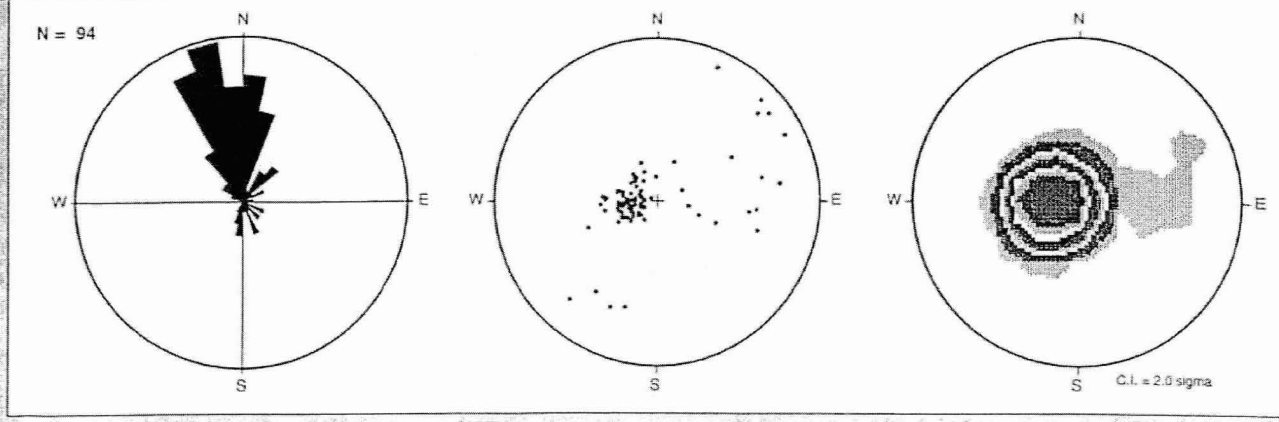

Open Fractures Interpreted from BIPS Image Data *Depth Interval 31–215 ft*

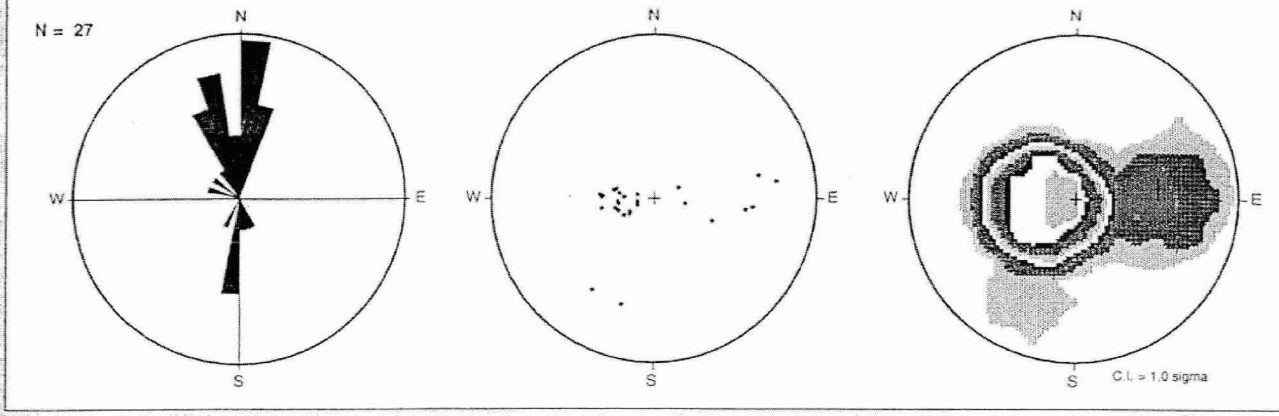

All Fractures Interpreted from FMI Image Data *Depth Interval 30–215 ft*

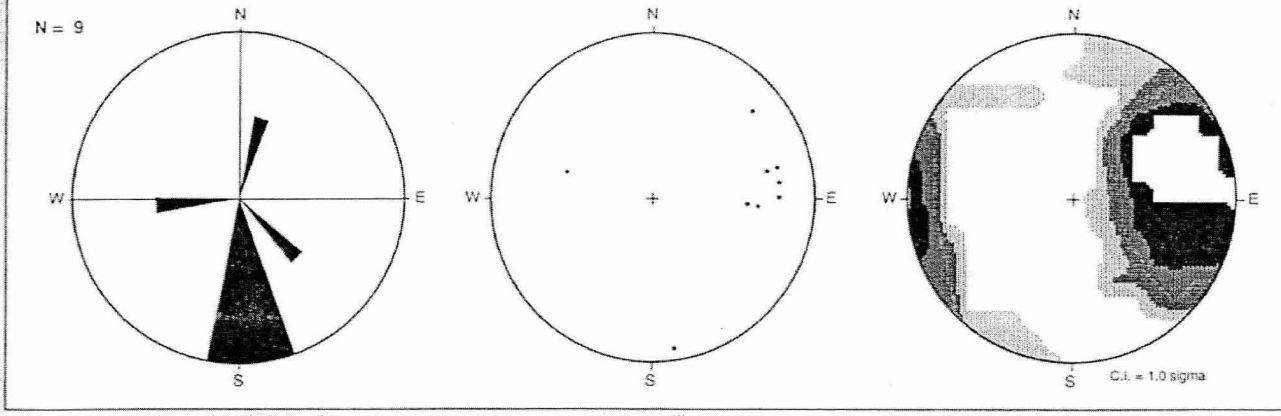

BIPS and FMI Fracture Analysis NCLLRWDF Site: Well W203

All Fractures Interpreted from BIPS Image Data ***Depth Interval 33–100 ft***

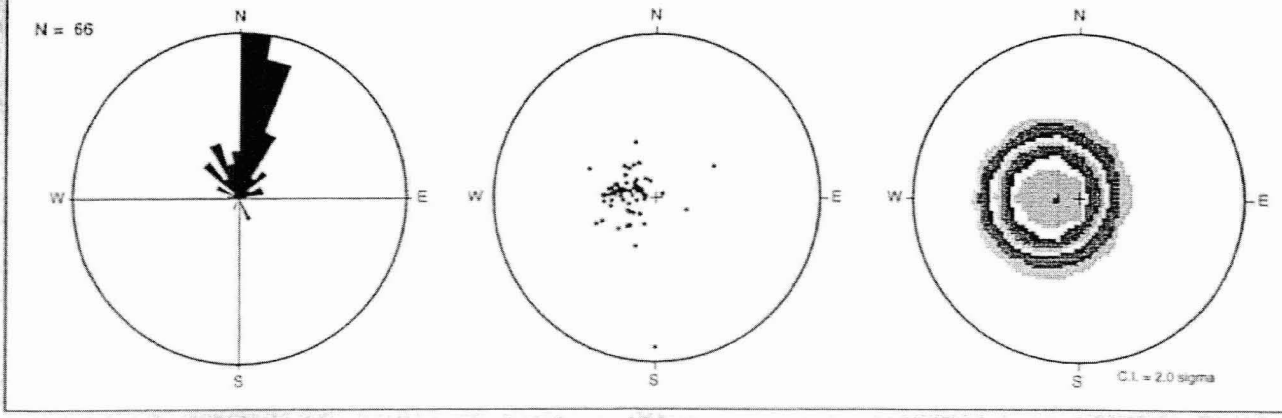

Open Fractures Interpreted from BIPS Image Data ***Depth Interval 33–100 ft***

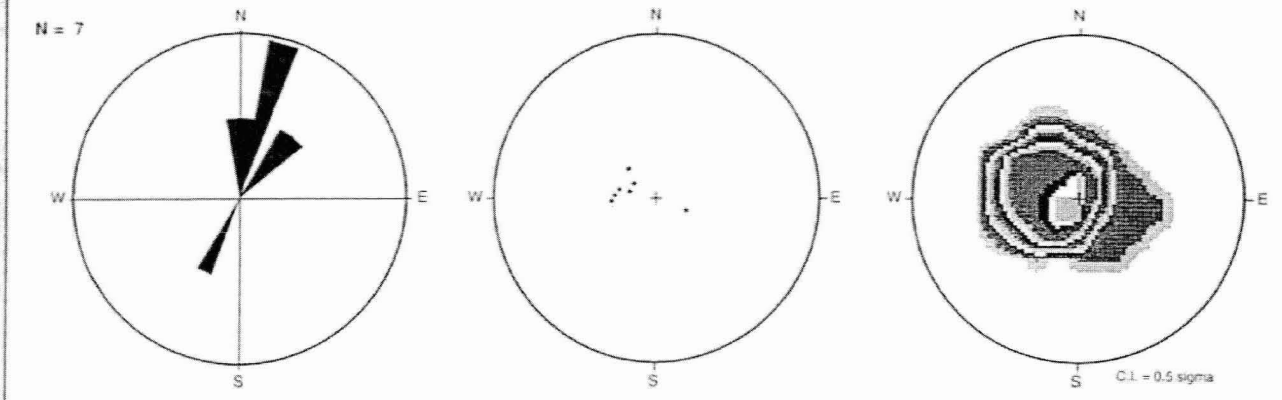

All Fractures Interpreted from FMI Image Data ***Depth Interval 50–362 ft***

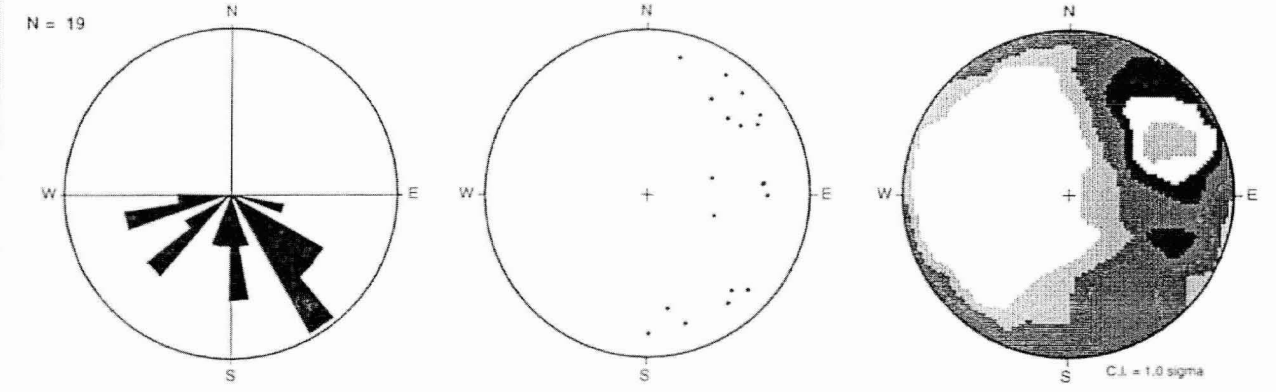

BIPS and FMI Fracture Analysis NCLLRWDF Site: Well W204

All Fractures Interpreted from BIPS Image Data *Depth Interval 32–100 ft*

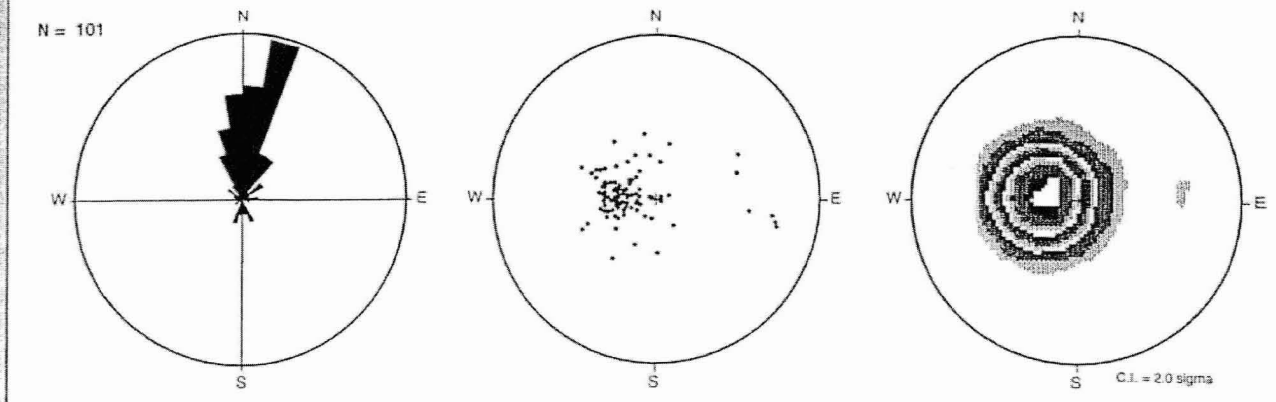

Open Fractures Interpreted from BIPS Image Data *Depth Interval 32–100 ft*

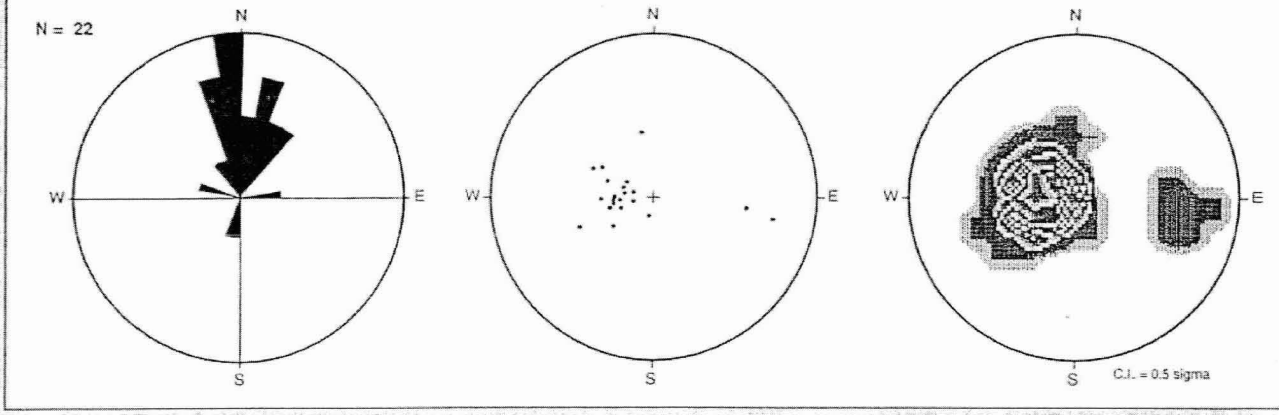

All Fractures Interpreted from FMI Image Data *Depth Interval 31–139 ft*

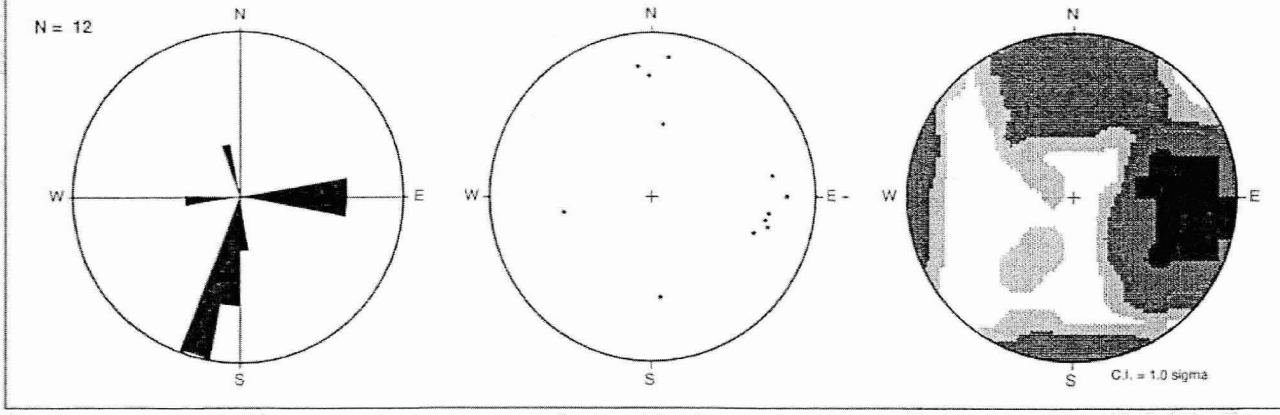

BIPS and FMI Fracture Analysis NCLLRWDF Site: Well W205

All Fractures Interpreted from BIPS Image Data ***Depth Interval 30–715 ft***

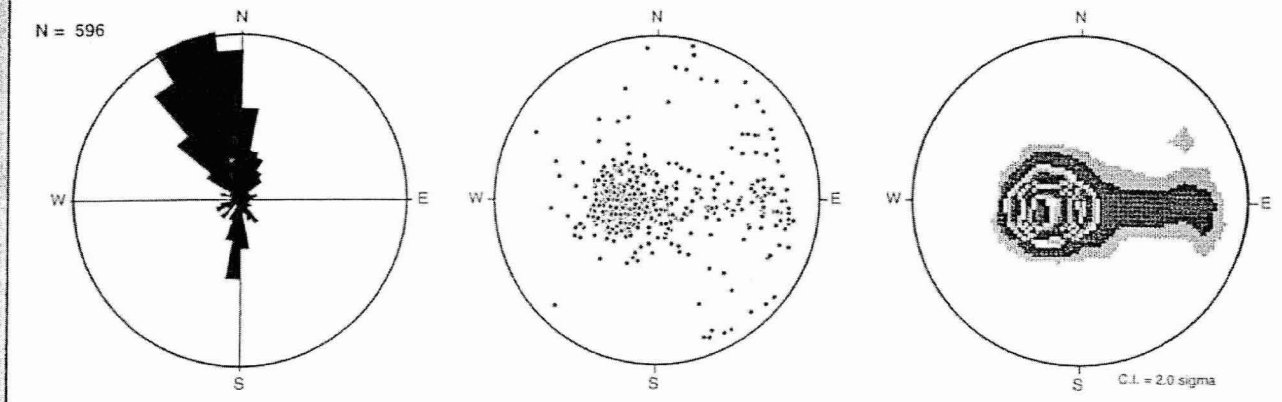

Open Fractures Interpreted from BIPS Image Data ***Depth Interval 30–715 ft***

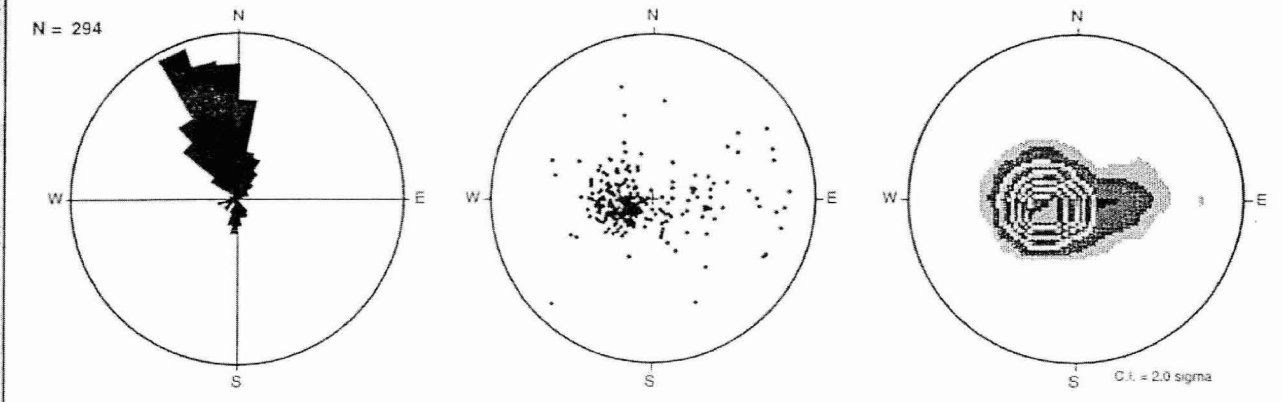

All Fractures Interpreted from FMI Image Data ***Depth Interval 38–712 ft***

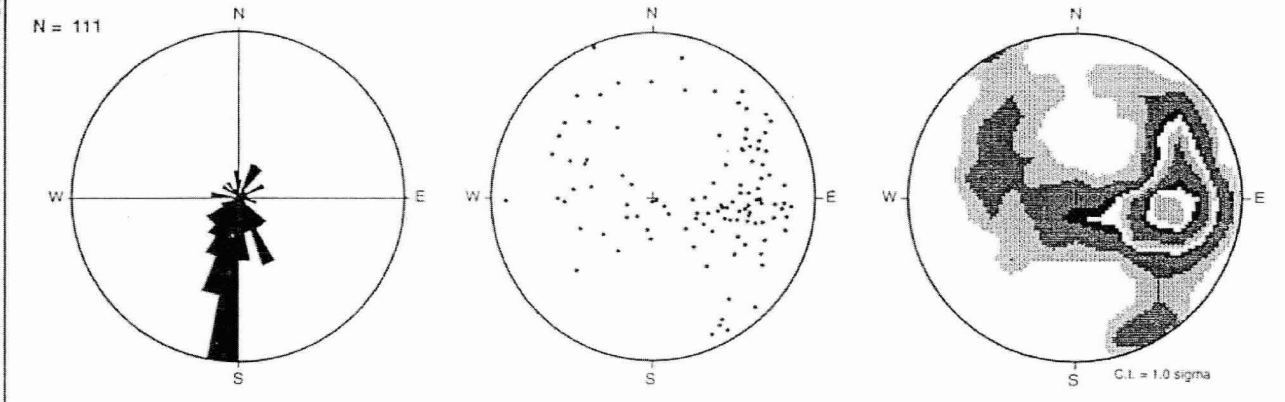

BIPS and FMI Fracture Analysis NCLLRWDF Site: Well W206

All Fractures Interpreted from BIPS Image Data *Depth Interval 34–415 ft*

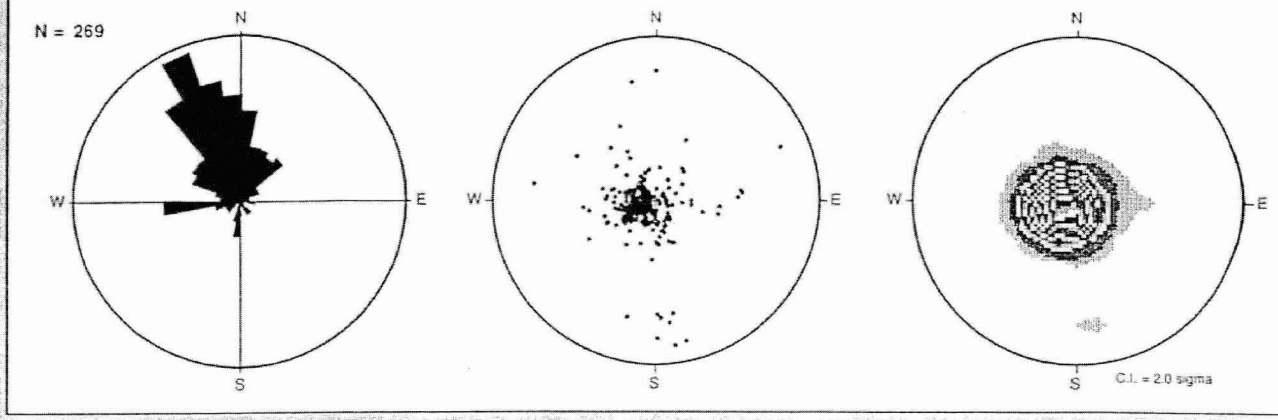

Open Fractures Interpreted from BIPS Image Data *Depth Interval 34–415 ft*

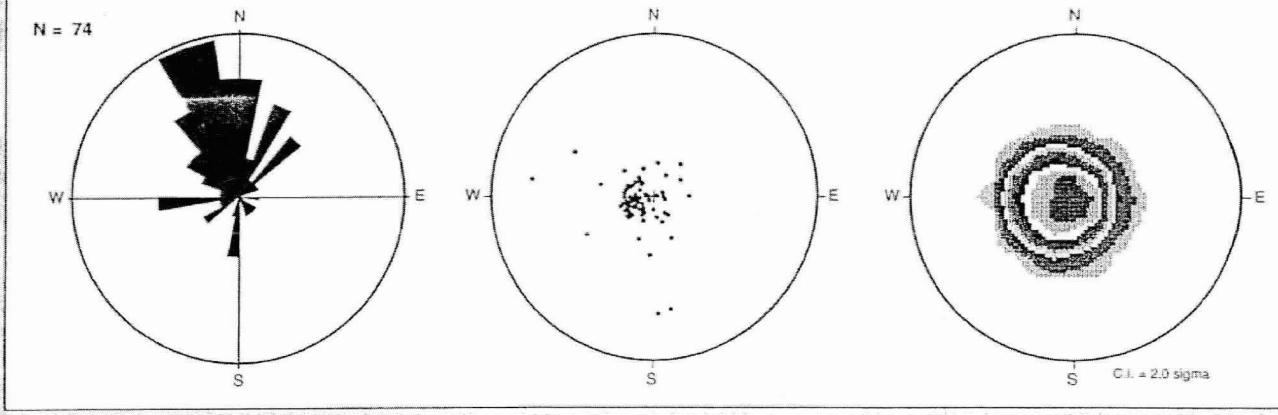

All Fractures Interpreted from FMI Image Data *Depth Interval 47–414 ft*

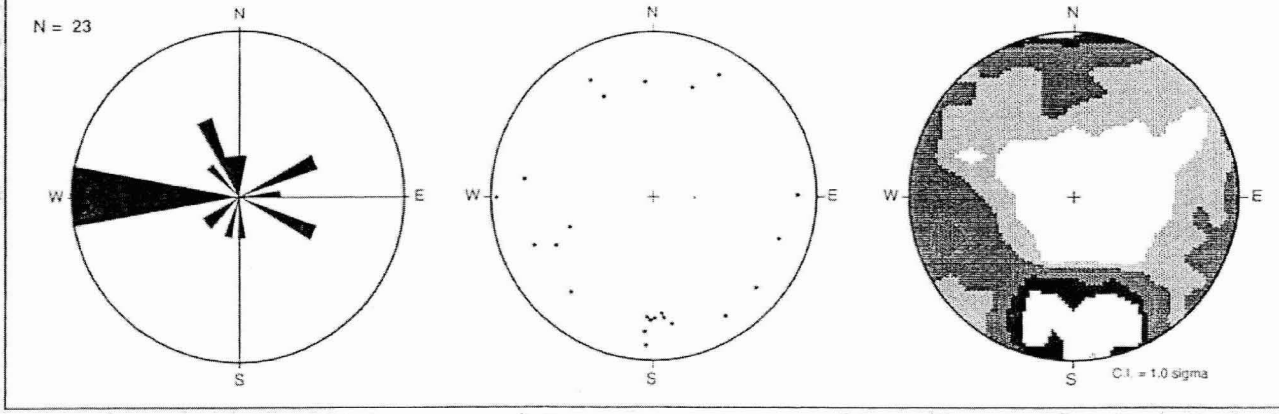

BIPS and FMI Fracture Analysis NCLLRWDF Site: Well W207

All Fractures Interpreted from BIPS Image Data ***Depth Interval 24–465 ft***

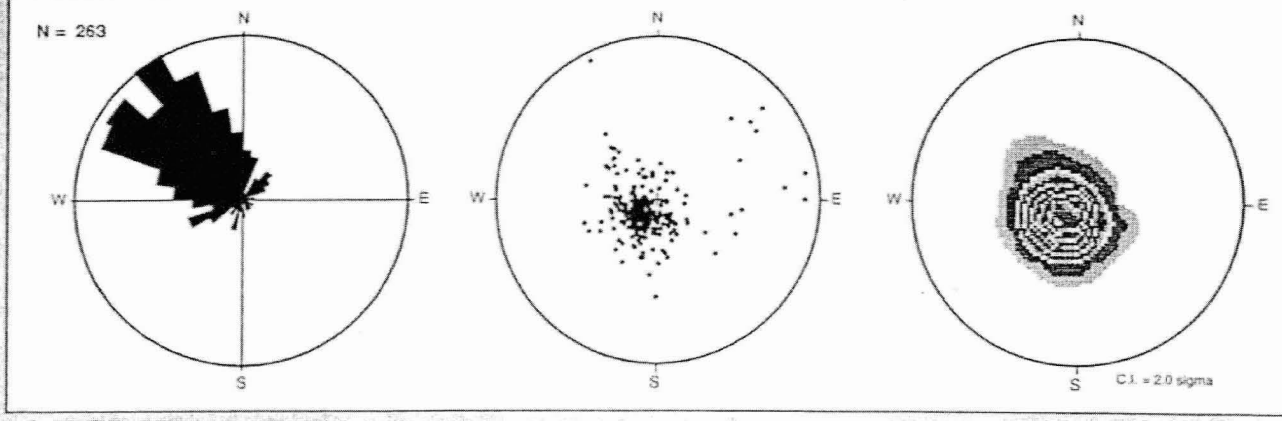

Open Fractures Interpreted from BIPS Image Data ***Depth Interval 24–465 ft***

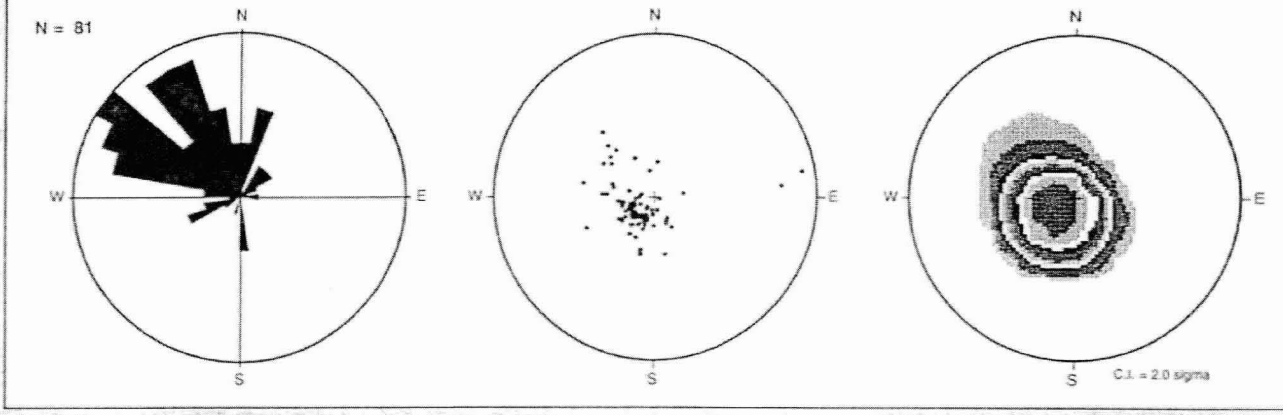

All Fractures Interpreted from FMI Image Data ***Depth Interval 42–461 ft***

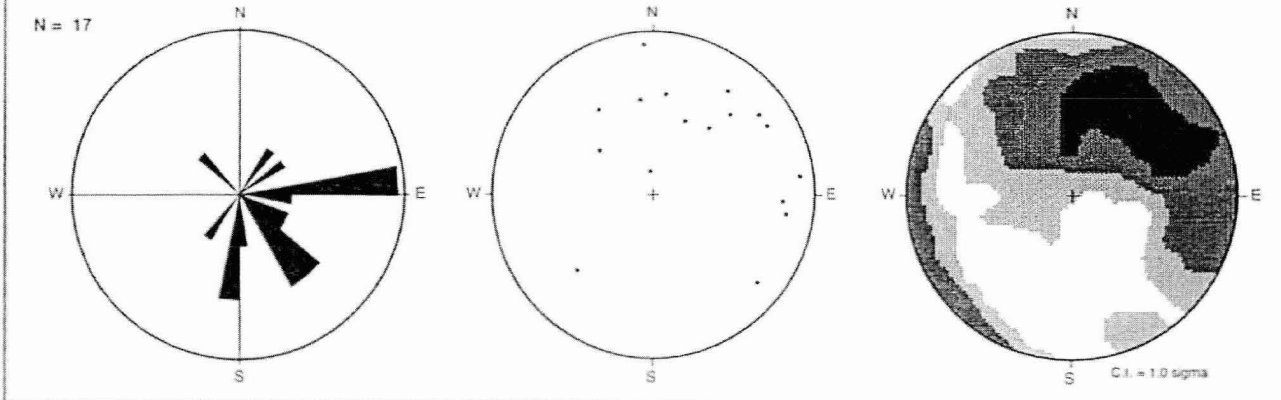

BIPS and FMI Fracture Analysis NCLLRWDF Site: Well W208

All Fractures Interpreted from BIPS Image Data ***Depth Interval 32–515 ft***

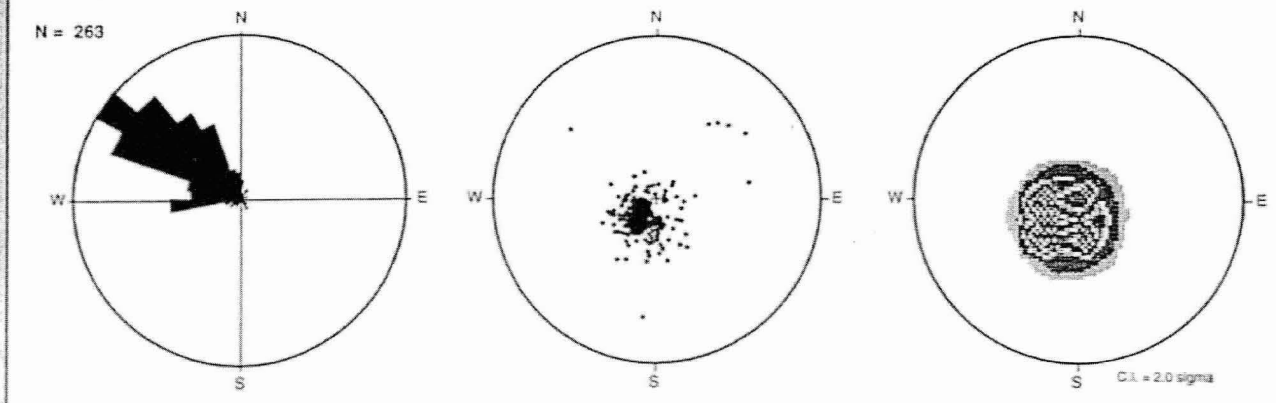

Open Fractures Interpreted from BIPS Image Data ***Depth Interval 32–515 ft***

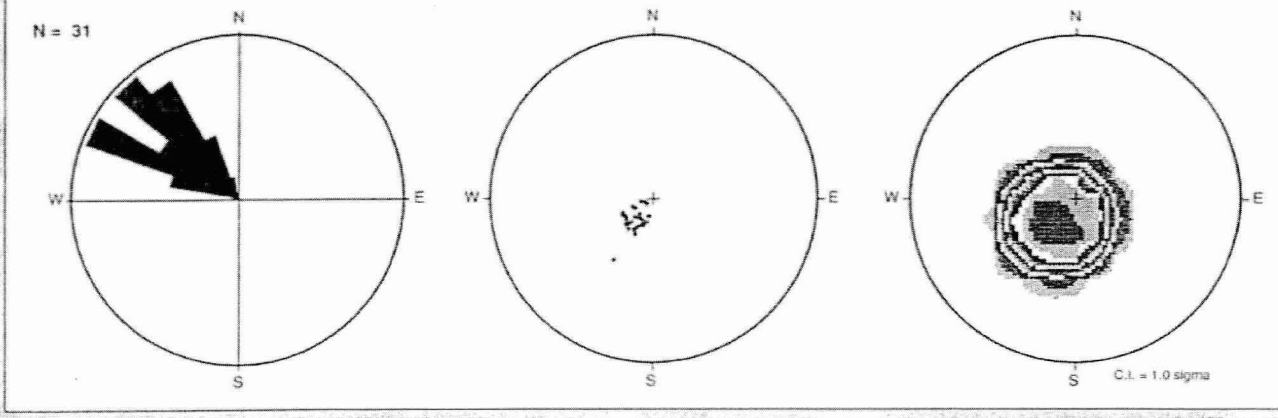

All Fractures Interpreted from FMI Image Data ***Depth Interval 33–516 ft***

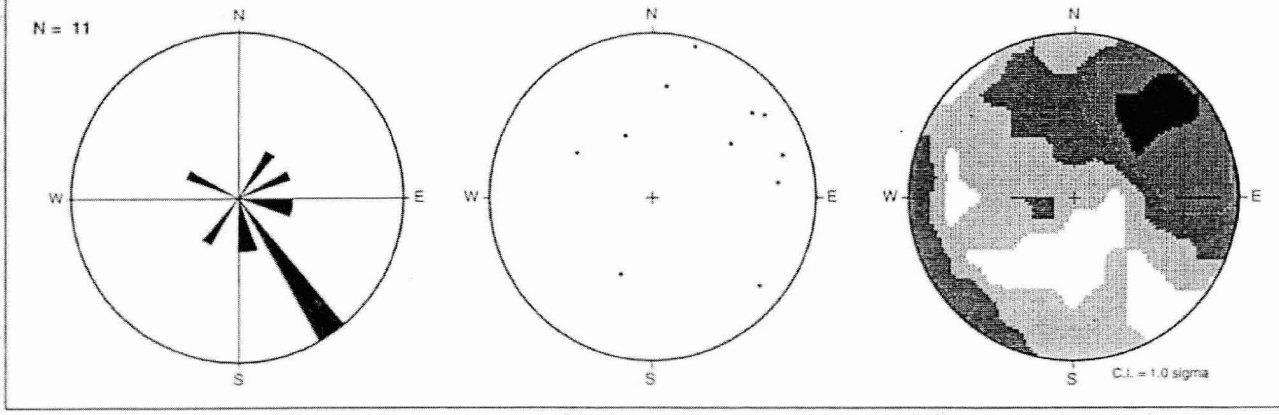

Appendix F

Hydrophysical Logging

FIGURE W201ARIA.5: SUMMARY OF HYDROPHYSICAL LOGS FOR SLUG TEST AFTER EMPLACEMENT; HLA-RALEIGH; NCLLRWSF; WELL: W201AR1A

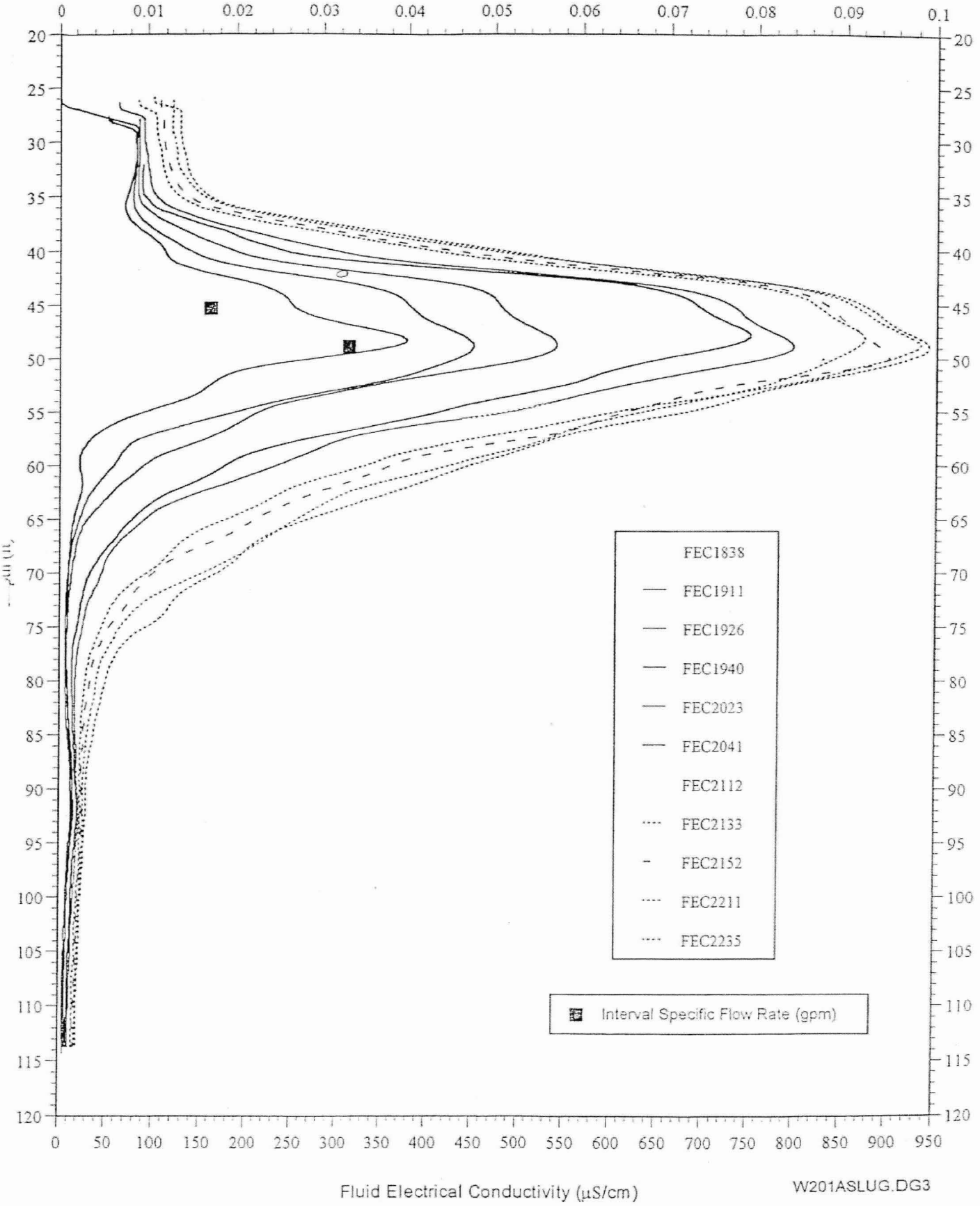

FIGURE W201ARB1B: SUMMARY OF HYDROPHYSICAL LOGS FOR SLUG TEST AFTER EMPLACEMENT TEST; HLA - RALEIGH; NCLLRWSF; WELL: W201AR1B

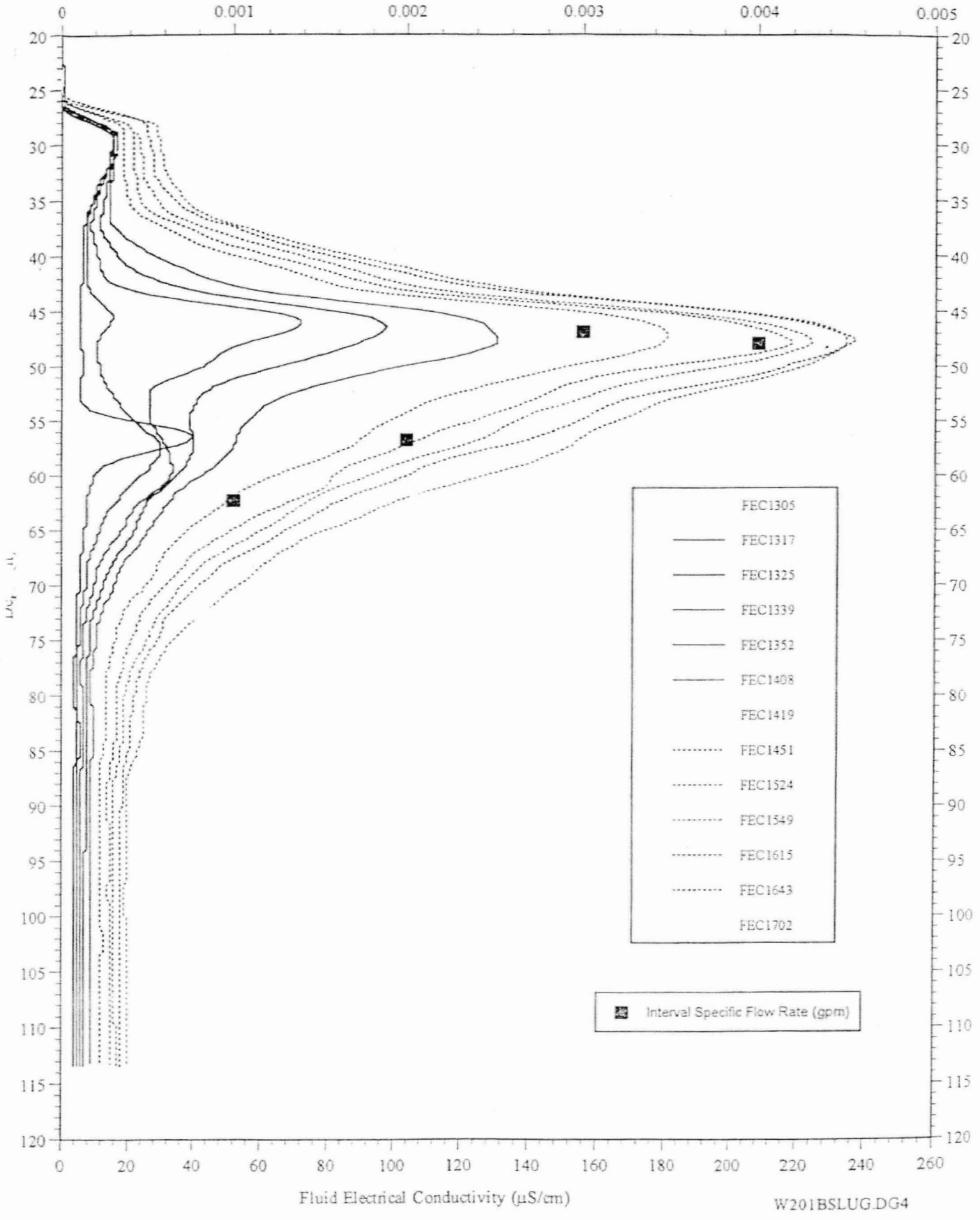

W201BSLUG.DG4

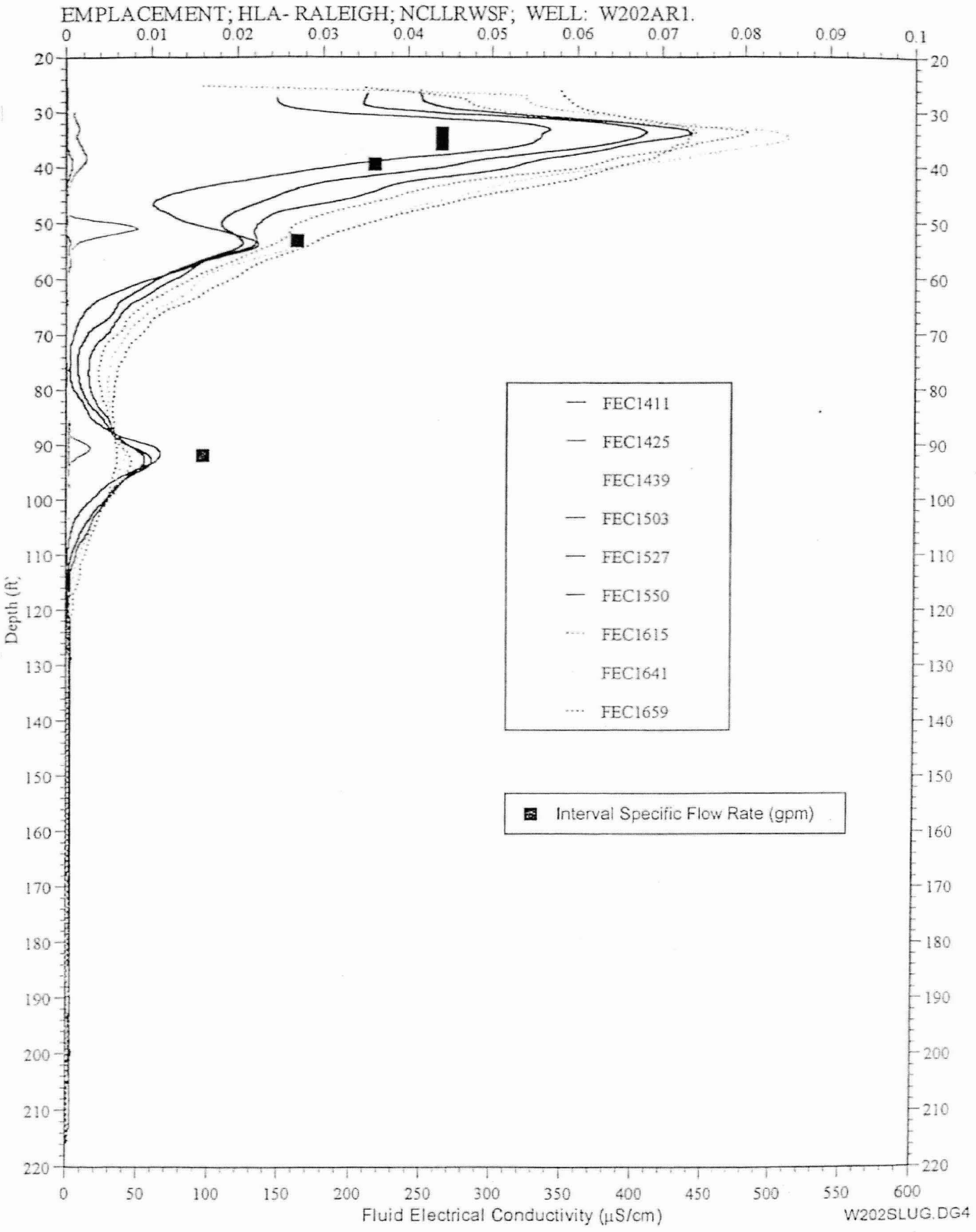
EMPLACEMENT; HLA- RALEIGH; NCLLRWSF; WELL: W202AR1.
0
0.01
0.02
0.03
0.04
0.05
0.06
0.07
0.08
0.09
0.1
20
30
40
50
60
70
80
90
100
110
120
130
140
150
160
170
180
190
200
210
220
Depth (ft)
FEC1411
FEC1425
FEC1439
FEC1503
FEC1527
FEC1550
FEC1615
FEC1641
FEC1659
Interval Specific Flow Rate (gpm)
0
50
100
150
200
250
300
350
400
450
500
550
600
Fluid Electrical Conductivity (µS/cm)
W202SLUG.DG4

FIGURE W203AR1.5: SUMMARY OF HYDROPHYSICAL LOGS FOR SLUG TEST AFTER EMPLACEMENT; HLA - RALEIGH; NCLLRSF; WELL: W203AR1

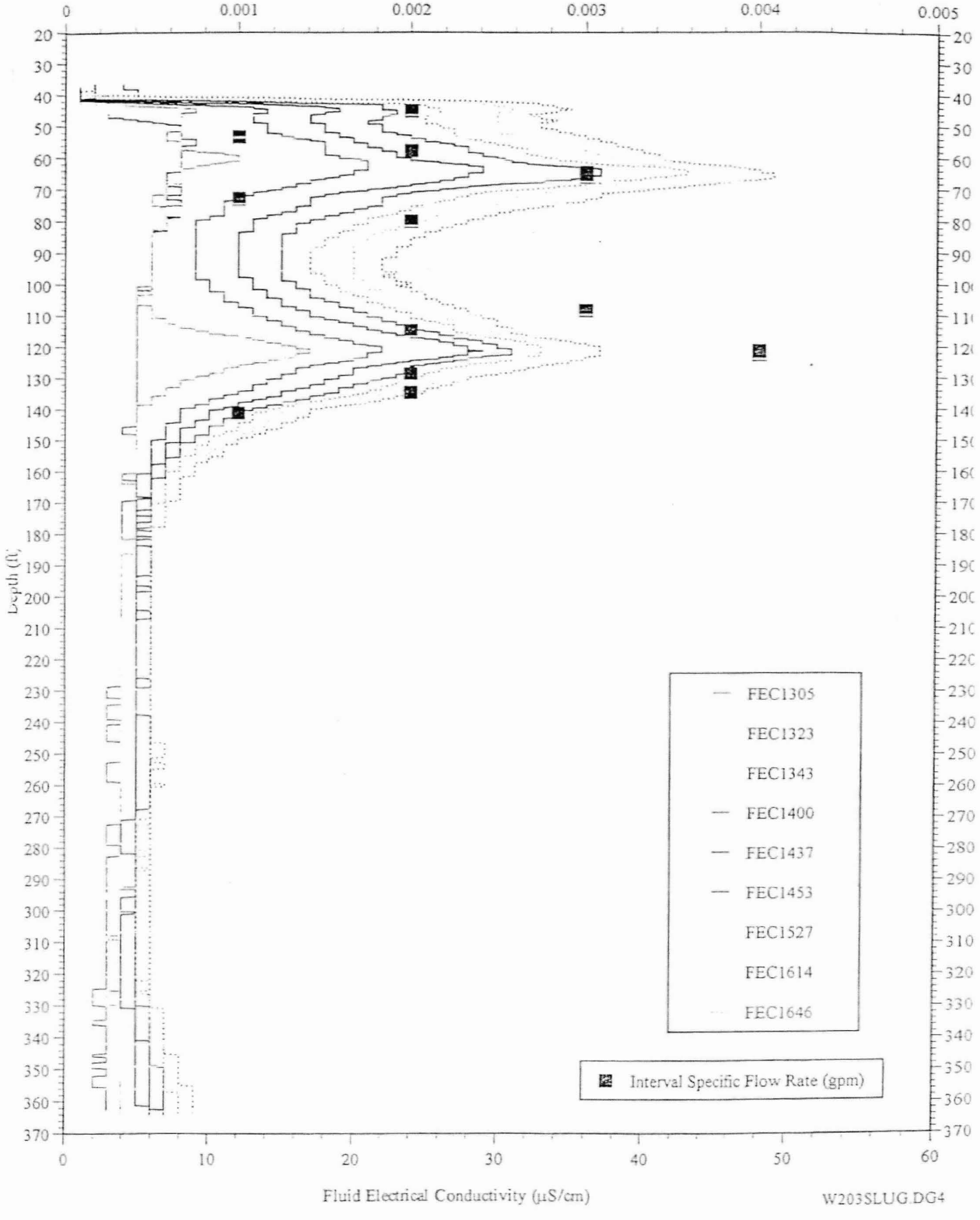

W203SLUG.DG4

FIGURE W204AR1.3: SUMMARY OF HYDROPHYSICAL LOGS FOR 5.6 FOOT SLUG TEST AFTE EMPLACEMENT; HLA-RALEIGH; NCLLRWSF; WELL: W204AR1.

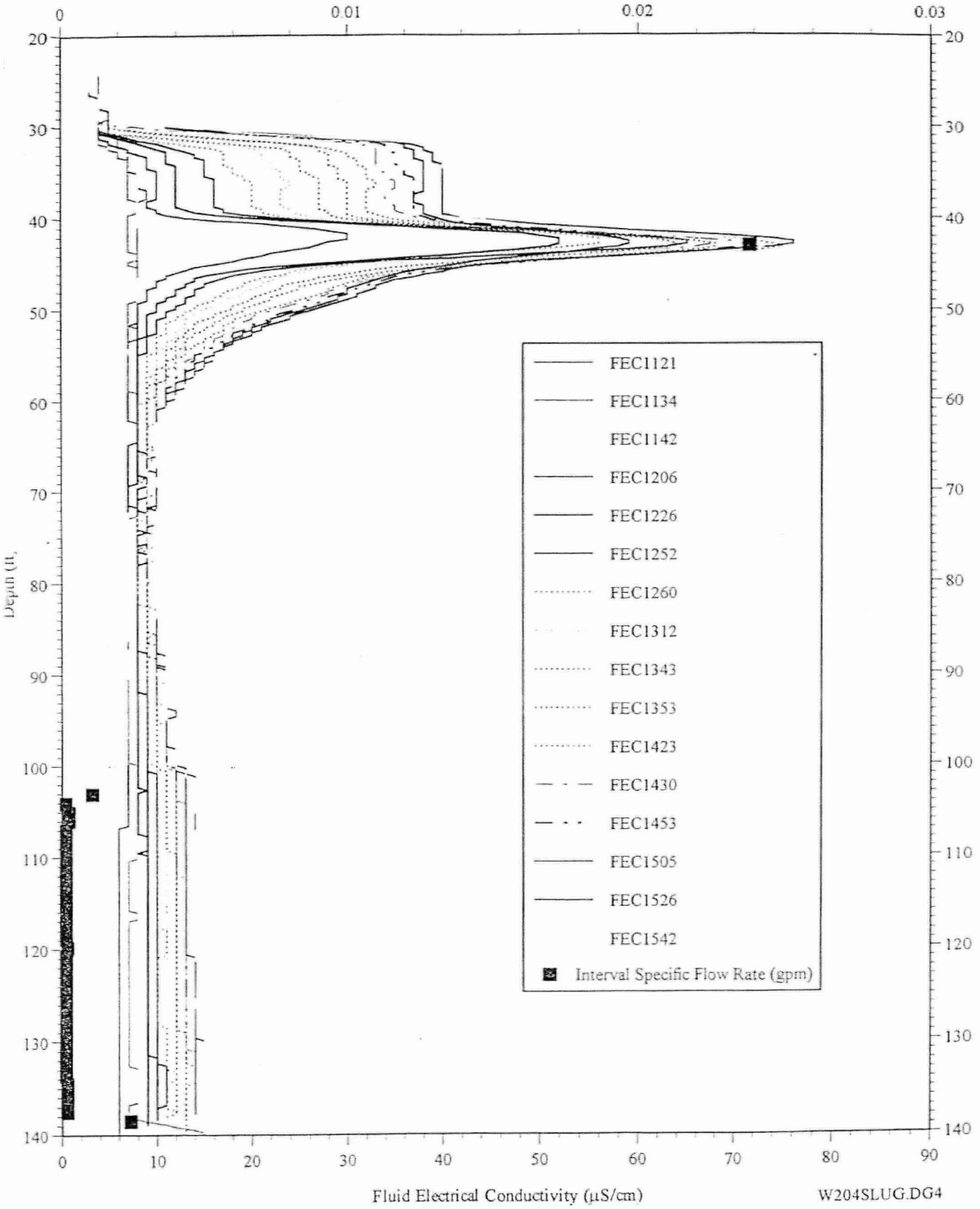

FIGURE W205CH1.3: SUMMARY OF HYDROPHYSICAL LOGS FOR PUMP AFTER EMPLACEMENT TEST; HLA-RALEIGH; NCLLRWSF; WELL: W205CH1

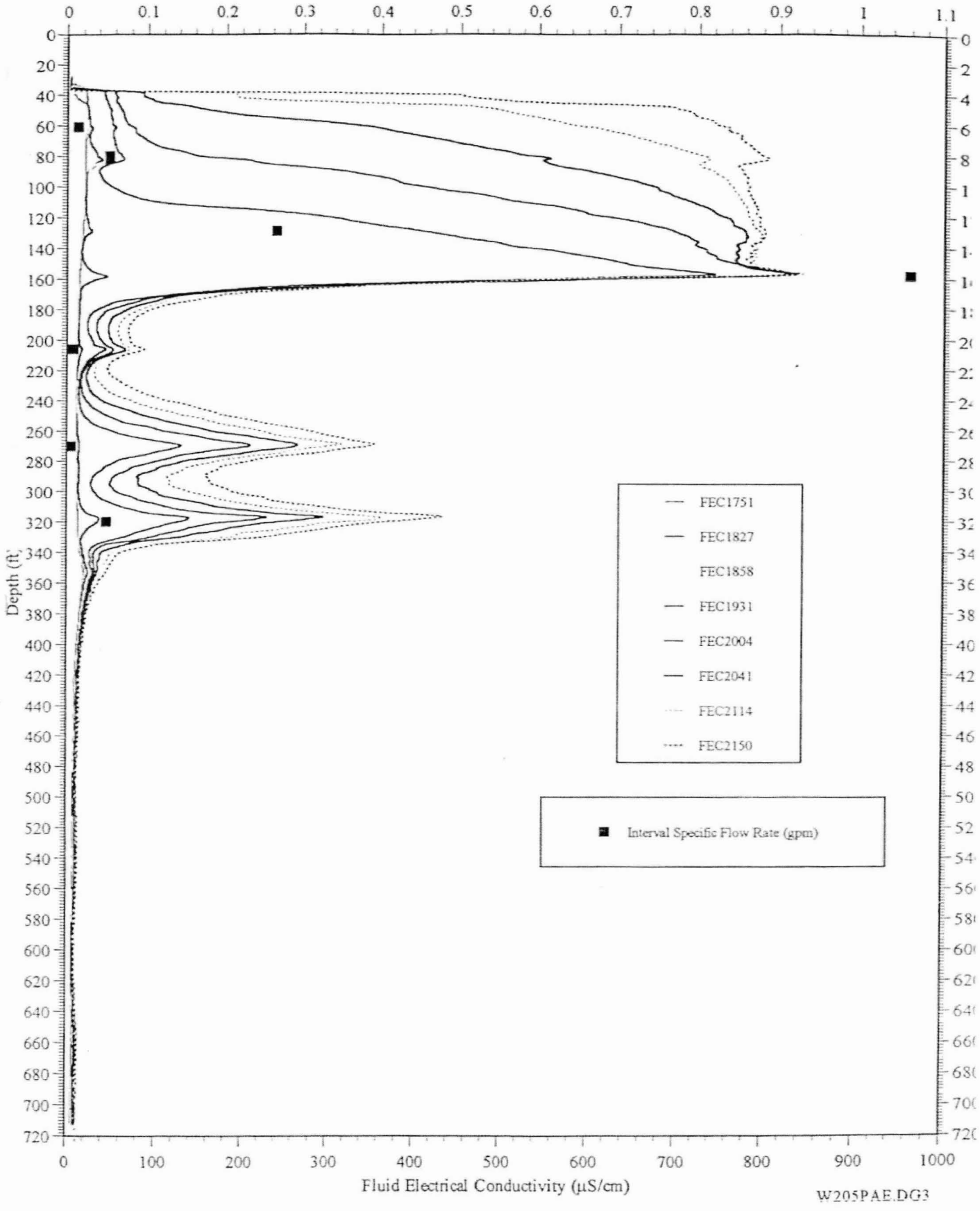

FIGURE W206AR1.3: SUMMARY OF HYDROPHYSICAL LOGS FOR 8.5 FOOT SLUG TEST; HLA RALEIGH; NCLLRWSF; WELL: W206AR1.

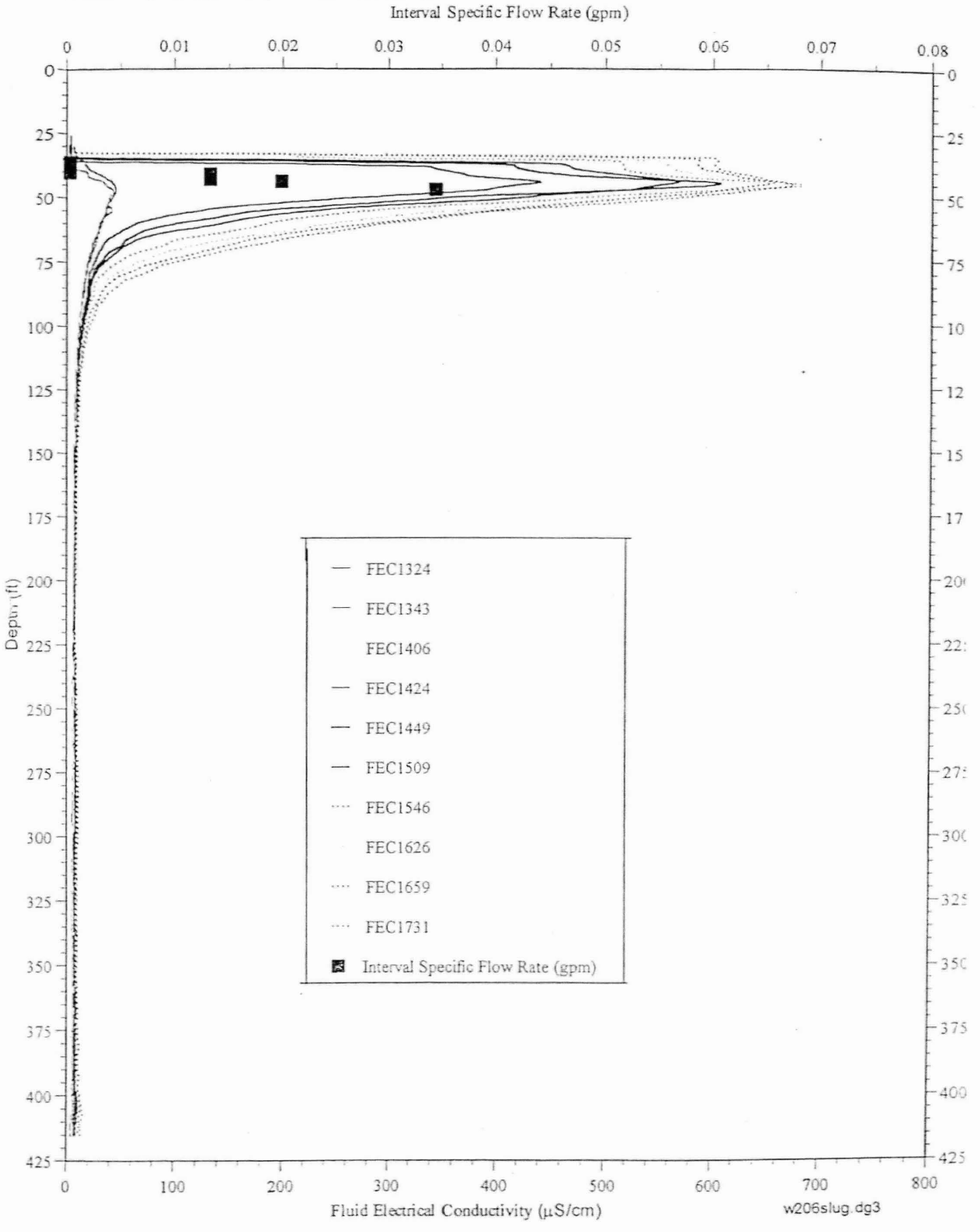

EMPLACEMENT TEST; HLA-RALEIGH; NCLLRWSF; WELL W207AR1

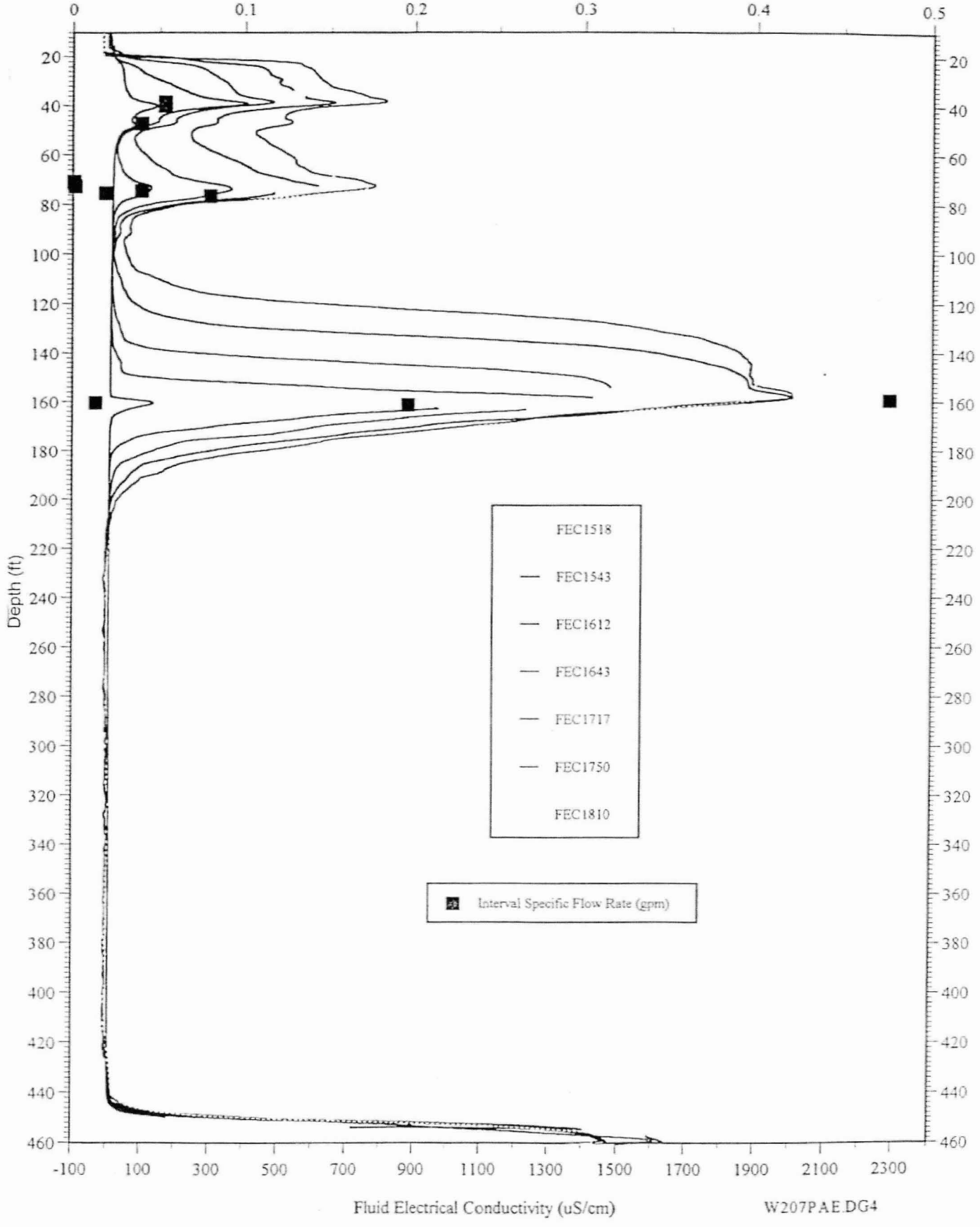

Appendix G

Packer Testing

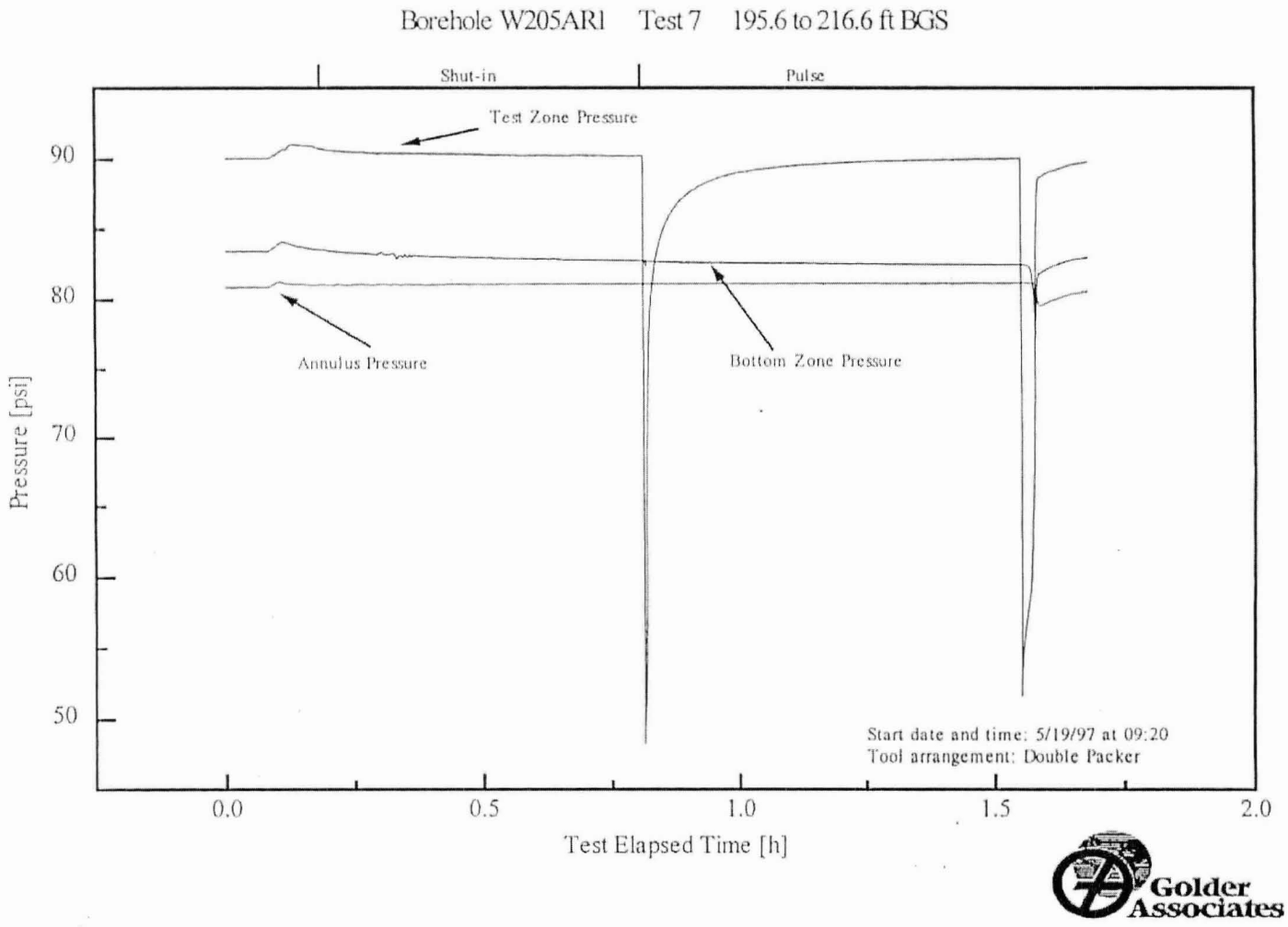

FIGURE 3-2A; TEST 7 IN BOREHOLE 205AR1; EXAMPLE FOR A PULSE TEST

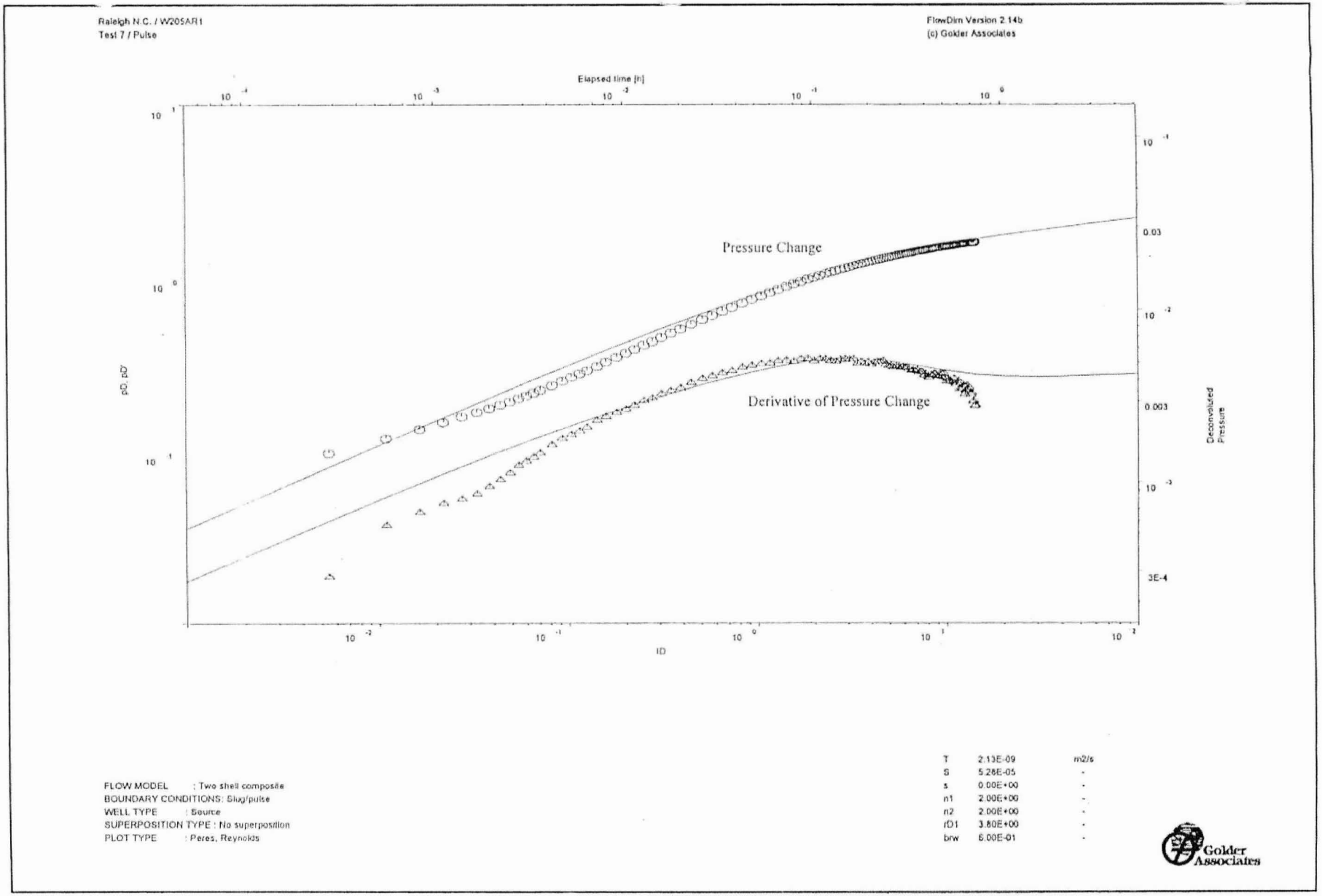

FIGURE 3-2B; Test 7 in Borehole W205AR1; Pulse Phase; Log-Log Deconvolution Plot

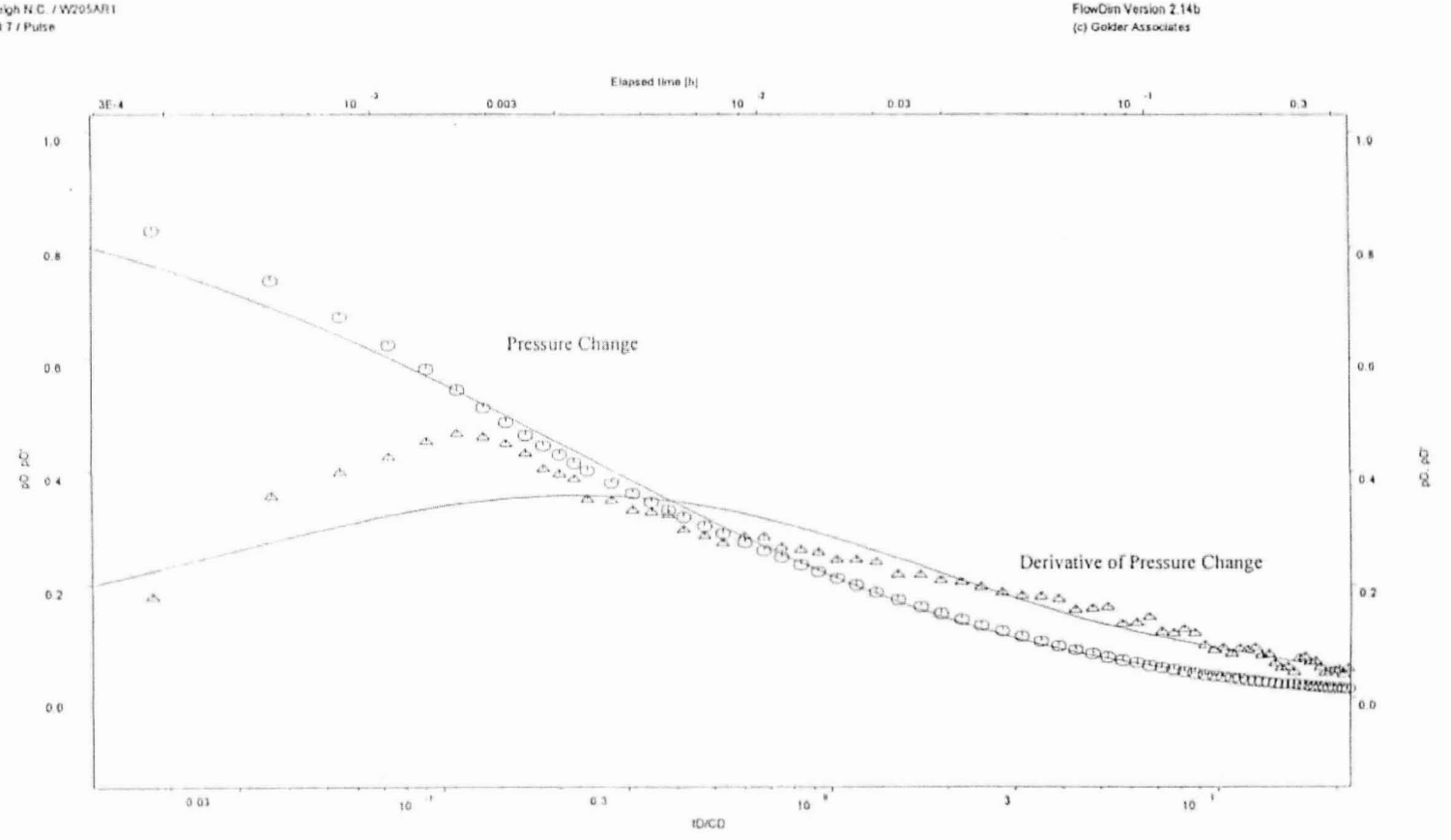

FIGURE 3-2C; Test 7 in Borehole W205ARI; Pulse Phase; Ramey A Analysis

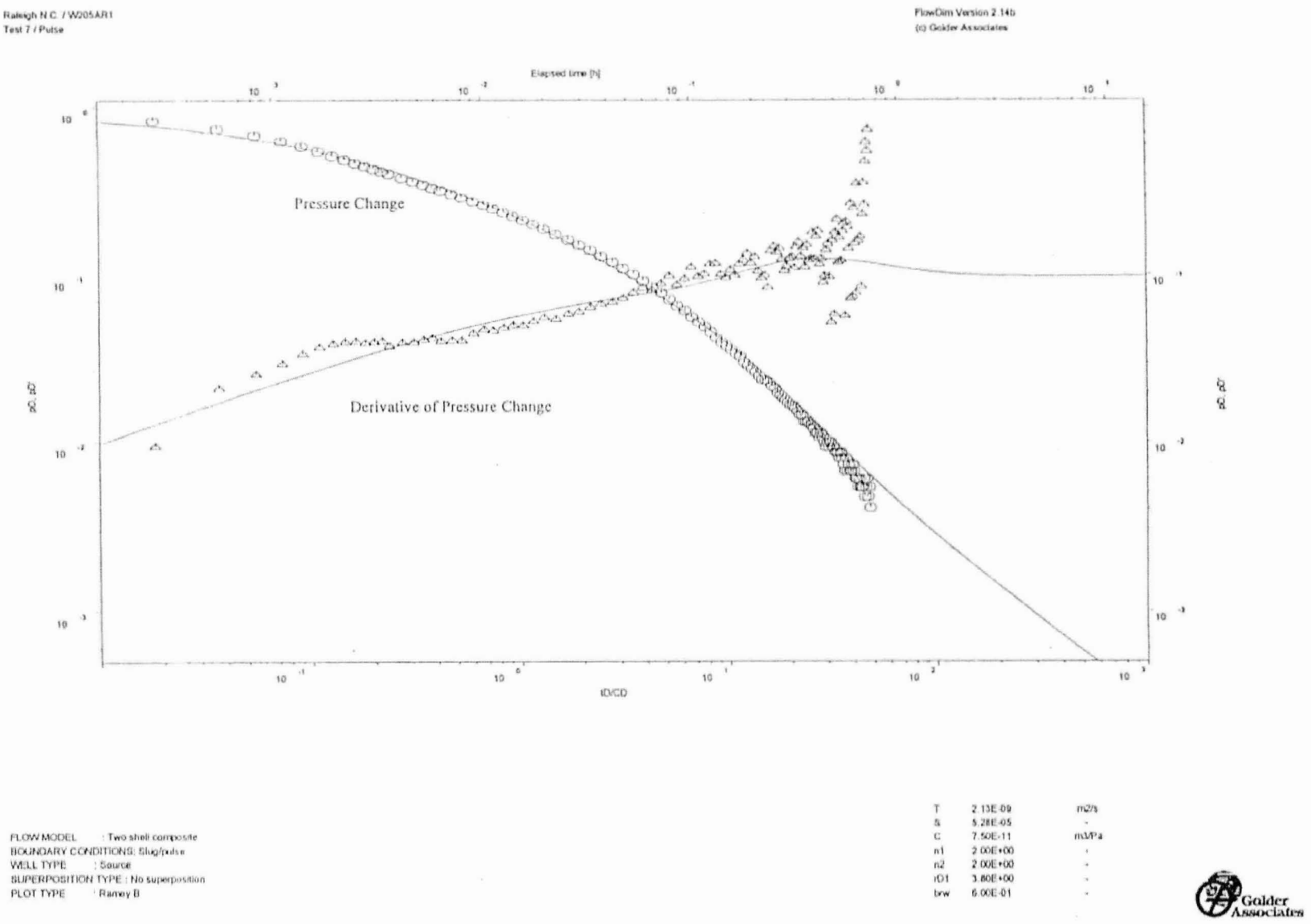

FIGURE 3-2D; Test 7 in Borehole W205ARI; Pulse Phase; Ramey B Analysis

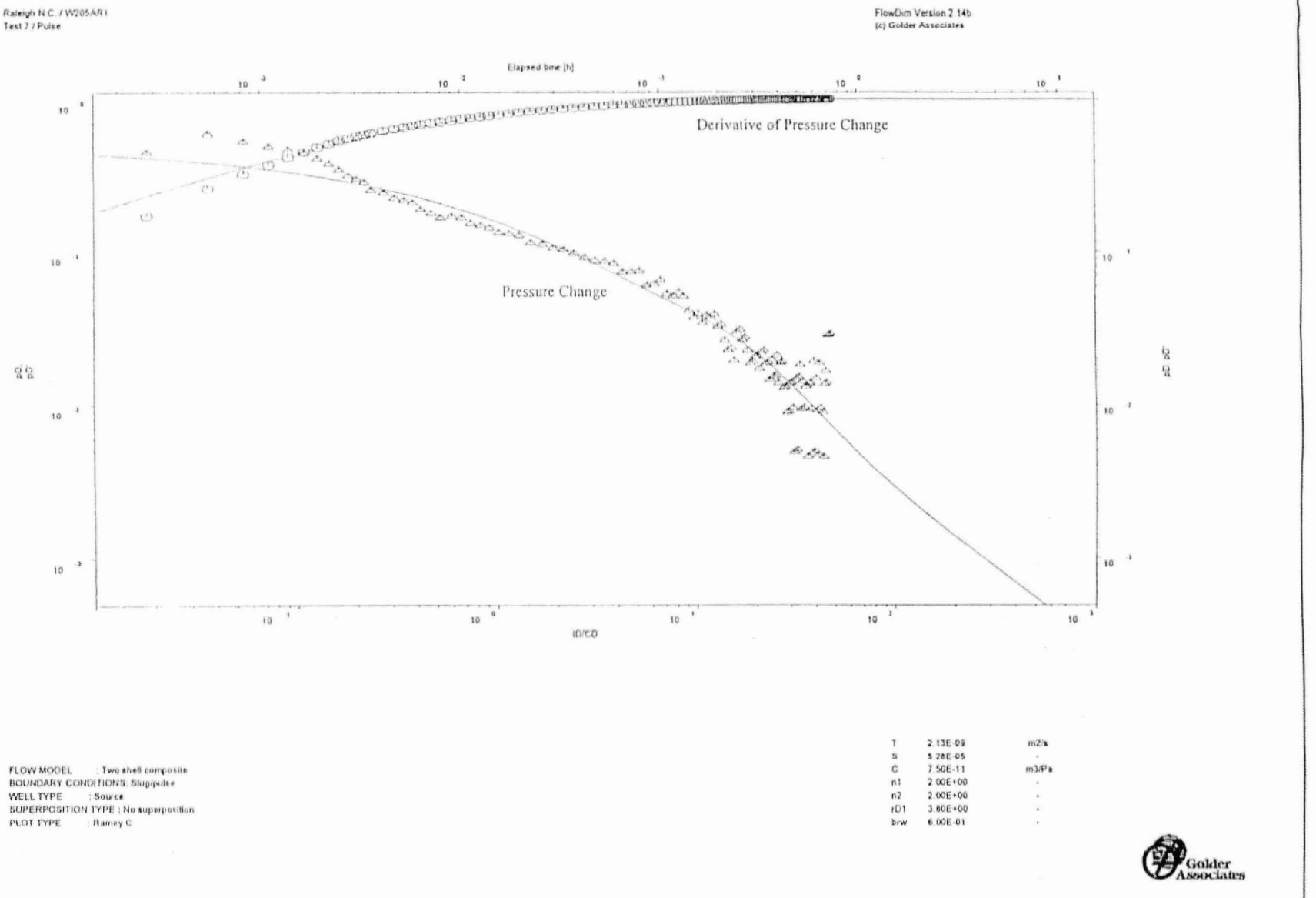

FIGURE 3-2E; Test 7 in Borehole W205AR1; Pulse Phase; Ramey C Analysis

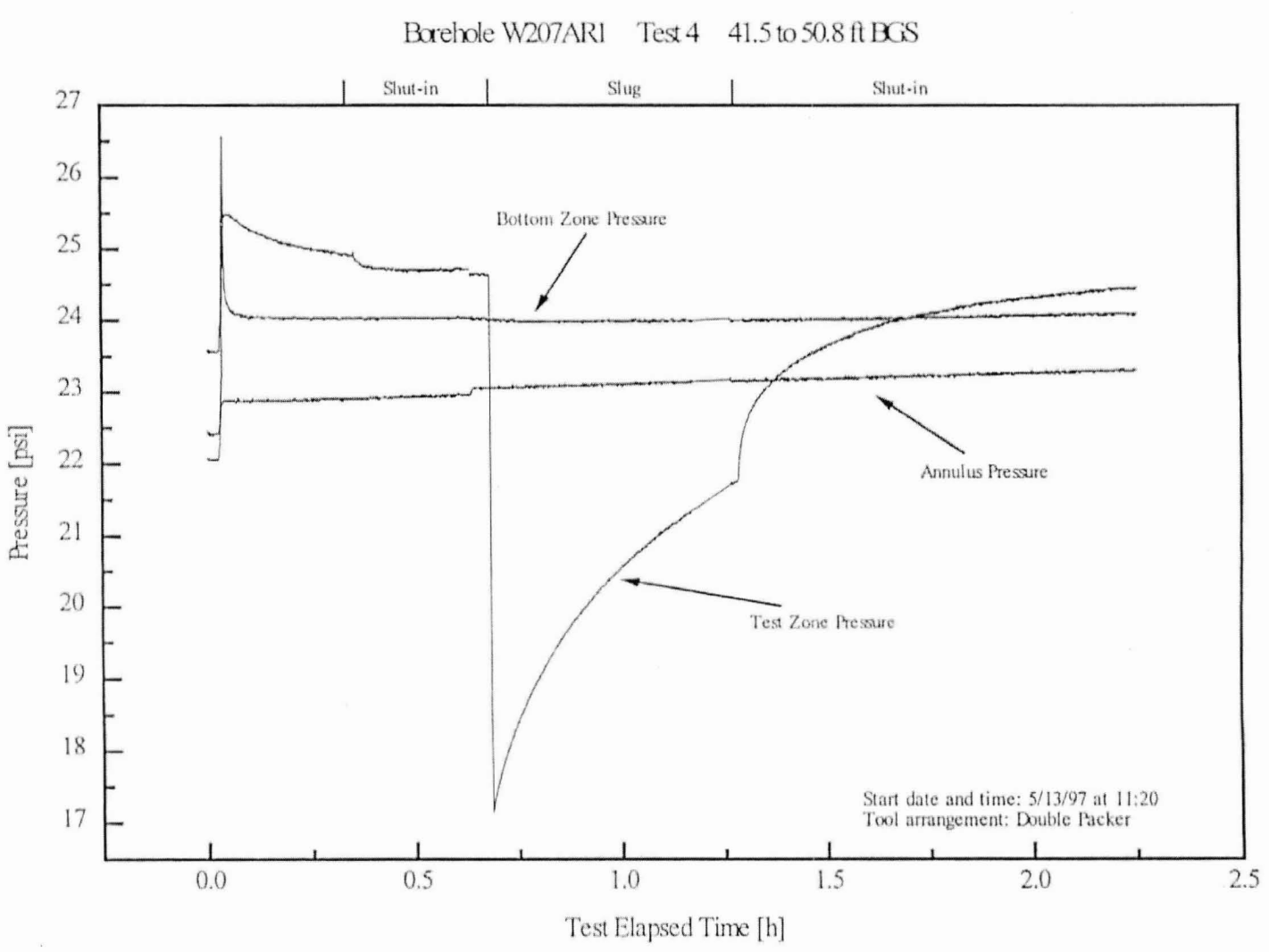

Golder Associates

FIGURE 3-3A; TEST 4 IN BOREHOLE 205AR1; EXAMPLE FOR A SLUG TEST

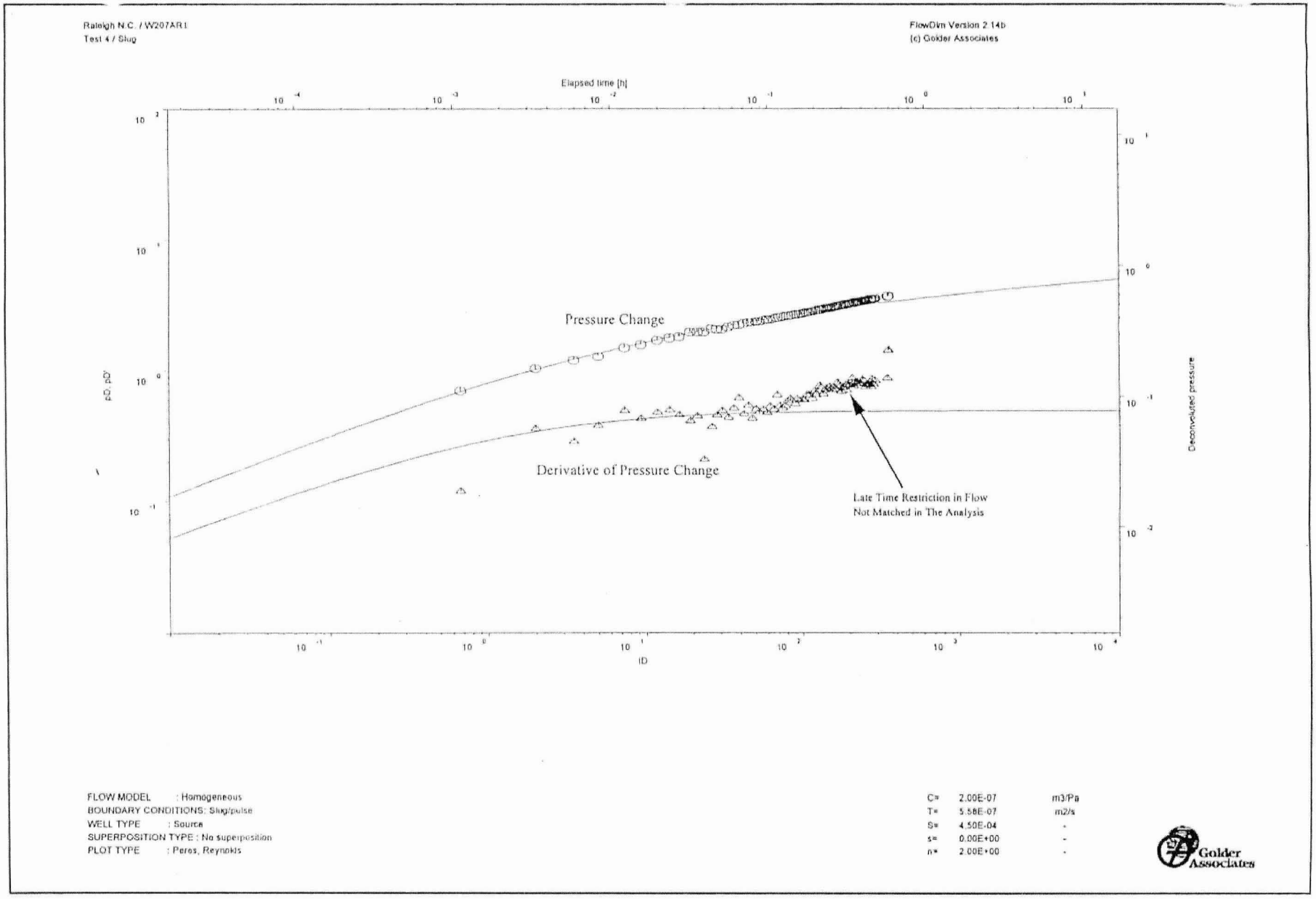

FIGURE 3-3B; TEST 4 IN BOREHOLE W207ARI; SLUG PHASE; DECONVOLUTION PLOT

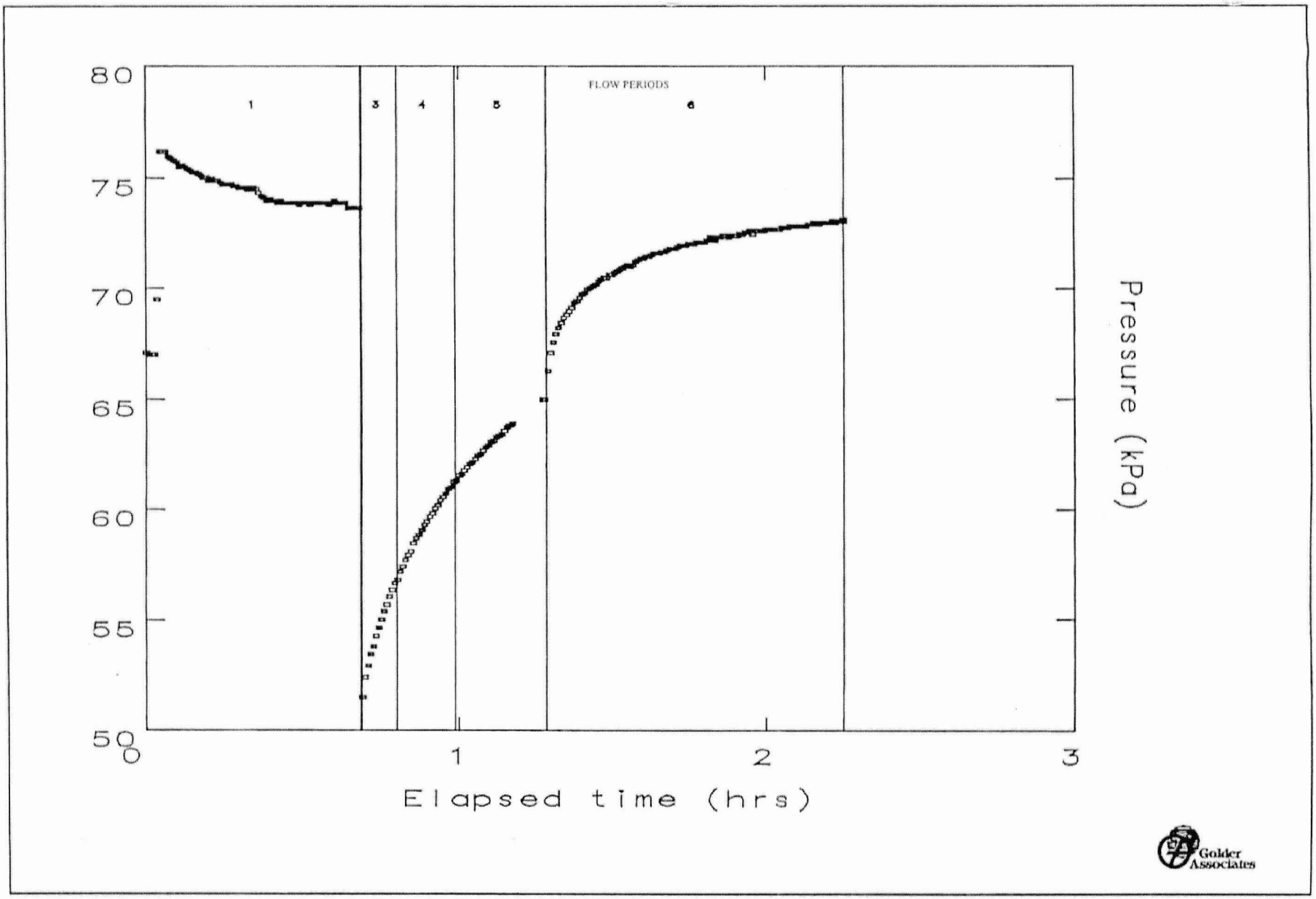

FIGURE 3-3C; TEST 4 IN BOREHOLE W207ARI; DISCRETISATION OF TEST FOR CONSTANT RATE ANALYSIS

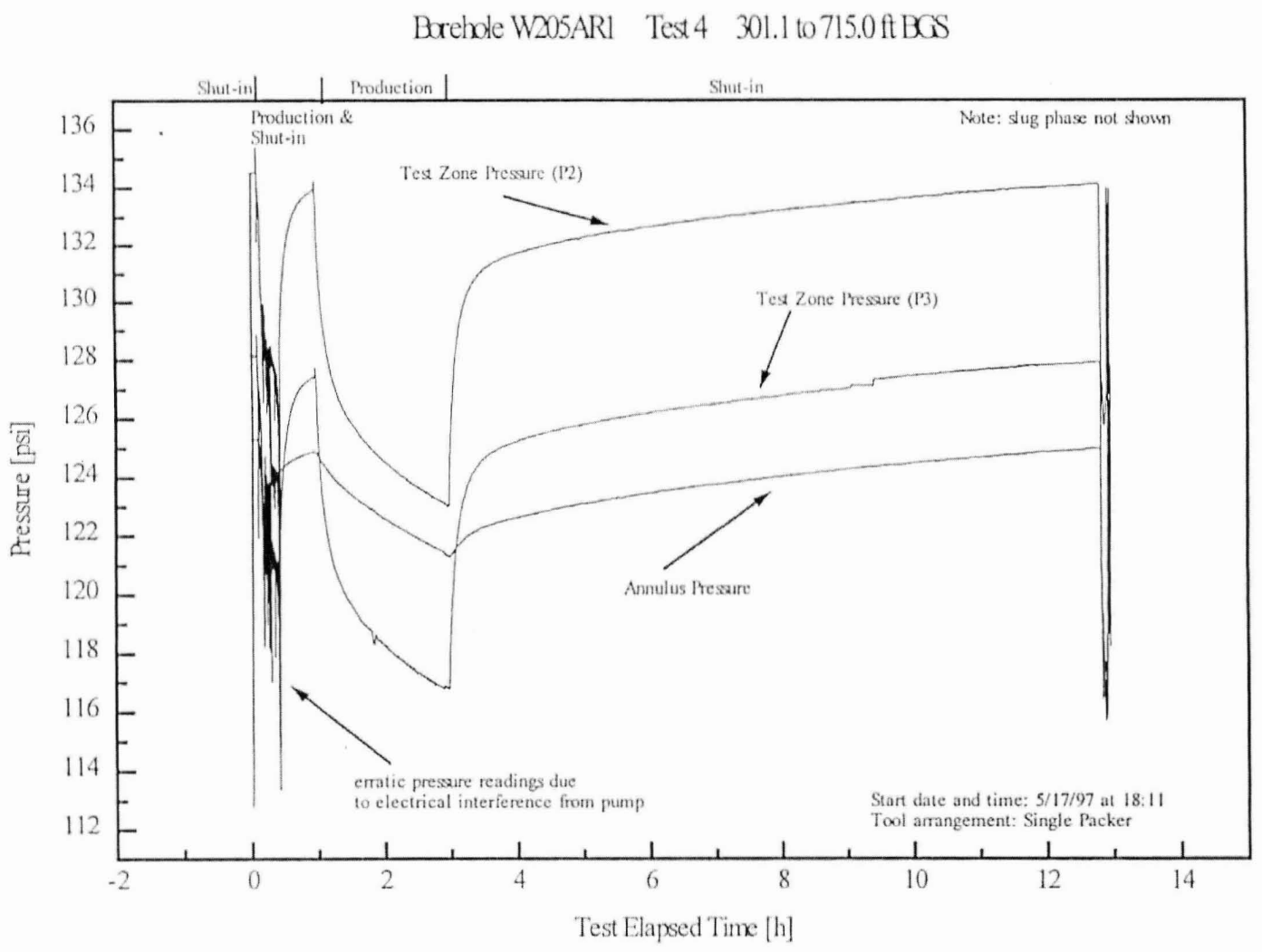

Golder Associates

FIGURE 3-4A; TEST 4 IN BOREHOLE W205AR1; EXAMPLE FOR A CONSTANT RATE TEST

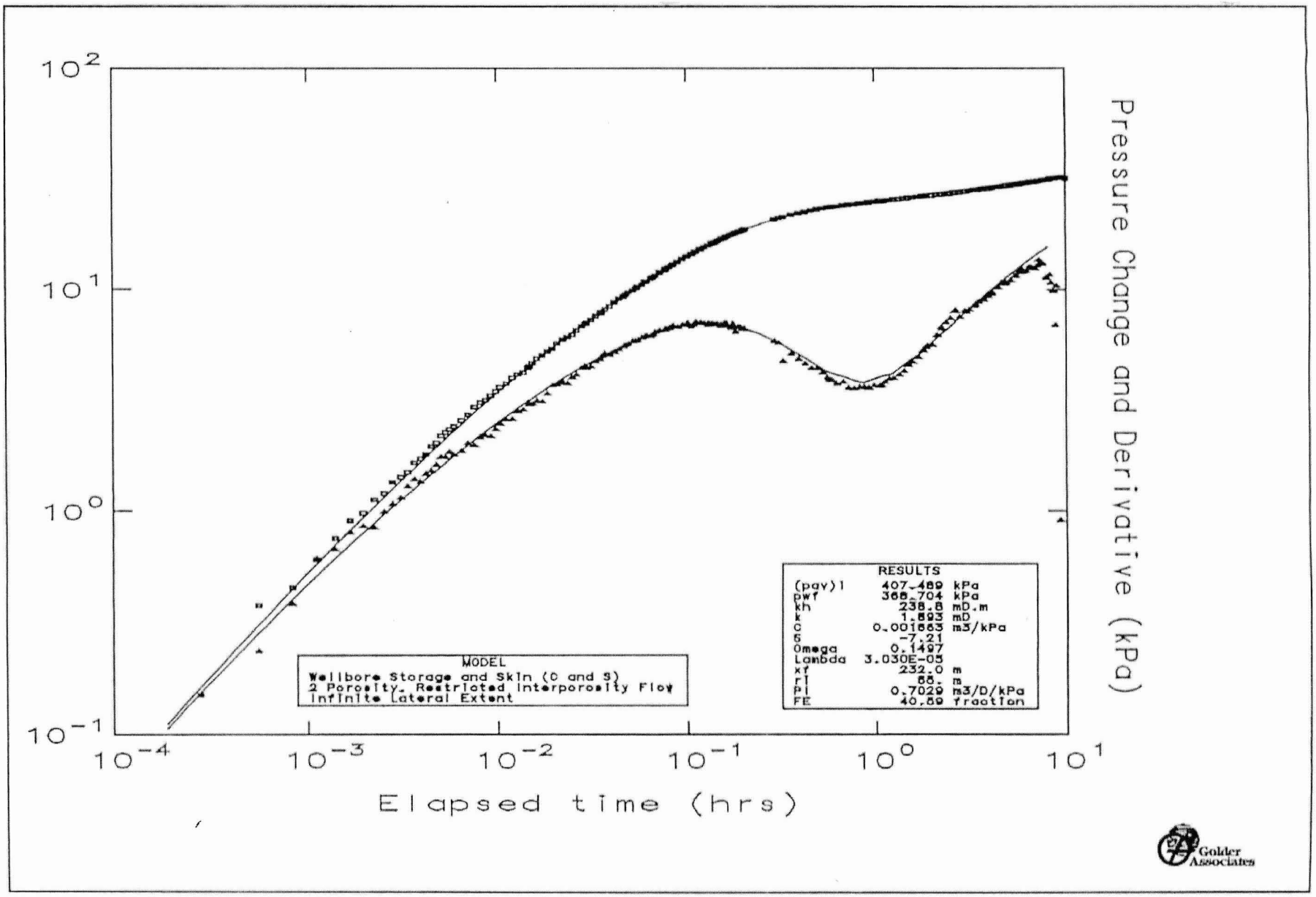

FIGURE 3-4B; TEST 4 IN BOREHOLE W205ARI; SHUT-IN PHASE; LOG-LOG PLOT

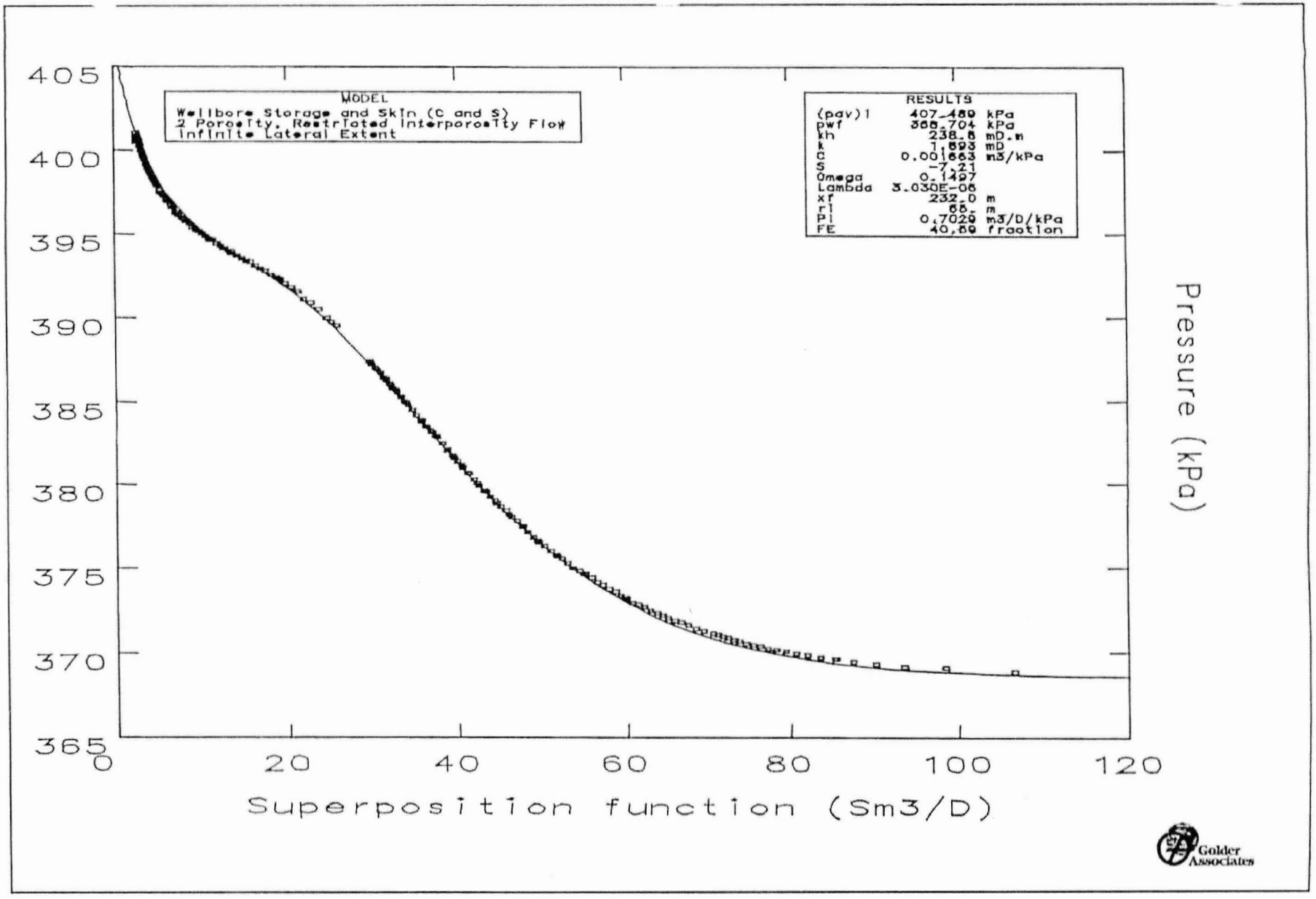

FIGURE 3-4C; TEST 4 IN BOREHOLE W205AR1; SHUT-IN PHASE; HORNER ANALYSIS

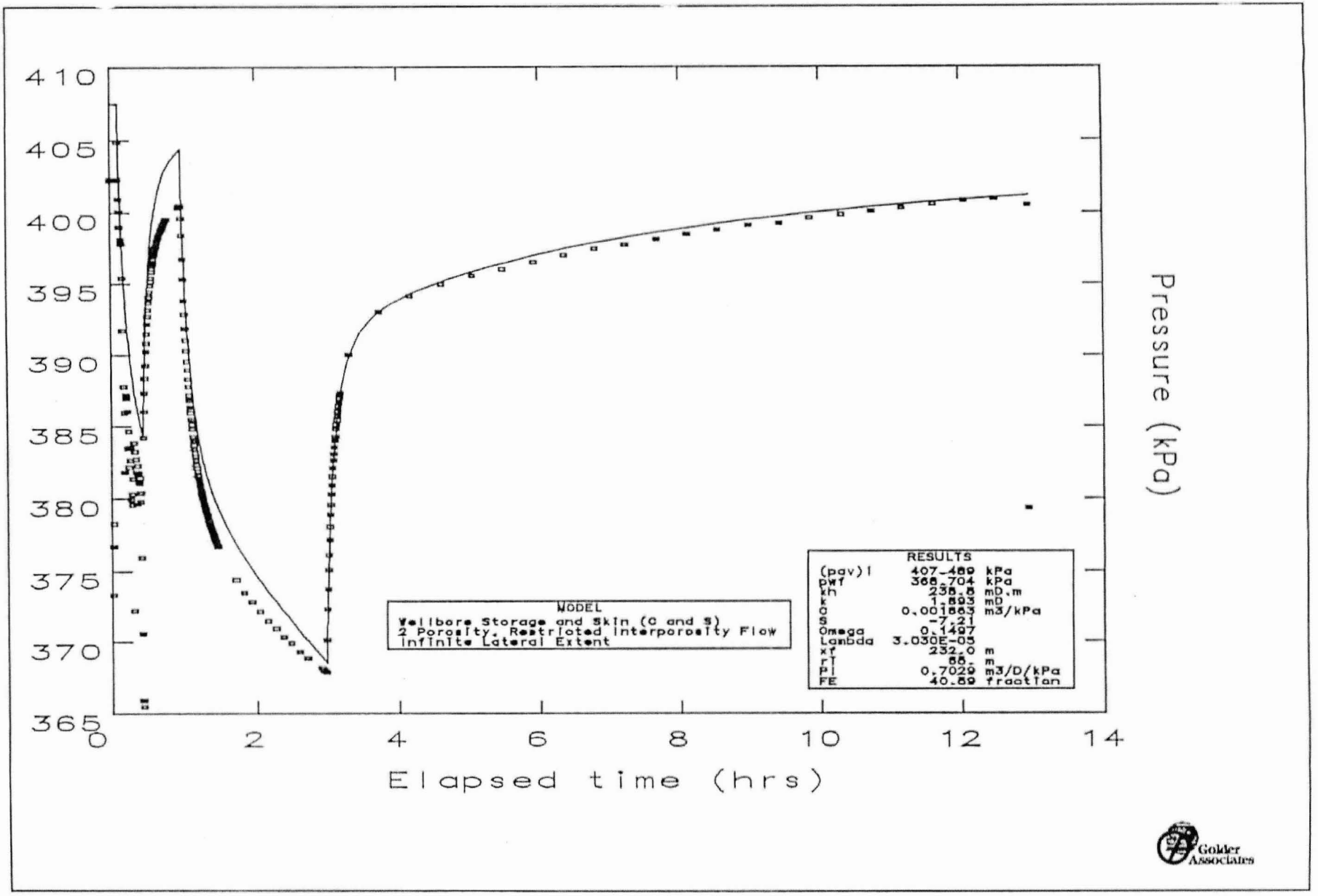

FIGURE 3-4D; TEST 4 IN BOREHOLE W205ARI; MATCH TO ENTIRE SIMULATION BASED ON RESULTS DERIVED IN ANALYSIS OF THE SHUT-IN PHASE

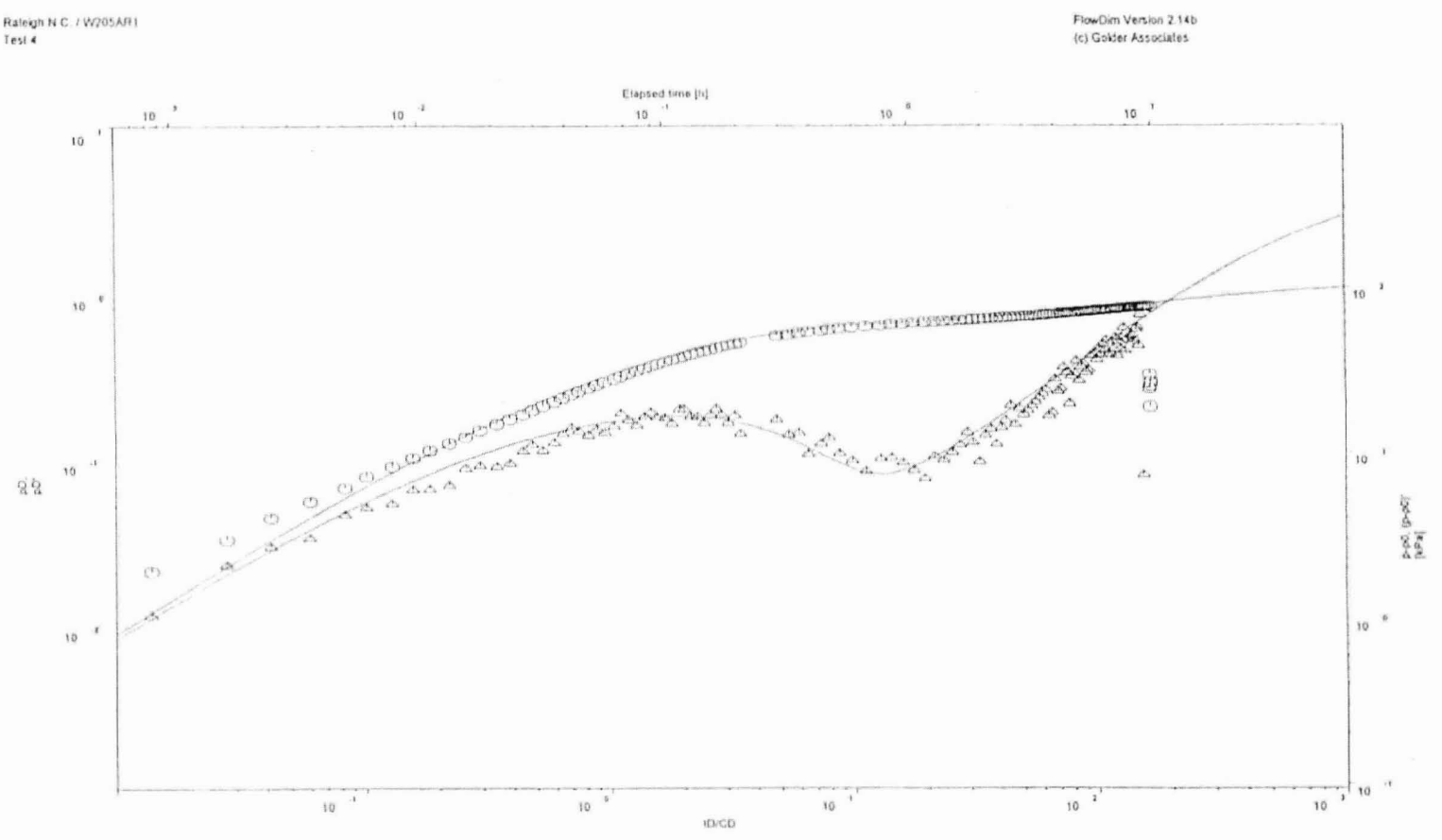

FIGURE 3-4E; TEST 4 IN BOREHOLE W205ARI; SHUT-IN PHASE; LOG-LOG PLOT; ALTERNATIVE FLOW MODEL USING THE FLOW DIMENSION APPROACH

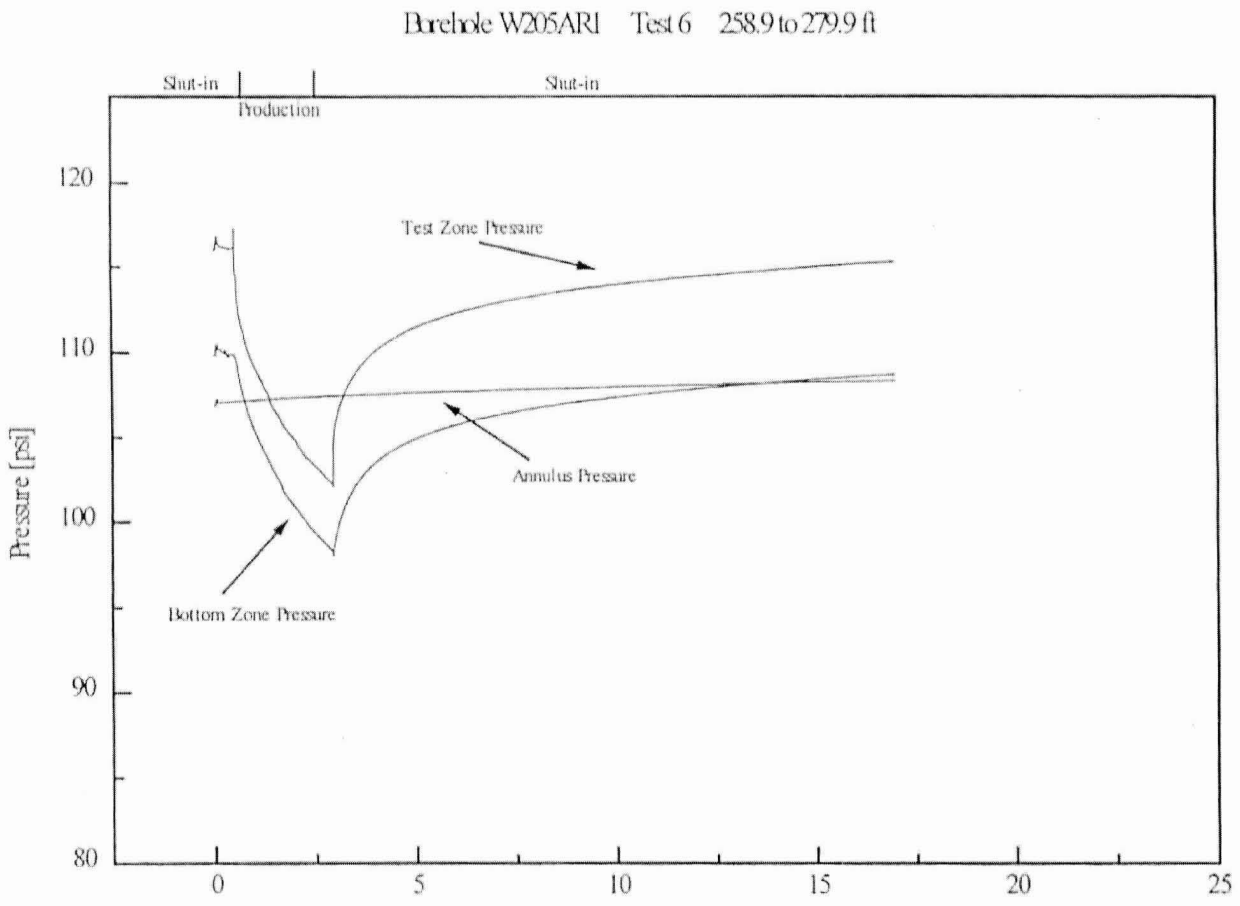

FIGURE 3-5A; TEST 6 IN BOREHOLE W205ARI; EXAMPLE FOR CONSTANT RATE TEST

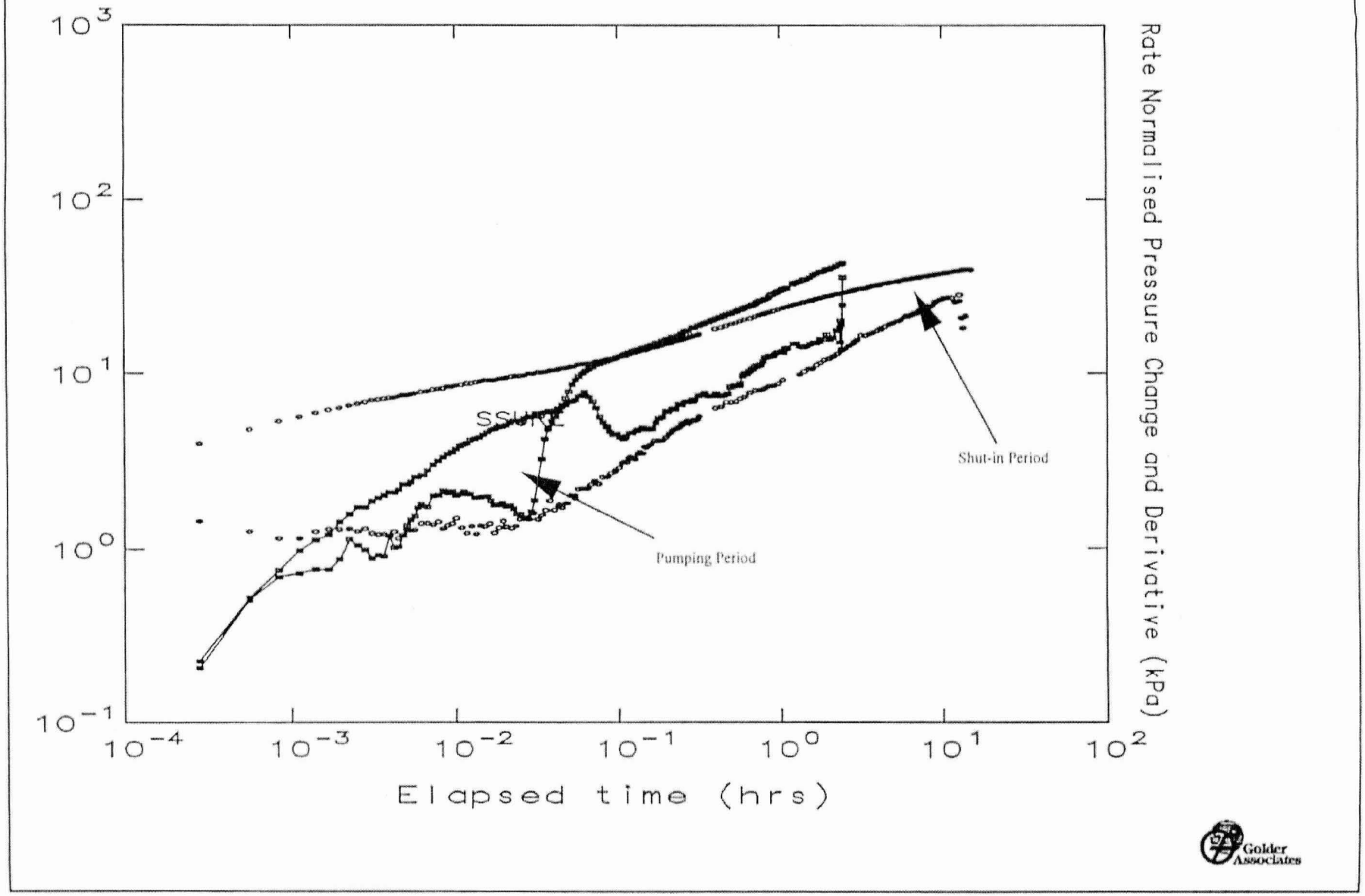

FIGURE 3-5C; TEST 6 IN BOREHOLE W205ARI; MULTI-PHASE DIAGNOSTIC PLOT

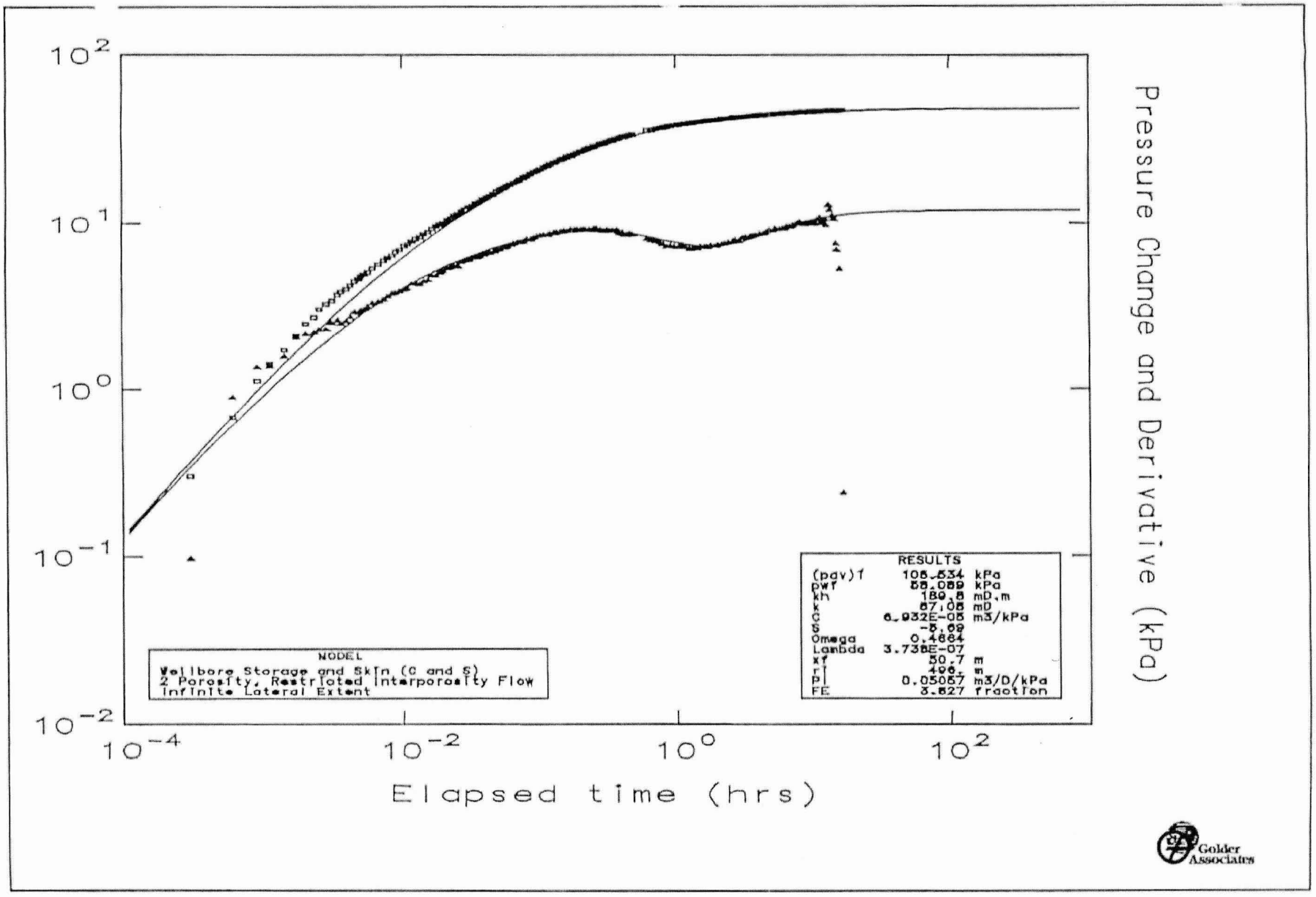

FIGURE 3-6; TEST 2 IN BOREHOLE W207I; SHUT-IN PHASE; LOG-LOG PLOT

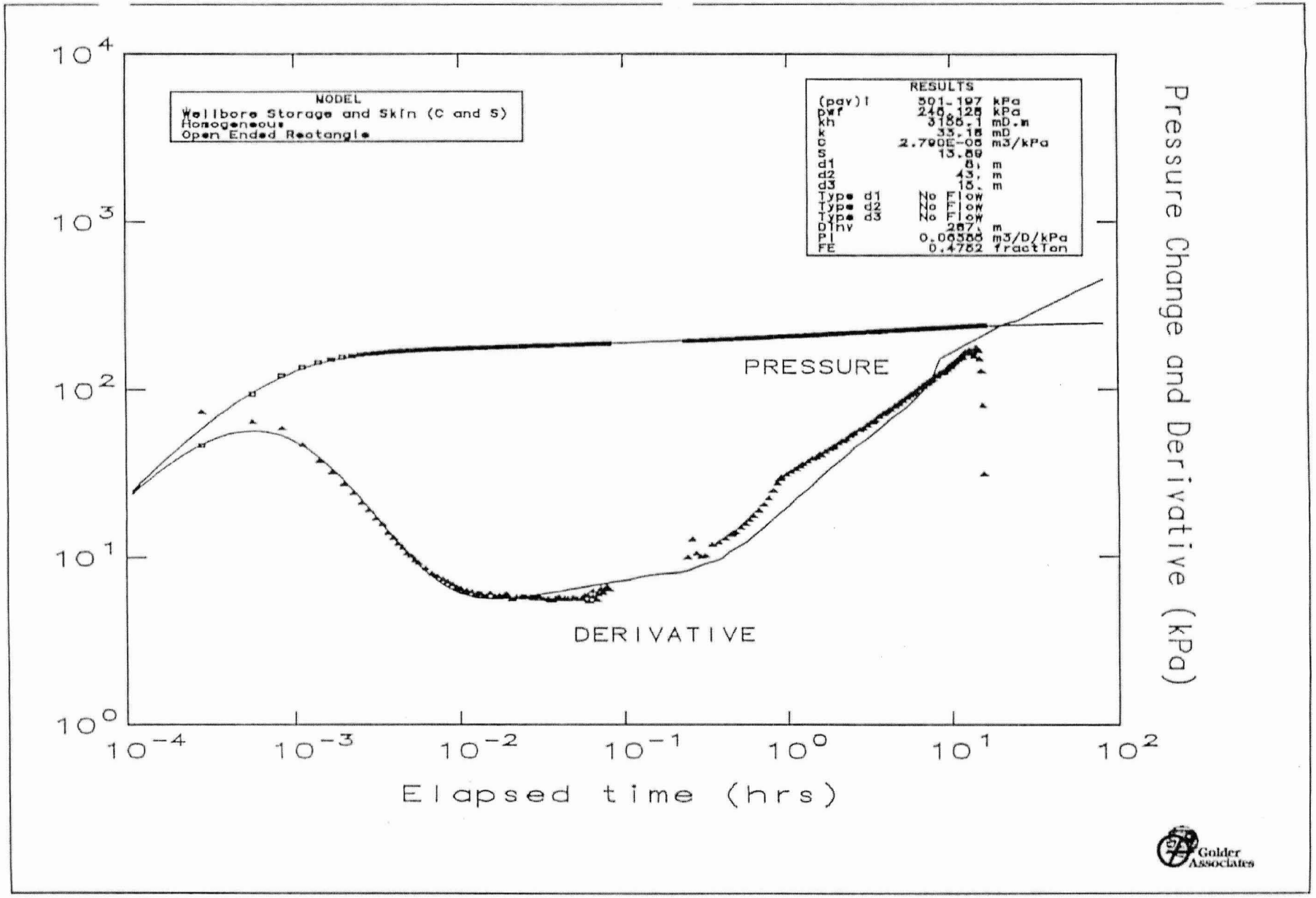

FIGURE 3-7; TEST 3 IN BOREHOLE W207ARI; SHUT-IN PHASE; LOG-LOG PLOT

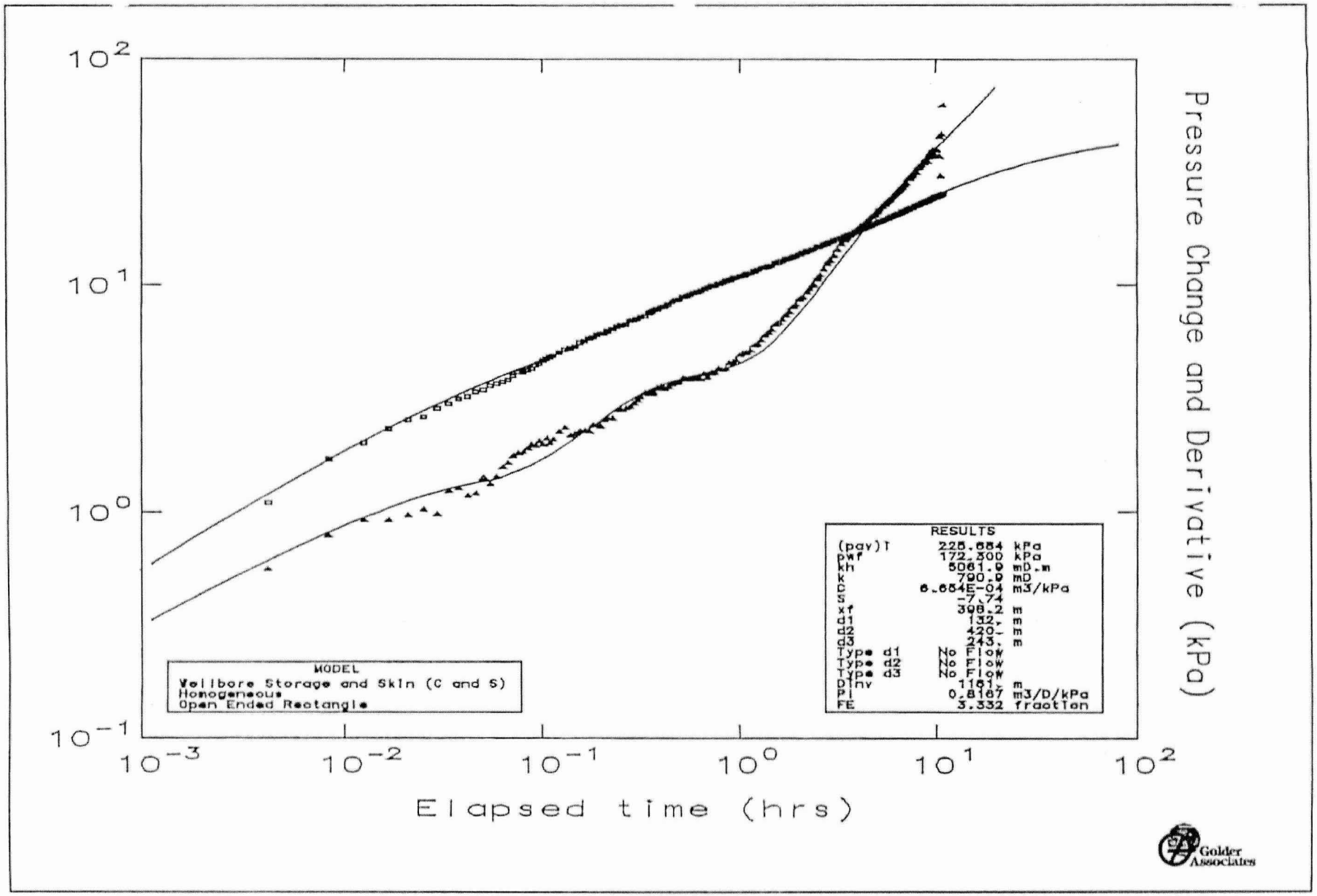

FIGURE 3-8; TEST 2 IN BOREHOLE W205ARI; SHUT-IN PHASE; LOG-LOG PLOT

Figure 4.2: Summary of Head Data for Borehole W203ARI

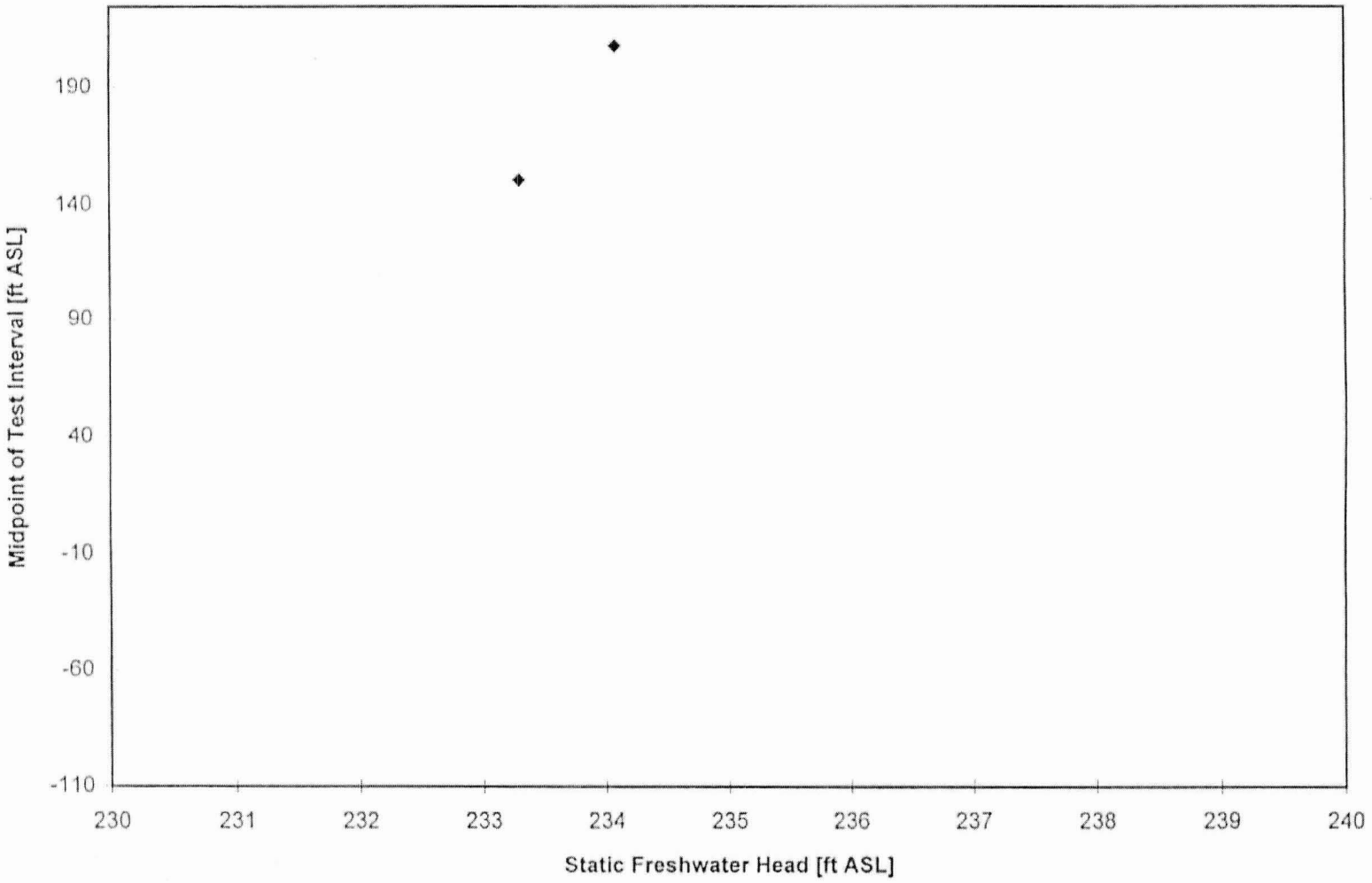

Figure 4-3: Summary of Head Data for Borehole W205ARI

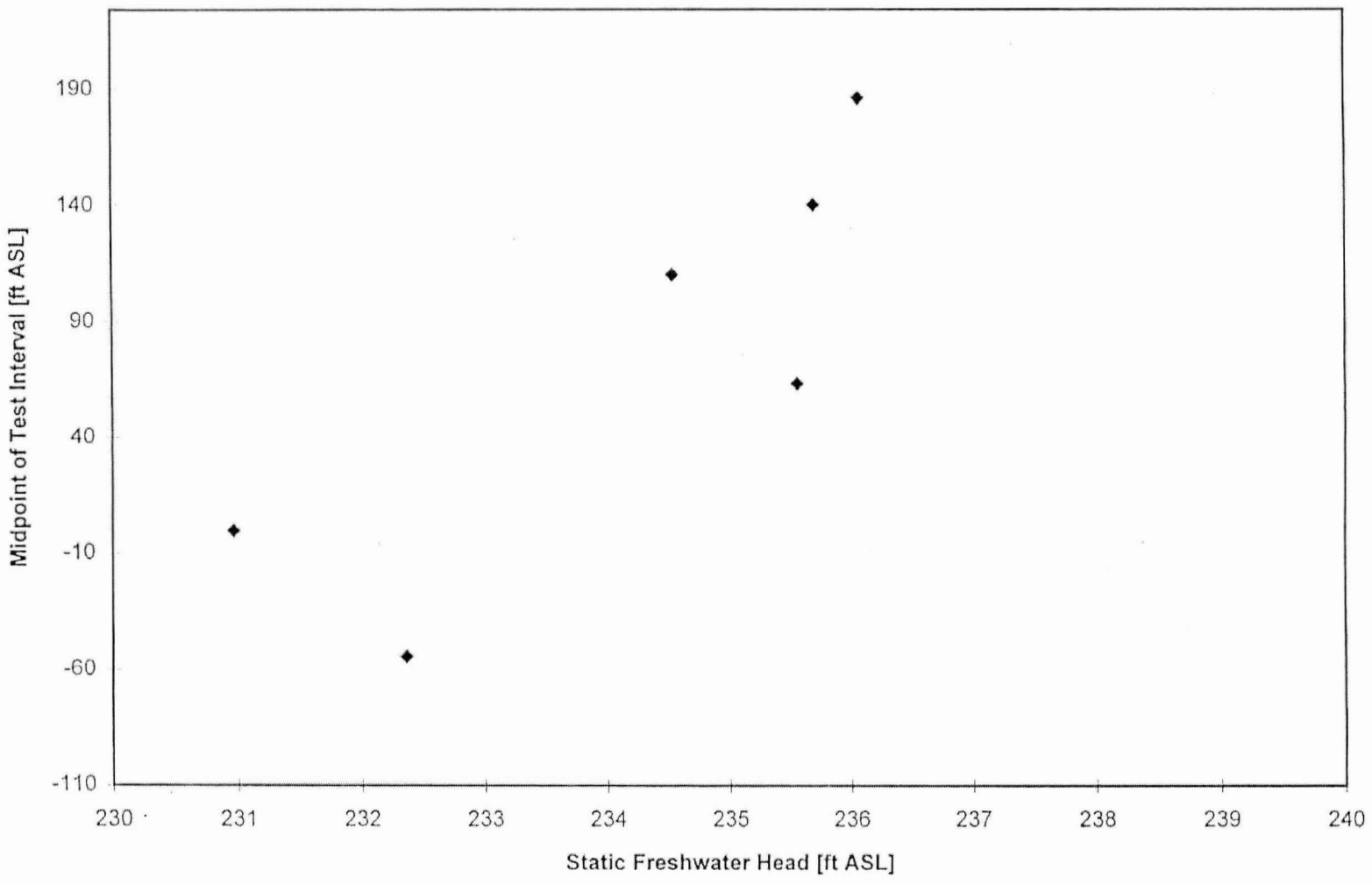

Figure 4-4: Summary of Head Data for Borehole W207ARI

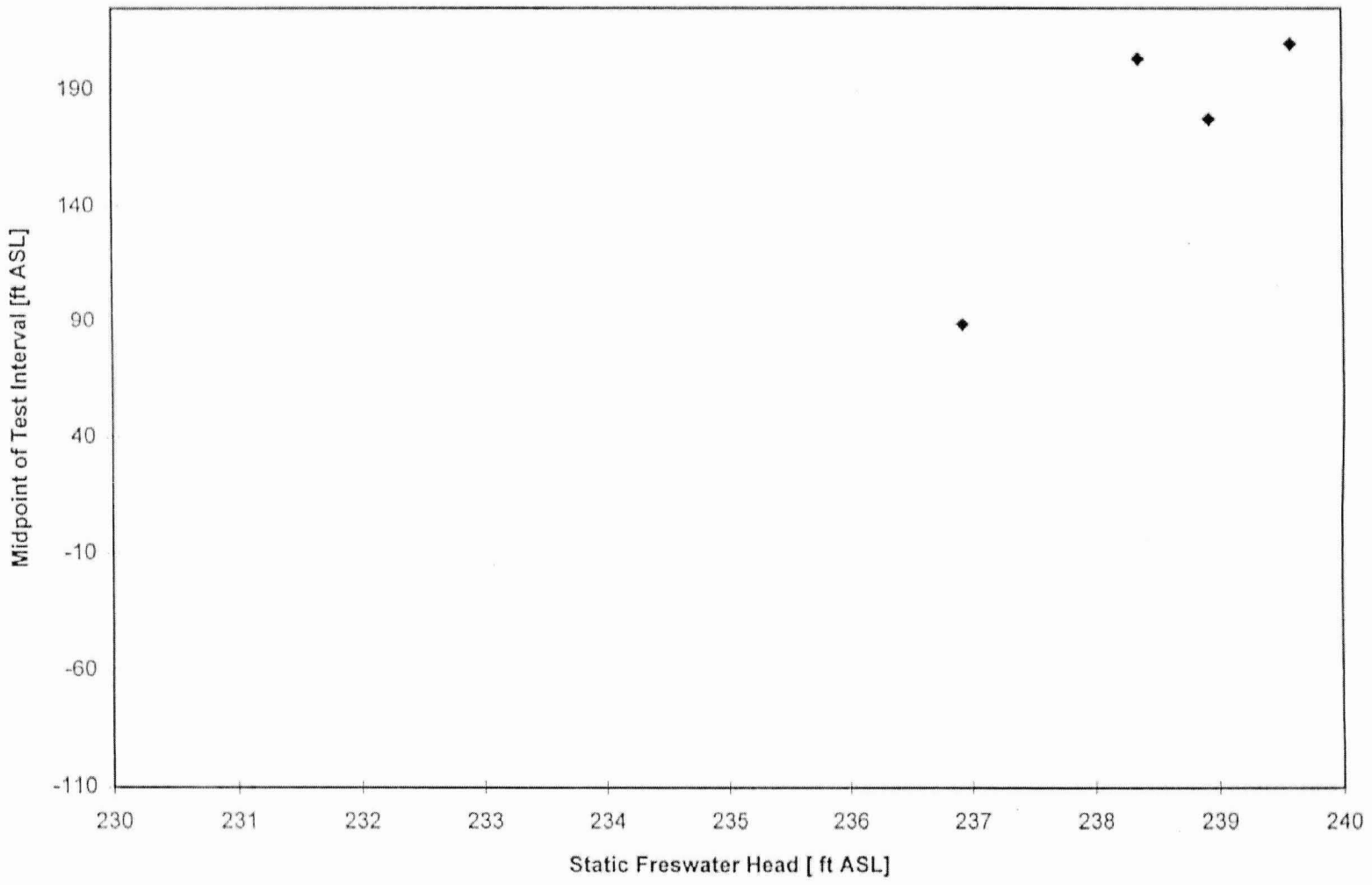

Appendix H

Geochemistry Data

Table H-1. Field Parameter Results for Time Series Plots Well W207AR1

NCLLRWDF
Wake County, North Carolina

Sample Description	Sample Date	Sample Time	Field Parameter pH	Temp (°C)	Specific Conductance (µS)	Pumping Rate (gpm)	Total Water Pumped (gal)
W207AR1/67.5-77.9	5/11/97	12:50	7.58	19.8	1845	NA	0
W207AR1/67.5-77.9	5/11/97	14:34	7.76	NR	NR	1.07	2.1
W207AR1/67.5-77.9	5/11/97	14:42	7.58	16.9	2580	1.07	10.7
W207AR1/67.5-77.9	5/11/97	14:45	7.55	16.9	2480	1.07	13.9
W207AR1/67.5-77.9	5/11/97	14:47	7.57	16.9	2550	1.07	16.1
W207AR1/67.5-77.9	5/11/97	15:08	7.62	NR	2540	0.45	17.0
W207AR1/67.5-77.9	5/11/97	15:10	7.68	18.9	2570	0.40	17.8
W207AR1/67.5-77.9	5/11/97	15:12	7.67	18.3	2620	0.30	18.4
W207AR1/67.5-77.9	5/11/97	15:14	7.65	18.3	2610	0.40	19.2
W207AR1/67.5-77.9	5/11/97	15:16	7.64	18.0	2610	0.40	20.0
W207AR1/67.5-77.9	5/11/97	15:18	7.63	17.8	2600	0.40	20.8
W207AR1/67.5-77.9	5/11/97	15:20	7.64	17.9	2580	0.40	21.6
W207AR1/67.5-77.9	5/11/97	15:22	7.64	17.9	2570	0.40	22.4
W207AR1/67.5-77.9	5/11/97	15:24	7.64	18.0	2550	0.40	23.2
W207AR1/67.5-77.9	5/11/97	15:26	7.67	17.9	2530	0.40	24.0
W207AR1/67.5-77.9	5/11/97	15:28	7.66	17.9	2520	0.40	24.8
W207AR1/67.5-77.9	5/11/97	15:30	7.67	17.7	2490	0.40	25.6
W207AR1/67.5-77.9	5/11/97	15:32	7.67	17.7	2480	0.40	26.4
W207AR1/67.5-77.9	5/11/97	15:34	7.68	17.9	2450	0.40	27.2
W207AR1/67.5-77.9	5/11/97	15:36	7.68	17.9	2420	0.40	28.0
W207AR1/67.5-77.9	5/11/97	15:38	7.69	17.9	2410	0.40	28.8
W207AR1/67.5-77.9	5/11/97	15:40	7.71	17.9	2390	0.40	29.6
W207AR1/67.5-77.9	5/11/97	15:42	7.71	17.8	2370	0.40	30.4
W207AR1/67.5-77.9	5/11/97	15:44	7.71	17.8	2350	0.40	31.2
W207AR1/67.5-77.9	5/11/97	15:46	7.73	17.8	2320	0.40	32.0
W207AR1/67.5-77.9	5/11/97	15:48	7.74	17.8	2290	0.40	32.8
W207AR1/67.5-77.9	5/11/97	15:50	7.74	17.8	2280	0.40	33.6
W207AR1/67.5-77.9	5/11/97	15:52	7.75	17.9	2260	0.40	34.4
W207AR1/67.5-77.9	5/11/97	15:54	7.75	17.8	2250	0.40	35.2
W207AR1/67.5-77.9	5/11/97	15:56	7.76	17.9	2230	0.40	36.0
W207AR1/67.5-77.9	5/11/97	15:58	7.77	17.9	2210	0.40	36.8
W207AR1/67.5-77.9	5/11/97	16:00	7.78	17.9	2200	0.40	37.6
W207AR1/67.5-77.9	5/11/97	16:05	7.75	17.9	2150	0.40	39.6
W207AR1/67.5-77.9	5/11/97	16:45	7.82	17.9	1936	0.40	55.5
W207AR1/67.5-77.9	5/11/97	16:50	7.89	17.9	1918	0.40	57.5
W207AR1/67.5-77.9	5/11/97	16:55	7.90	17.9	1908	0.40	59.5
W207AR1/67.5-77.9	5/11/97	17:00	7.91	17.9	1898	0.40	61.5

Table H-1. Field Parameter Results for Time Series Plots Well W207AR1

NCLLRWDF
Wake County, North Carolina

			Field Parameter				
Sample Description	Sample Date	Sample Time	pH	Temp (°C)	Specific Conductance (µS)	Pumping Rate (gpm)	Total Water Pumped (gal)
W207AR1/67.5-77.9	5/11/97	17:18	7.93	17.9	1845	0.40	68.7
W207AR1/153	5/12/97	16:55	8.02	16.6	1573	NR	15
W207AR1/153	5/12/97	17:00	8.19	16.8	1474	NR	30
W207AR1/153	5/12/97	17:05	8.28	16.6	1454	NR	45
W207AR1/153	5/12/97	17:10	8.31	16.8	1461	NR	60
W207AR1/153	5/12/97	17:15	8.31	16.7	1472	NR	75
W207AR1/153	5/12/97	17:25	8.29	16.7	1500	NR	91
W207AR1/153	5/12/97	17:30	8.29	16.7	1517	NR	104
W207AR1/153	5/12/97	17:35	8.29	16.7	1539	NR	138
W207AR1/153	5/12/97	17:45	8.31	16.7	1545	NR	170

NA - Not Applicable
NR - Not Recorded
°C- Degrees Centigrade
µS - Microsiems or micromhos
gal- Gallons of water produced total
gpm - Gallons per minute

Table H-2. Field Parameter Results for Time Series Plots Well W205ARI

NCLLRWDF
Wake County, North Carolina

Sample Description	Sample Date	Sample Time	Field Parameter pH	Temp (°C)	Specific Conductance (mS)	Total Water Pumped (gal)
W205AR1/118.1-139.1	5/16/97	12:15	8.61	18.4	166	3
W205AR1/145.18-166	5/16/97	15:47	8.81	17.6	261	9
W205AR1/145.18-166	5/16/97	15:54	8.27	16.6	804	31
W205AR1/145.18-166	5/16/97	15:57	8.29	16.7	794	36
W205AR1/145.18-166	5/16/97	15:59	8.31	16.8	796	39
W205AR1/145.18-166	5/16/97	16:01	8.30	16.9	780	49
W205AR1/145.18-166	5/16/97	16:06	8.25	16.9	777	71
W205AR1/145.18-166	5/16/97	16:11	8.29	16.9	771	83
W205AR1/145.18-166	5/16/97	16:16	8.27	16.9	771	102
W205AR1/145.18-166	5/16/97	16:21	8.29	16.9	771	118
W205AR1/145.18-166	5/16/97	16:27	8.28	17.0	767	136
W205AR1/145.18-166	5/16/97	16:31	8.25	17.0	767	149
W205AR1/145.18-166	5/16/97	16:36	8.25	17.0	764	172
W205AR1/145.18-166	5/16/97	16:54	8.25	17.0	759	221
W205AR1/145.18-166	5/16/97	17:00	8.25	17.0	757	247
W205AR1/145.18-166	5/16/97	17:10	8.32	17.0	755	268
W205AR1/145.18-166	5/16/97	17:15	8.28	17.0	754	288
W205AR1/148.2-169.2	5/16/97	18:30	8.29	16.9	757	36
W205AR1/148.2-169.2	5/16/97	18:44	8.27	17.6	763	94
W205AR1/148.2-169.2	5/16/97	18:55	8.27	16.8	743	166
W205AR1/148.2-169.2	5/16/97	19:00	8.23	16.5	737	216
W205AR1/148.2-169.2	5/16/97	19:09	8.23	16.5	737	275
W205AR1/148.2-169.2	5/16/97	19:21	8.21	16.5	736	373
W205AR1/148.2-169.2	5/16/97	19:30	8.20	16.5	734	447
W205AR1/148.2-169.2	5/16/97	19:41	8.15	16.4	732	522
W205AR1/148.2-169.2	5/16/97	19:52	8.16	16.2	728	613
W205AR1/148.2-169.2	5/16/97	20:01	8.21	16.3	730	664
W205AR1/148.2-169.2	5/16/97	20:13	8.20	16.2	730	807
W205AR1/148.2-169.2	5/16/97	20:26	8.20	16.1	729	884
W205AR1/148.2-169.2	5/16/97	20:36	8.23	16.3	730	934
W205AR1/148.2-169.2	5/16/97	20:41	8.29	16.3	730	NR
W205AR1/148.2-169.2	5/16/97	20:50	8.24	16.2	731	1098
W205AR1/148.2-169.2	5/16/97	21:10	8.25	16.2	732	1259
W205AR1/148.2-169.2	5/16/97	21:18	8.25	16.0	726	1332
W205AR1/148.2-169.2	5/16/97	21:32	8.23	16.2	730	1443
W205AR1/262.88-283.88	5/18/97	09:33	8.97	19.1	867	2
W205AR1/262.88-283.88	5/18/97	09:35	8.87	17.5	653	5
W205AR1/262.88-283.88	5/18/97	09:37	8.80	17.2	655	8
W205AR1/262.88-283.88	5/18/97	09:40	8.78	17.2	650	13

Table H-2. Field Parameter Results for Time Series Plots Well W205ARI

NCLLRWDF
Wake County, North Carolina

Sample Description	Sample Date	Sample Time	Field Parameter pH	Temp (°C)	Specific Conductance (mS)	Total Water Pumped (gal)
W205AR1/262.88-283.88	5/18/97	09:45	8.72	17.4	657	23
W205AR1/262.88-283.88	5/18/97	09:52	8.14	17.3	799	35
W205AR1/262.88-283.88	5/18/97	09:57	8.10	17.4	804	42
W205AR1/266.88-287.88	5/18/97	11:03	8.13	18.9	814	3
W205AR1/266.88-287.88	5/18/97	11:06	8.10	17.3	798	10
W205AR1/266.88-287.88	5/18/97	11:08	8.10	17.2	795	13
W205AR1/266.88-287.88	5/18/97	11:10	8.10	17.2	794	16
W205AR1/266.88-287.88	5/18/97	11:13	8.12	17.3	794	22
W205AR1/266.88-287.88	5/18/97	11:20	8.10	17.4	822	37
W205AR1/266.88-287.88	5/18/97	11:25	8.09	17.5	808	46
W205AR1/266.88-287.88	5/18/97	11:30	8.23	17.5	792	59
W205AR1/266.88-287.88	5/18/97	11:35	8.17	17.6	791	68
W205AR1/266.88-287.88	5/18/97	11:40	8.17	18.2	784	77
W205AR1/266.88-287.88	5/18/97	11:47	8.27	17.5	780	91
W205AR1/266.88-287.88	5/18/97	11:55	8.30	17.5	775	107
W205AR1/266.88-287.88	5/18/97	12:00	8.30	17.4	773	117
W205AR1/266.88-287.88	5/18/97	12:06	8.33	17.4	769	131
W205AR1/266.88-287.88	5/18/97	12:10	8.34	17.5	769	140
W205AR1/266.88-287.88	5/18/97	12:15	8.36	17.5	768	148
W205AR1/266.88-287.88	5/18/97	12:20	8.33	17.6	770	158
W205AR1/266.88-287.88	5/18/97	12:25	8.35	17.5	767	167
W205AR1/266.88-287.88	5/18/97	12:30	8.35	17.7	769	178
W205AR1/266.88-287.88	5/18/97	12:35	8.37	17.6	767	187
W205AR1/266.88-287.88	5/18/97	12:40	8.35	17.5	765	198
W205AR1/266.88-287.88	5/18/97	12:45	8.31	17.7	765	209
W205AR1/266.88-287.88	5/18/97	12:52	8.30	17.7	764	221
W205AR1/266.88-287.88	5/18/97	12:58	8.36	18.2	763	234
W205AR1/266.88-287.88	5/18/97	13:06	8.31	17.7	763	253
W205AR1/266.88-287.88	5/18/97	13:15	8.39	17.6	763	267
W205AR1/266.88-287.88	5/18/97	13:20	8.40	17.7	764	282
W205AR1/266.88-287.88	5/18/97	13:25	8.34	17.5	761	289
W205AR1/266.88-287.88	5/18/97	13:30	8.36	17.5	762	298
W205AR1/301-715	5/17/97	17:55	8.12	19.1	568	32
W205AR1/301-715	5/17/97	17:59	8.71	17.9	561	52
W205AR1/301-715	5/17/97	18:01	8.85	17.9	566	61
W205AR1/301-715	5/17/97	18:03	8.89	17.5	572	72
W205AR1/301-715	5/17/97	18:05	8.84	17.4	571	82
W205AR1/301-715	5/17/97	18:39	7.98	17.8	700	108
W205AR1/301-715	5/17/97	18:42	8.37	17.4	592	114
W205AR1/301-715	5/17/97	18:44	8.47	17.3	582	123

Table H-2. Field Parameter Results for Time Series Plots Well W205AR1

NCLLRWDF
Wake County, North Carolina

Sample Description	Sample Date	Sample Time	Field Parameter pH	Temp (°C)	Specific Conductance (mS)	Total Water Pumped (gal)
W205AR1/301-715	5/17/97	18:47	8.52	17.5	601	131
W205AR1/301-715	5/17/97	18:49	8.55	17.5	605	143
W205AR1/301-715	5/17/97	18:54	8.56	17.7	619	167
W205AR1/301-715	5/17/97	18:59	8.57	17.6	621	195
W205AR1/301-715	5/17/97	19:04	8.59	17.6	634	216
W205AR1/301-715	5/17/97	19:09	8.94	17.4	648	247
W205AR1/301-715	5/17/97	19:13	8.96	17.5	653	272
W205AR1/301-715	5/17/97	19:25	8.91	17.4	669	323
W205AR1/301-715	5/17/97	19:30	9.00	17.4	673	346
W205AR1/301-715	5/17/97	19:37	8.99	17.4	678	384
W205AR1/301-715	5/17/97	19:45	9.00	17.4	684	417
W205AR1/301-715	5/17/97	19:51	9.04	17.3	688	453
W205AR1/301-715	5/17/97	19:56	9.06	17.3	690	476
W205AR1/301-715	5/17/97	20:01	9.08	17.3	691	502
W205AR1/301-715	5/17/97	20:07	9.10	17.3	693	534
W205AR1/301-715	5/17/97	20:11	9.12	17.2	694	547
W205AR1/301-715	5/17/97	20:16	9.13	17.3	695	578
W205AR1/301-715	5/17/97	20:23	9.16	17.2	696	611
W205AR1/301-715	5/17/97	20:30	9.18	17.2	696	637
W205AR1/301-715	5/17/97	20:35	9.21	17.3	698	666
W205AR1/301-715	5/17/97	20:36	9.23	17.3	698	677
W205AR1/313-334	5/17/97	14:59	8.56	17.3	882	6
W205AR1/313-334	5/17/97	15:01	8.69	17.3	857	8
W205AR1/313-334	5/17/97	15:03	9.08	17.5	782	11
W205AR1/313-334	5/17/97	15:06	8.79	17.4	713	15
W205AR1/313-334	5/17/97	15:08	9.24	17.4	691	17
W205AR1/313-334	5/17/97	15:11	8.79	17.1	616	24
W205AR1/313-334	5/17/97	15:13	8.70	17.2	585	28
W205AR1/313-334	5/17/97	15:15	8.74	17.3	553	32
W205AR1/313-334	5/17/97	15:17	8.74	17.3	560	37
W205AR1/313-334	5/17/97	15:19	8.73	17.3	561	39
W205AR1/313-334	5/17/97	15:21	8.55	17.4	586	44

NA - Not Applicable
NR - Not Recorded
°C- Degrees Centigrade
µS - Microsiems or micromhos
gal- Gallons of water produced total
gpm - Gallons per minute

Table H-3. Summary of Data Qualifiers Based on Charge Calculations

NCLLRWDF
Wake County, North Carolina

Sample Designation	Sample Date	Total Cations (meq/l)	Total Anions (meq/l)	Charge Balance (%)	Data Qualifier
1993 GroundWater Results					
W10MC13	3/8/93	1.09	0.96	6.10%	CBE
W10MC15	3/17/93	7.48	7.37	0.75%	
W11MC28	2/22/93	43.08	32.14	14.55%	CBR
W11MC29	2/22/93	38.08	34.51	4.92%	
W12MC24	3/4/93	53.24	56.69	-3.13%	
W13MC19	3/8/93	75.54	77.22	-1.10%	
W13MC20	3/8/93	43.09	47.99	-5.38%	CBE
W16DB4	2/23/93	9.21	9.10	0.64%	
W16OW33	2/23/93	15.42	16.41	-3.11%	
W16OW37	2/23/93	12.27	12.02	1.06%	
W16OW39	2/23/93	8.89	9.36	-2.62%	
W160W41	2/23/93	8.30	7.88	2.61%	
W160W44	2/23/93	15.49	16.05	-1.78%	
W18OW7	3/10/93	7.71	7.40	2.08%	
W2DC4	3/4/93	3.75	3.41	4.68%	
W2DC5	3/11/93	3.99	3.29	9.64%	CBE
W31DC10	3/9/93	7.39	7.10	1.98%	
W31DC9	3/8/93	22.21	21.47	1.69%	
W32MC41	3/7/93	7.40	6.95	3.18%	
W3MC4	3/10/93	2.56	2.06	10.75%	CBR
W3MC6	3/9/93	8.46	7.87	3.62%	
W4MC2	2/23/93	24.46	25.77	-2.60%	
W4MC3	2/24/93	81.31	87.76	-3.82%	
W52SW26	3/8/93	28.07	27.94	0.22%	
W6SW51	3/10/93	55.00	56.98	-1.77%	
W7MC8	3/10/93	68.73	71.25	-1.80%	
W7MC9	3/11/93	31.63	208.96	-73.71%	CBR
W8MC10	2/22/93	3.99	3.81	2.23%	
W8MC11	2/23/93	4.32	3.90	5.06%	CBE
W9MC31	3/8/93	23.23	21.93	2.90%	
W9MC32	3/10/93	7.90	7.57	2.13%	
1995 Drainage Study Results					
W10MC13	7/18/95	1.17	1.61	-15.65%	CBR
W10MC14	7/18/95	7.67	7.08	4.01%	
W10MC15	7/18/95	8.12	8.69	-3.35%	
W12MC24	7/18/95	51.59	57.53	-5.44%	CBE
W12MC25	7/18/95	55.98	62.82	-5.76%	CBE
W13MC20	7/18/95	44.88	45.48	-0.67%	
W32MC41	7/18/95	7.44	7.76	-2.12%	
W33SW13	7/18/95	5.88	6.10	-1.86%	
W3MC4	7/18/95	2.56	2.06	10.75%	CBR
W3MC5	7/18/95	6.70	7.11	-2.97%	
W3MC6	7/18/95	8.04	9.06	-5.95%	CBE
W52SW26	7/18/95	19.64	21.91	-5.45%	CBE

Table H-3. Summary of Data Qualifiers Based on Charge Calculations

NCLLRWDF
Wake County, North Carolina

Sample Designation	Sample Date	Total Cations (meq/l)	Total Anions (meq/l)	Charge Balance (%)	Data Qualifier
W6MC34	7/18/95	25.26	25.92	-1.28%	
W7MC7	7/18/95	39.56	48.15	-9.79%	CBE
W13MC19	7/25/95	61.24	67.47	-4.84%	
W31DC10	7/25/95	6.82	6.22	4.61%	
W31DC9	7/25/95	34.93	36.72	-2.51%	
W7MC8	7/25/95	64.48	69.18	-3.51%	
W80W99	7/25/95	24.26	24.56	-0.62%	
W9MC31	7/25/95	17.19	17.06	0.36%	
W101SW47	11/18/95	44.02	46.66	-2.90%	
W103MC49	11/18/95	7.47	7.82	-2.26%	
W103OW90	11/18/95	7.11	3.91	28.99%	CBR
W103OW93	11/18/95	13.70	14.54	-2.97%	
W103SW129	11/18/95	25.40	19.56	13.00%	CBR
W106SW50	11/18/95	22.03	23.55	-3.35%	
W119SW52	11/18/95	1.32	2.23	-25.63%	CBR
W119SW53	11/18/95	2.05	2.29	-5.61%	CBE
W120SW56	11/16/95	40.36	44.67	-5.08%	CBE
W121SW58	11/18/95	30.87	32.64	-2.78%	
W122SW62	11/16/95	1.92	10.18	-68.32%	CBR
W122SW63	11/16/95	27.80	31.47	-6.18%	CBE
W123MC45	11/18/95	6.64	5.92	5.72%	CBE
W123SW69	11/18/95	42.18	43.08	-1.07%	
W124SW46	11/19/95	8.52	7.80	4.46%	
W124SW73	11/19/95	47.80	53.39	-5.52%	CBE
W125SW80	11/16/95	7.22	8.29	-6.89%	CBE
W125SW82	11/16/95	43.09	46.69	-4.01%	
W125SW84	11/16/95	12.59	14.59	-7.36%	CBE
W125SW86	11/16/95	44.24	49.46	-5.57%	CBE
W125SW89	11/17/95	57.57	66.84	-7.46%	CBE
W125SW97	11/17/95	10.50	12.38	-8.25%	CBE
W126SW94	11/17/95	63.44	69.89	-4.84%	
W126SW95	11/17/95	65.55	104.81	-23.04%	CBR
W126SW96	11/17/95	52.43	56.01	-3.30%	
W126SW99	11/17/95	37.32	41.39	-5.17%	CBE
W127SW104	11/16/95	25.61	17.61	18.49%	CBR
W128SW108	11/17/95	10.87	8.59	11.72%	CBR
W130MC50	11/20/95	5.57	5.41	1.42%	
W130SW115	11/19/95	29.06	28.77	0.49%	
W131SW122	11/16/95	75.75	85.59	-6.10%	CBE
W132SW123	11/16/95	44.46	49.88	-5.75%	CBE
W132SW124	11/16/95	4.20	4.17	0.34%	
W21MC47	11/17/95	6.27	5.71	4.66%	
W21SW113	11/17/95	65.20	67.19	-1.50%	
W21SW114	11/17/95	34.47	38.42	-5.42%	CBE
W25SW67	11/18/95	12.79	13.38	-2.26%	
W37SW17	11/17/95	31.67	38.99	-10.36%	CBR

Table H-3. Summary of Data Qualifiers Based on Charge Calculations

NCLLRWDF
Wake County, North Carolina

Sample Designation	Sample Date	Total Cations (meq/l)	Total Anions (meq/l)	Charge Balance (%)	Data Qualifier
W38SW18	11/17/95	10.96	15.05	-15.71%	CBR
W21MC47	11/17/95	6.27	5.71	4.66%	
W21SW113	11/17/95	65.20	67.19	-1.50%	
W21SW114	11/17/95	34.47	38.42	-5.42%	CBE
W25SW67	11/18/95	12.79	13.38	-2.26%	
W37SW17	11/17/95	31.67	38.99	-10.36%	CBR
W38SW18	11/17/95	10.96	15.05	-15.71%	CBR
W6SW77	11/19/95	54.56	57.32	-2.47%	
W94OW84	11/19/95	34.33	38.30	-5.47%	CBE
W94OW85	11/19/95	19.55	17.81	4.64%	
W94SW40	11/19/95	31.90	34.69	-4.20%	
1997 GroundWater Results					
PRODUCTION-01	4/21/97	5.91	4.85	9.82%	CBE
PRODUCTION-02	4/21/97	5.81	5.10	6.49%	CBE
W103MC49	5/8/97	7.42	6.99	3.01%	
W103SW129	5/1/97	17.72	11.98	19.32%	CBR
W106SW50	4/30/97	21.66	19.58	5.05%	CBE
W119SW52	4/30/97	1.42	0.95	19.63%	CBR
W119SW54	5/8/97	0.003	0.13	-95.31%	CBR
W119SW54	5/8/97	2.50	2.70	-3.94%	
W120SW56	4/30/97	26.75	41.70	-21.84%	CBR
W122SW62	4/24/97	1.56	1.27	10.38%	CBR
W123SW68	5/1/97	1.59	4.99	-51.77%	CBR
W123SW69	5/1/97	22.08	19.75	5.56%	CBE
W124SW73	4/30/97	50.81	53.65	-2.72%	
W125SW82	4/24/97	55.43	55.06	0.34%	
W125SW83	4/24/97	26.05	22.12	8.16%	CBE
W126SW94	4/24/97	74.24	65.76	6.05%	CBE
W126SW95	4/24/97	67.91	58.68	7.29%	CBE
W130MC50	5/1/97	6.49	6.81	-2.42%	
W130SW115	5/1/97	30.94	34.17	-4.95%	
W132SW123	5/1/97	44.19	45.90	-1.89%	
W21SW113	4/24/97	62.66	87.35	-16.46%	CBR
W21SW3	4/24/97	0.78	0.54	17.56%	CBR
W32MC39	5/7/97	2.62	2.38	4.69%	
W32MC40	5/7/97	6.44	5.96	3.85%	
W37SW17	4/30/97	45.31	40.34	5.80%	CBE
W6SW76	4/24/97	20.00	18.33	4.37%	
W7MC8	5/1/97	60.97	80.46	-13.78%	CBR
W8MC10	4/30/97	5.36	4.53	8.44%	CBE
W8MC11	4/30/97	3.63	2.87	11.71%	CBR
W8OW50	5/7/97	2.75	5.33	-31.93%	CBR
W94OW84	5/7/97	42.03	41.22	0.96%	
W94OW85	5/7/97	18.54	19.57	-2.70%	

Table H-3. Summary of Data Qualifiers Based on Charge Calculations

NCLLRWDF
Wake County, North Carolina

Sample Designation	Sample Date	Total Cations (meq/l)	Total Anions (meq/l)	Charge Balance (%)	Data Qualifier
Packer Test Ground Water					
W202AR1-1	5/20/97	5.05	10.17	-33.63%	CBR
W201AR1B-44.58-65.08	5/15/97	15.80	15.56	0.75%	
W203AR1-117-126.4-1	5/21/97	2.11	2.22	-2.61%	
W203AR1-117-126.4-2	5/21/97	1.98	1.94	1.11%	
W203AR1-58-67.4-1	5/21/97	1.88	1.96	-2.13%	
W203AR1-61-70.4-1	5/21/97	2.26	2.41	-3.17%	
W204AR1-1	5/20/97	1.20	1.17	1.39%	
W204AR1-2	5/20/97	1.20	1.21	-0.57%	
W205AR1-118.1-139.1-1	5/19/97	7.37	7.74	-2.50%	
W205AR1-145.18-166-1	5/16/97	2.93	3.06	-2.04%	
W205AR1-145.18-166-2	5/16/97	8.42	7.73	4.29%	
W205AR1-145.18-166-3	5/16/97	8.20	8.04	1.04%	
W205AR1-145.18-166-4	5/16/97	8.23	8.22	0.11%	
W205AR1-148.2-169.2-1	5/16/97	8.40	7.09	8.43%	CBE
W205AR1-148.2-169.2-2	5/16/97	8.36	7.44	5.83%	CBE
W205AR1-148.2-169.2-3	5/16/97	8.08	7.49	3.80%	
W205AR1-148.2-169.2-4	5/16/97	8.02	7.59	2.81%	
W205AR1-148.2-169.2-5	5/16/97	8.12	7.59	3.43%	
W205AR1-148.2-169.2-6	5/16/97	7.84	7.47	2.39%	
W205AR1-195.6-216.6-1	5/19/97	7.12	6.99	0.92%	
W205AR1-262.88-283.88-1	5/18/97	6.11	5.75	3.04%	
W205AR1-262.88-283.88-2	5/18/97	6.08	6.08	-0.07%	
W205AR1-266.88-287.88-1	5/18/97	7.56	7.54	0.14%	
W205AR1-266.88-287.88-2	5/18/97	7.74	7.30	2.92%	
W205AR1-266.88-287.88-3	5/18/97	7.27	7.05	1.53%	
W205AR1-266.88-287.88-4	5/18/97	7.16	7.14	0.15%	
W205AR1-266.88-287.88-5	5/18/97	6.96	7.18	-1.56%	
W205AR1-266.88-287.88-6	5/18/97	6.95	7.08	-0.88%	
W205AR1-266.88-287.88-7	5/18/97	7.09	7.10	-0.05%	
W205AR1-301-715-1	5/17/97	5.21	4.79	4.14%	
W205AR1-301-715-2	5/17/97	5.31	5.14	1.62%	
W205AR1-301-715-3	5/17/97	5.72	5.67	0.44%	
W205AR1-301-715-4	5/17/97	5.76	5.90	-1.26%	
W205AR1-301-715-5	5/17/97	6.04	5.91	1.09%	
W205AR1-301-715-6	5/17/97	6.12	5.82	2.49%	
W205AR1-313-334-1	5/17/97	6.90	6.28	4.71%	
W205AR1-313-334-2	5/17/97	5.03	4.85	1.80%	
W205AR1-71.98-92.98-1	5/19/97	8.74	9.60	-4.71%	
W119SW52-118-23	5/20/97	0.72	0.84	-7.41%	CBE
W119SW52-136-19	5/20/97	0.53	0.98	-29.47%	CBR
W119SW52-152-20	5/14/97	0.52	1.72	-53.89%	CBR
W119SW52-162-85	5/14/97	0.57	0.73	-12.04%	CBR
W205AR1-71.98-92.98-2	5/19/97	9.81	10.63	-4.03%	
W206AR1-42-57	5/14/97	5.33	4.73	5.93%	CBE
W207AR1-153-3	5/12/97	11.87	11.64	0.98%	

Table H-3. Summary of Data Qualifiers Based on Charge Calculations

NCLLRWDF
Wake County, North Carolina

Sample Designation	Sample Date	Total Cations (meq/l)	Total Anions (meq/l)	Charge Balance (%)	Data Qualifier
W207AR1-153-4	5/12/97	13.06	11.98	4.32%	
W207AR1-153-5	5/12/97	13.93	12.18	6.69%	CBE
W207AR1-156-166-1	5/12/97	13.15	13.12	0.11%	
W207AR1-67.5-77.9-1	5/11/97	17.24	15.73	4.57%	
W207AR1-67.5-77.9-2	5/11/97	19.42	17.93	3.99%	
W207AR1-67.5-77.9-3	5/11/97	17.52	16.88	1.85%	
W207AR1-67.5-77.9-4	5/11/97	17.25	16.41	2.50%	
W207AR1-67.5-77.9-5	5/11/97	15.94	11.49	16.21%	CBR
1997 Surface Water Results					
CHURCH CREEK-01	4/23/97	0.28	0.20	16.50%	CBR
CHURCH CREEK-03	4/23/97	0.35	0.20	27.28%	CBR
CHURCH CREEK-170-20	5/20/97	0.93	0.85	4.09%	
I1-01	5/4/97	0.27	0.28	-1.47%	
I5-05-92.7	5/4/97	0.30	0.29	2.10%	
I7-07-149.2	5/4/97	0.31	0.34	-5.29%	CBE
W103OW79-270-62.4	5/5/97	0.30	0.20	18.75%	CBR
W103OW79-274-100.2	5/5/97	0.29	0.23	12.20%	CBR
W103OW79-XX-164	5/5/97	0.31	0.19	24.15%	CBR
W103OW93-142-104	5/5/97	0.30	0.16	29.55%	CBR
W103OW93-142-52	5/5/97	0.18	0.15	8.66%	CBE
W103OW93-298-115	5/5/97	0.29	0.29	-0.73%	
W103SW129-220-19.5	5/5/97	0.31	0.26	9.39%	CBE
W119SW52-168-19	5/20/97	0.54	1.26	-39.50%	CBR
W119SW52-178-20	5/20/97	0.53	1.64	-50.83%	CBR
W119SW52-63-90	5/20/97	0.51	0.68	-14.44%	CBR
W119SW52-72-35	5/20/97	0.60	1.93	-52.67%	CBR
W121SW58-XX-XX	4/22/97	0.23	0.28	-8.57%	CBE
W122SW62-56-12.3	5/4/97	0.35	0.20	25.57%	CBR
W122SW62-56-12.3	4/24/97	0.35	0.43	-10.32%	CBR
W122SW62-76-14.8	5/4/97	0.33	0.25	14.16%	CBR
W122SW62-76-14.8	4/24/97	0.34	0.27	11.39%	CBR
W125SW80-334-66	4/21/97	0.58	0.45	12.95%	CBR
W125SW82-50-50	5/12/97	0.68	0.72	-2.69%	
W125SW82-50-50	5/12/97	0.72	0.74	-1.50%	
W126SW94-280-125	5/12/97	3.64	3.25	5.71%	CBE
W126SW94-290-17	5/12/97	1.74	1.67	2.04%	
W126SW97-54-48	4/23/97	0.77	0.59	13.18%	CBR
W127SW104-36-125	5/5/97	0.32	0.29	5.62%	CBE
W130SW115-146-80	5/6/97	0.28	0.18	22.32%	CBR
W130SW115-202-13	5/6/97	0.27	0.17	23.81%	CBR
W130SW115-264-35	5/6/97	0.37	0.30	9.32%	CBE
W130SW115-XX-160	5/6/97	0.27	0.23	6.44%	CBE
W132SW123-210-30	5/12/97	0.53	0.62	-7.92%	CBE
W132SW123-310-350	5/12/97	5.43	4.62	8.07%	CBE
W19SW52-XX-XX	4/22/97	0.25	0.18	15.34%	CBR

Table H-3. Summary of Data Qualifiers Based on Charge Calculations

NCLLRWDF
Wake County, North Carolina

Sample Designation	Sample Date	Total Cations (meq/l)	Total Anions (meq/l)	Charge Balance (%)	Data Qualifier
W205CH1-XX-XX	4/21/97	0.52	1.21	-39.89%	CBR
W21SW113-262-385	5/12/97	0.39	0.31	11.84%	CBR
W21SW113-88-110	5/12/97	0.29	0.44	-20.27%	CBR
W22SW4-280-33	5/12/97	1.26	1.18	3.25%	
W25SW66-208-164	4/27/97	0.67	0.60	6.00%	CBE
W25SW66-322-152	4/27/97	1.08	2.36	-37.35%	CBR
W25SW66-328-67	4/27/97	1.14	1.27	-5.34%	CBE
W37SW17-XX-XX	4/22/97	0.51	0.42	10.03%	CBR
W37SW17-XX-XX	4/28/97	0.32	0.19	25.88%	CBR
W37SW17-XX-XX	4/30/97	0.32	0.36	-6.07%	CBE
W94MC48-220-32.2	5/6/97	0.50	0.50	-0.69%	
W94MC48-296-36	5/6/97	0.23	0.36	-20.94%	CBR

meq/l milliequivalents/liter

CBE Estimated Value due to charge balance considerations, not to ba used in quantitative evaluation.

CBR Estimated Value due to charge balance considerations, to be used only for descriptive purposes.

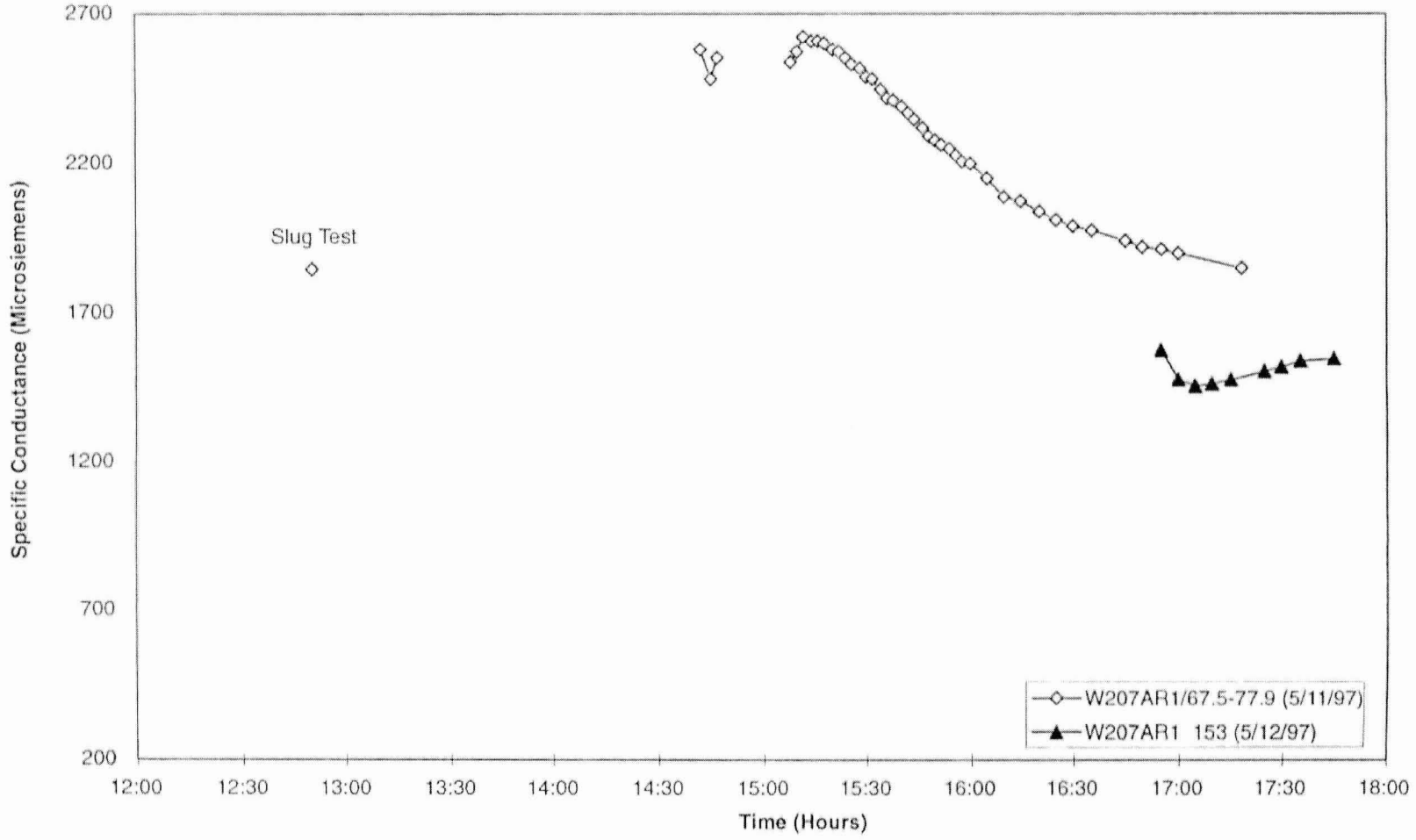

NCLL_4b 9-25-97 GEA

Harding Lawson Associates
Engineering and
Environmental Services

Specific Conductance Versus Time for Well W207AR1
North Carolina Low-Level Radioactive
Waste Disposal Facility Project
Wake County, North Carolina

FIGURE
H-1

DRAWN	JOB NUMBER	APPROVED	DATE	REVISED DATE
LDZ	36595,301	RAH	9/97	

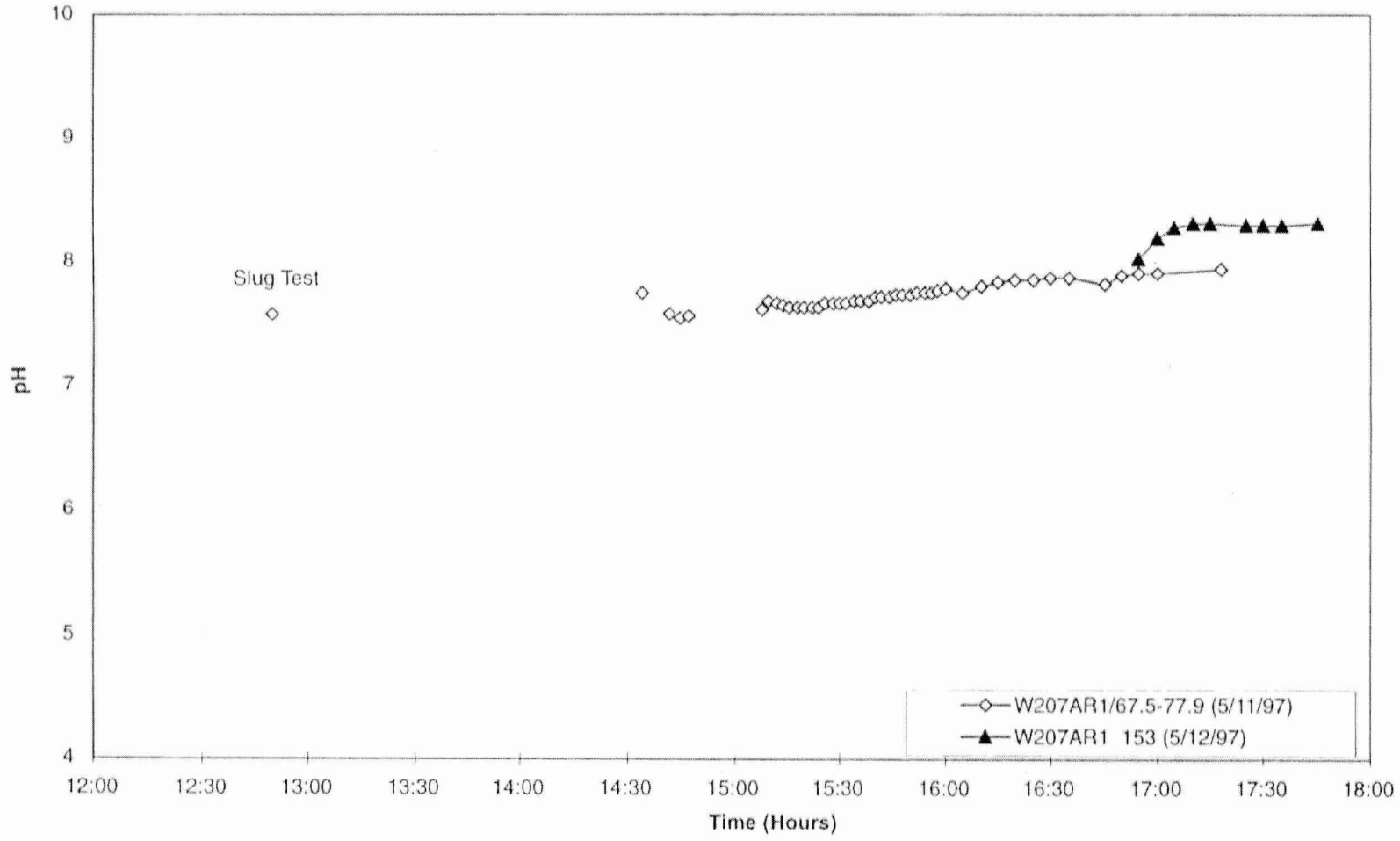

Harding Lawson Associates
Engineering and
Environmental Services

pH Versus Time for Well W207AR1
North Carolina Low-Level Radioactive
Waste Disposal Facility Project
Wake County, North Carolina

FIGURE
H-2

DRAWN	JOB NUMBER	APPROVED	DATE	REVISED DATE
LDZ	36595,301	RAH	9/97	

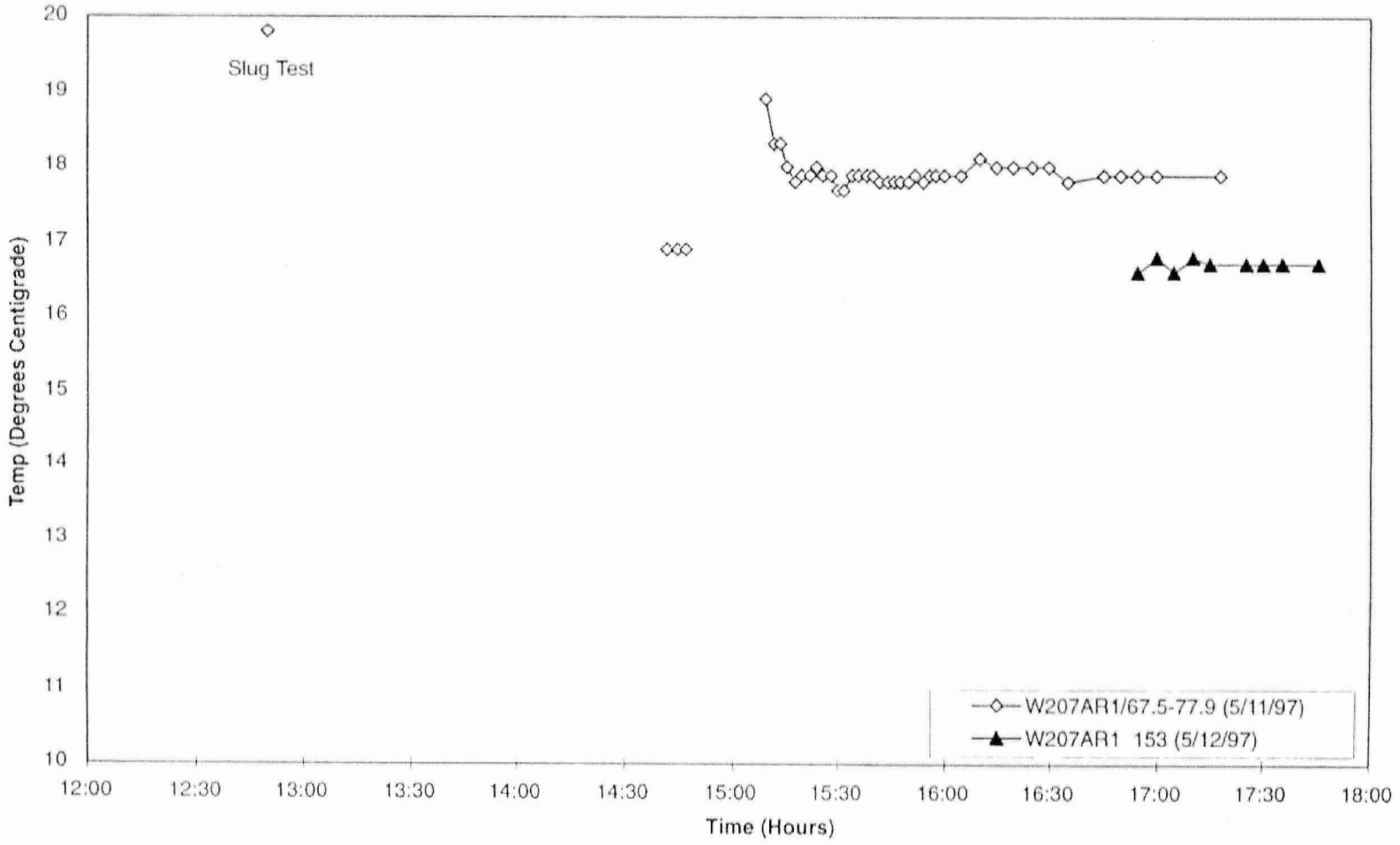

Harding Lawson Associates
Engineering and
Environmental Services

Temperature Versus Time for Well W207AR1
North Carolina Low-Level Radioactive
Waste Disposal Facility Project
Wake County, North Carolina

FIGURE
H-3

DRAWN	JOB NUMBER	APPROVED	DATE	REVISED DATE
LDZ	36595,301	RAH	9/97	

NCLL_41 9/25/97 GEA

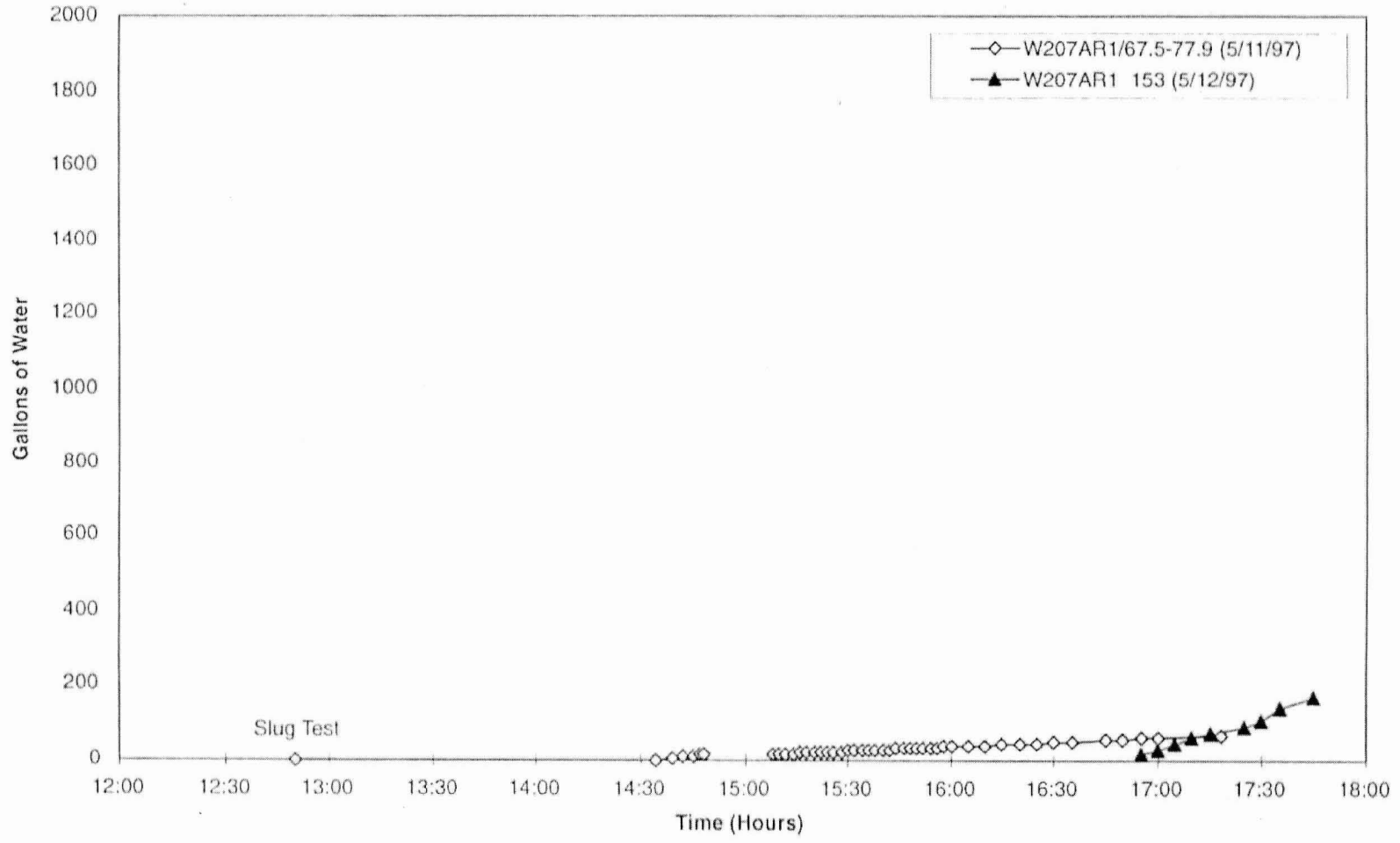

Harding Lawson Associates
Engineering and
Environmental Services

Gallons of Water Versus Time for Well W207AR1
North Carolina Low-Level Radioactive
Waste Disposal Facility Project
Wake County, North Carolina

FIGURE
H-4

DRAWN	JOB NUMBER	APPROVED	DATE	REVISED DATE
LDZ	36595,301	RAH	9/97	

NCLL-49 9/25/97 GEA

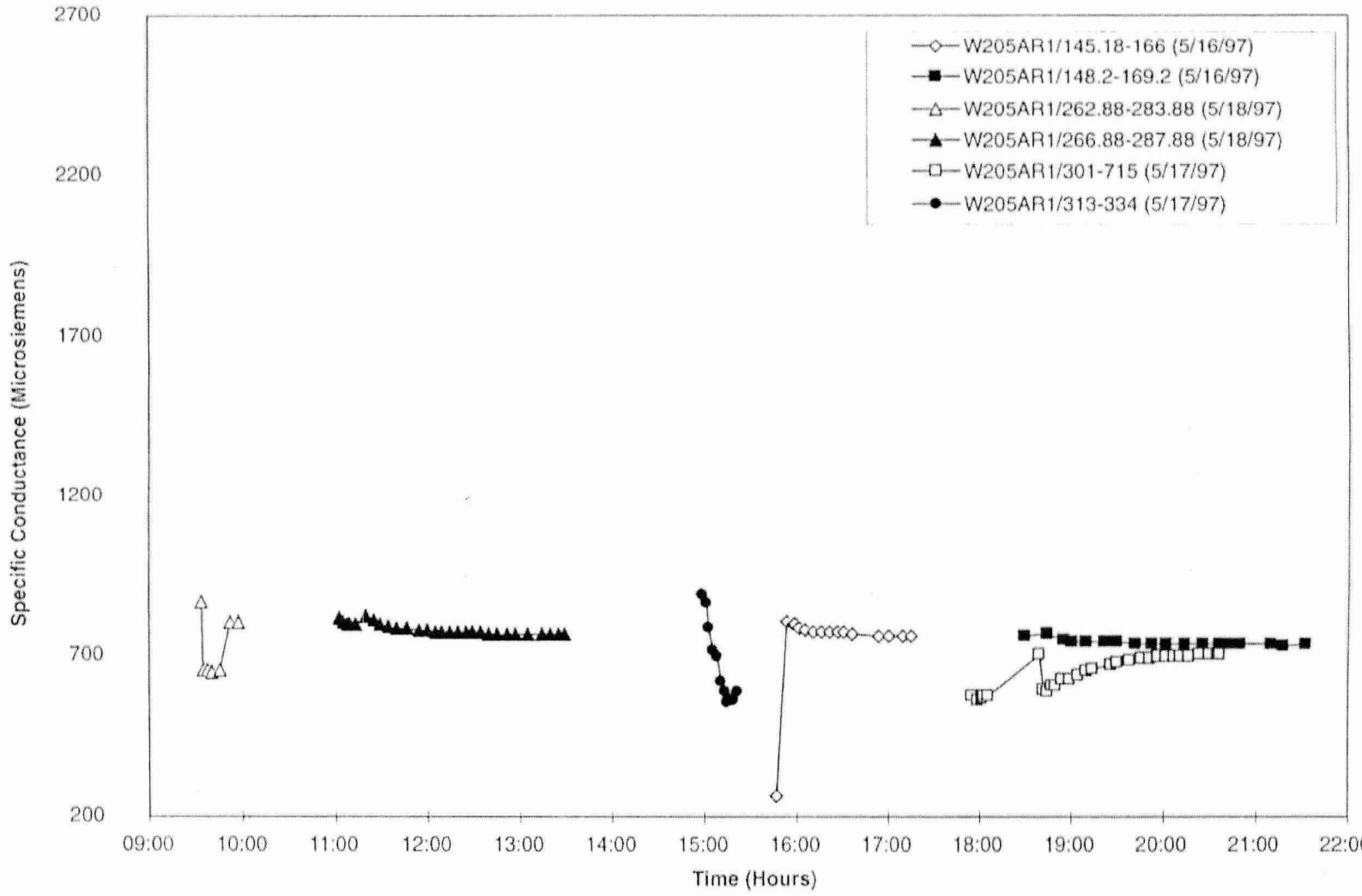

Harding Lawson Associates
Engineering and
Environmental Services

Specific Conductance Versus Time for Well W205AR1
North Carolina Low-Level Radioactive
Waste Disposal Facility Project
Wake County, North Carolina

FIGURE
H-5

DRAWN	JOB NUMBER	APPROVED	DATE	REVISED DATE
LDZ	36595,301	RAH	9/97	

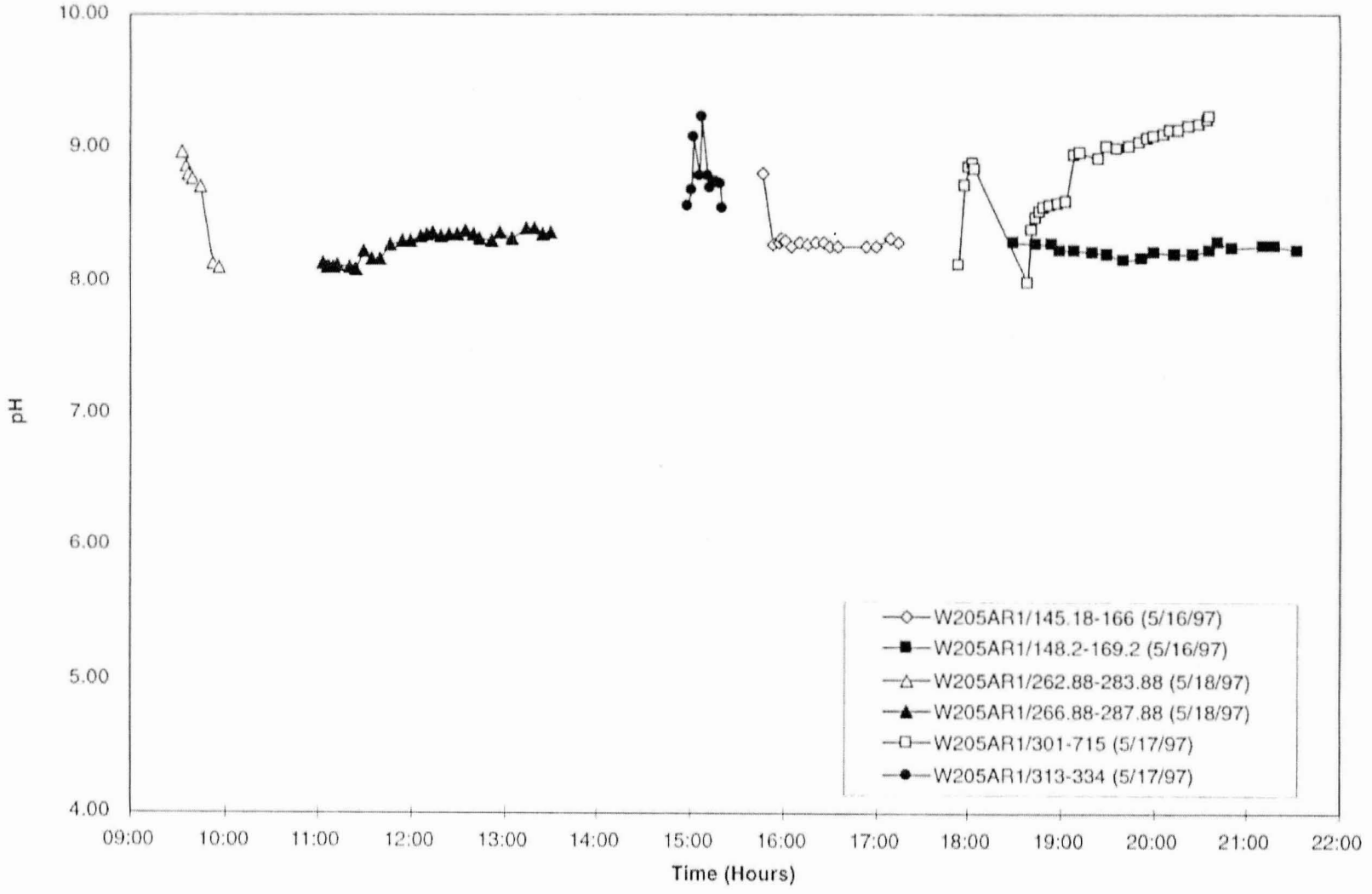

NCLL_49 9/25/97 GEA

Harding Lawson Associates
Engineering and
Environmental Services

pH Versus Time for Well W205AR1
North Carolina Low-Level Radioactive
Waste Disposal Facility Project
Wake County, North Carolina

FIGURE
H-6

DRAWN	JOB NUMBER	APPROVED	DATE	REVISED DATE
LDZ	36595,301	RAH	9/97	

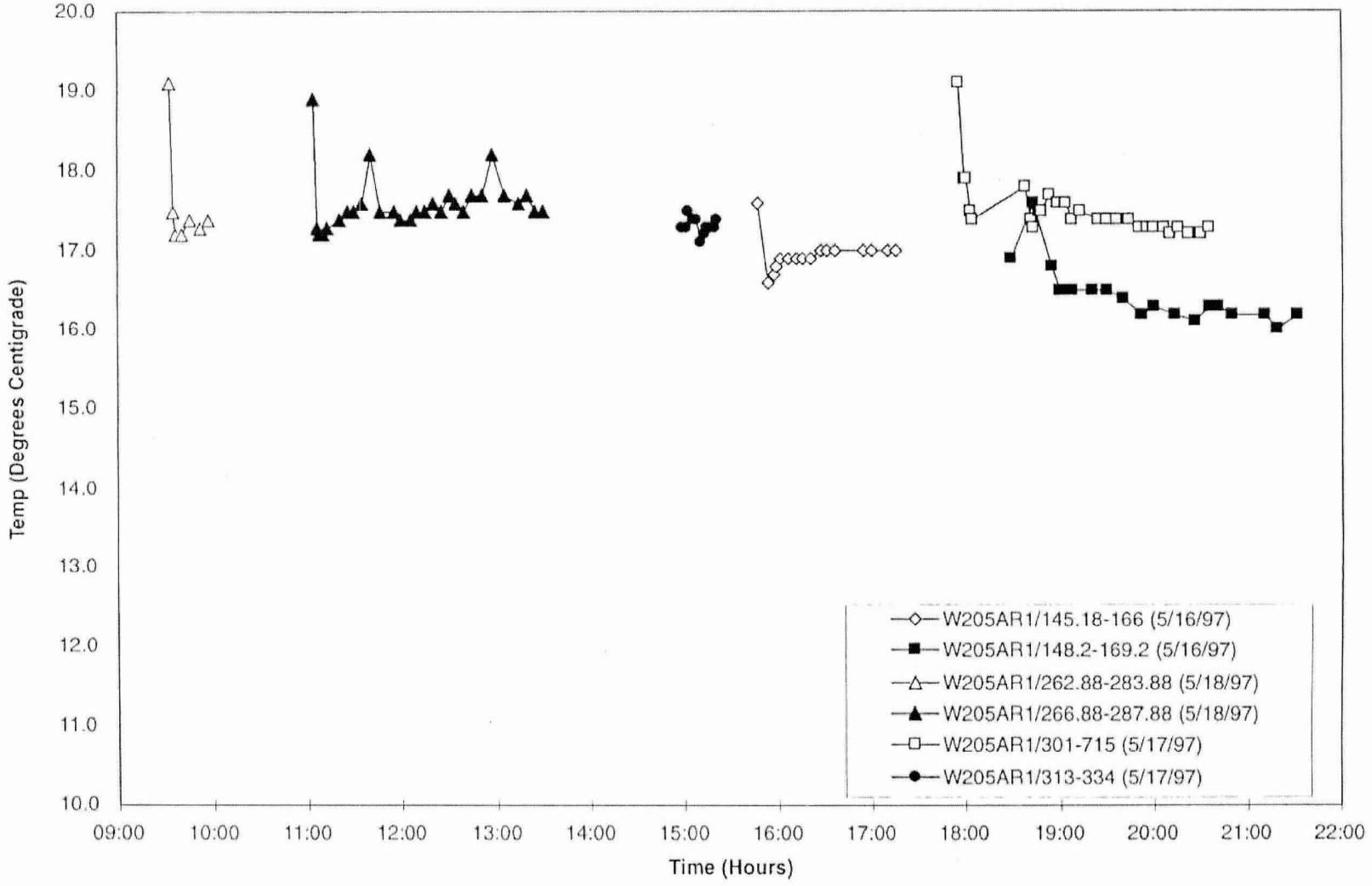

NGLL_4h 9/2597 GEA

Harding Lawson Associates
Engineering and
Environmental Services

Temperature Versus Time for Well W205AR1
North Carolina Low-Level Radioactive
Waster Disposal Facility Project
Wake County, North Carolina

FIGURE
H-7

DRAWN	JOB NUMBER	APPROVED	DATE	REVISED DATE
LDZ	36595,301	RAH	9/97	

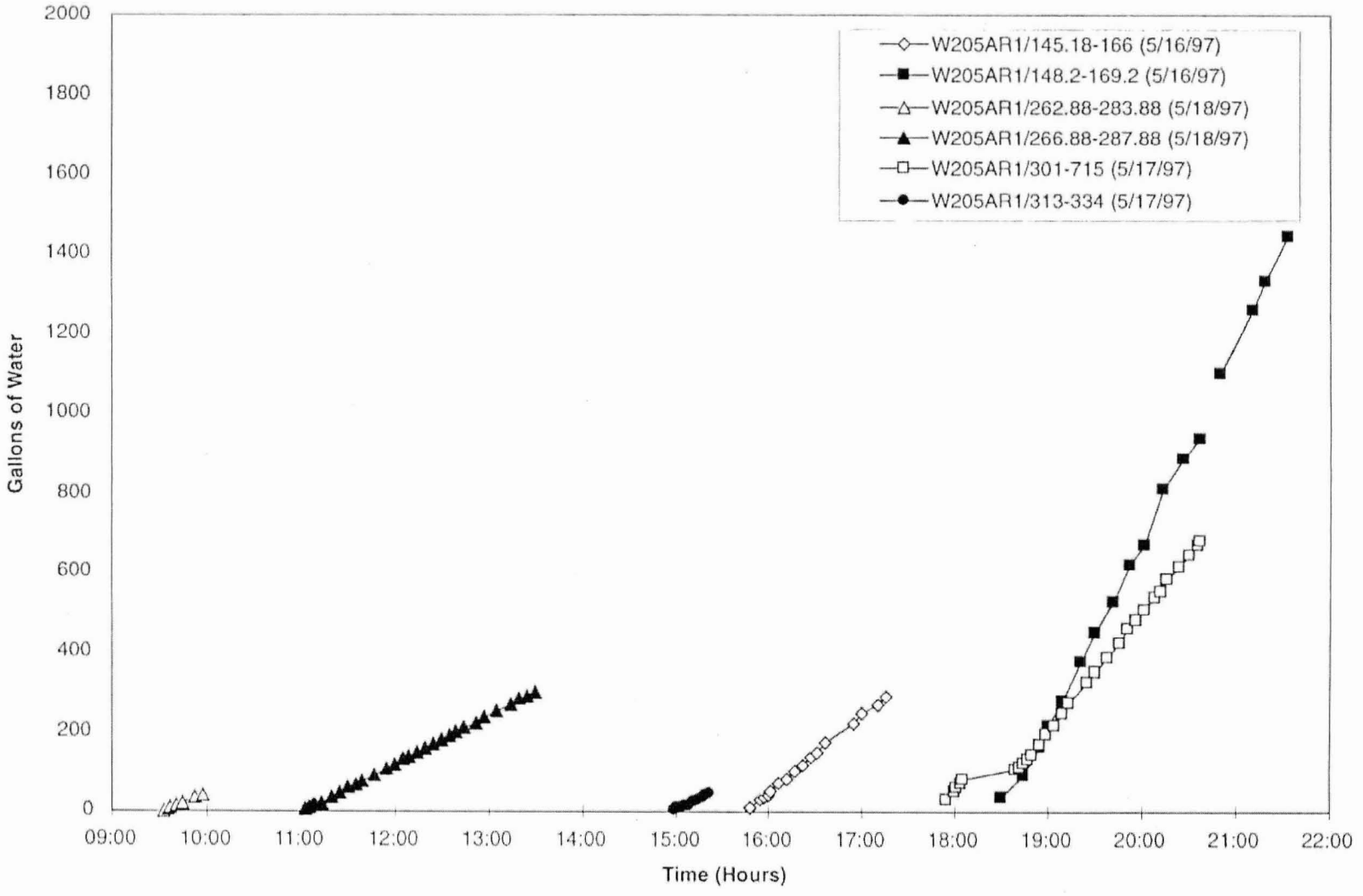

NCLL_4 9/25/97 GEA

Harding Lawson Associates
Engineering and
Environmental Services

Gallons of Water Versus Time for Well W205AR1
North Carolina Low-Level Radioactive
Waste Disposal Facility Project
Wake County, North Carolina

FIGURE
H-8

DRAWN	JOB NUMBER	APPROVED	DATE	REVISED DATE
LDZ	36595,301	RAH	9/97	

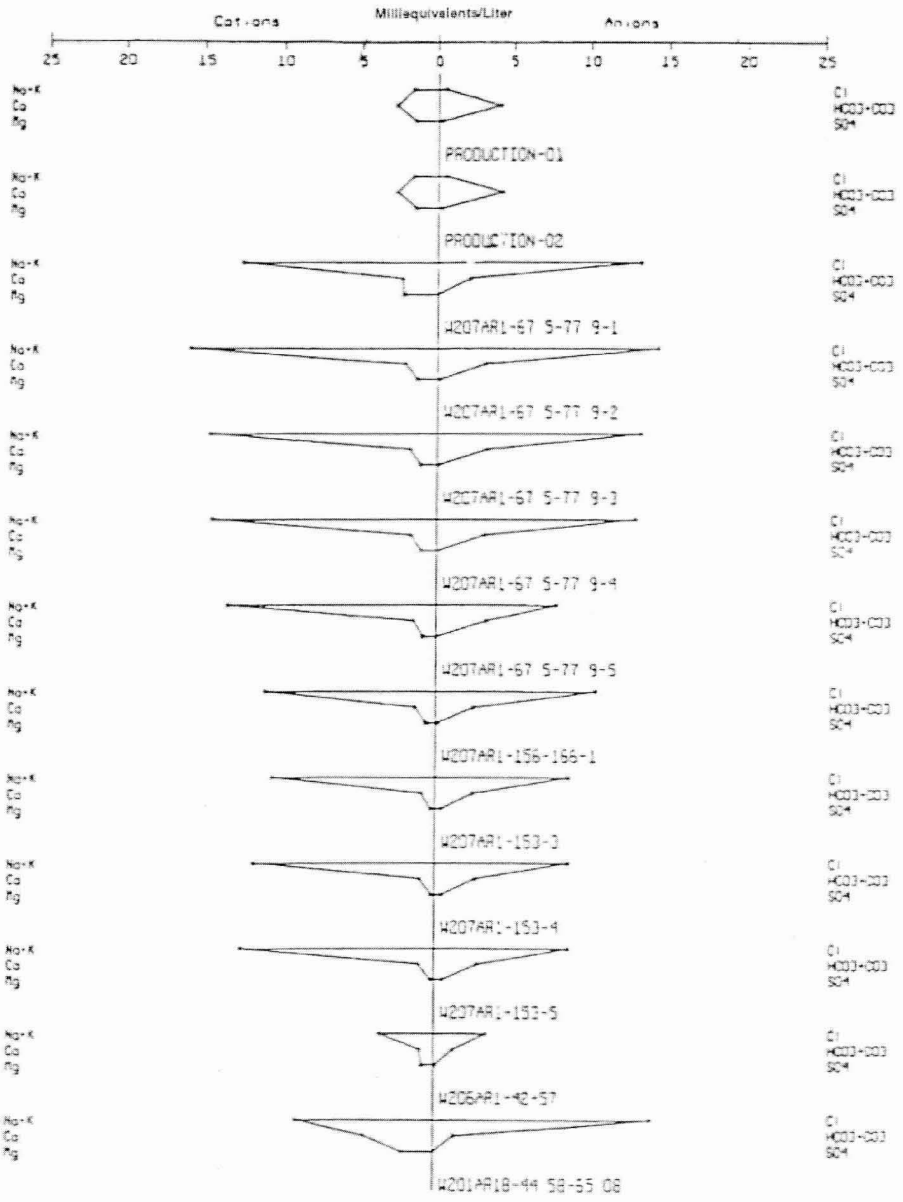

Harding Lawson Associates
Engineering and
Environmental Services

Stiff Plots Presented in the Order of Collection for 1997 Packer Test Wells
North Carolina Low-Level Radioactive
Waste Disposal Facility Project
Wake County, North Carolina

FIGURE
H-9a

DRAWN	JOB NUMBER	APPROVED	DATE	REVISED DATE
LDZ	36595.301	RAH	9/97	

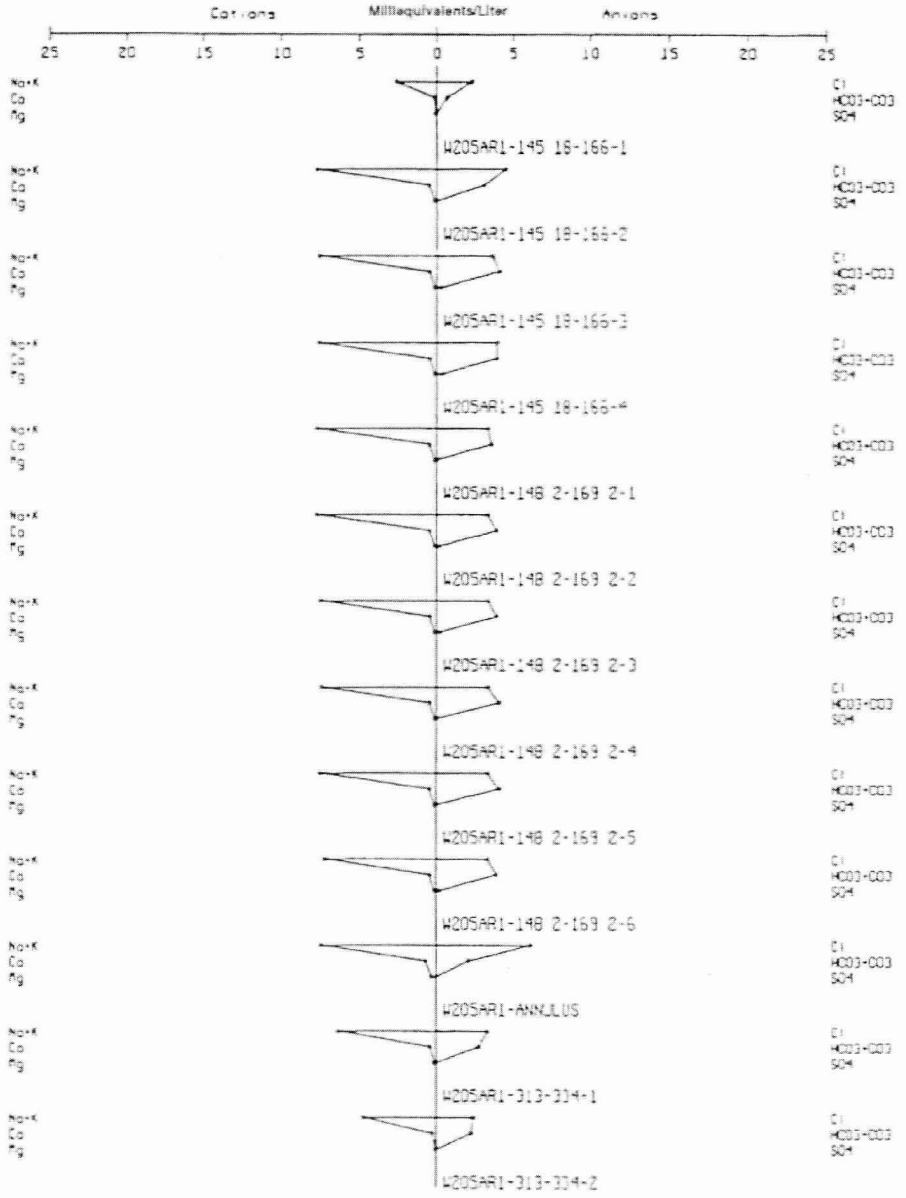

Harding Lawson Associates
Engineering and
Environmental Services

Stiff Plots Presented in the Order of Collection for 1997 Packer Test Wells
North Carolina Low-Level Radioactive
Waste Disposal Facility Project
Wake County, North Carolina

FIGURE
H-9b

DRAWN	JOB NUMBER	APPROVED	DATE	REVISED DATE
LDZ	36595,301	RAH	9/97	

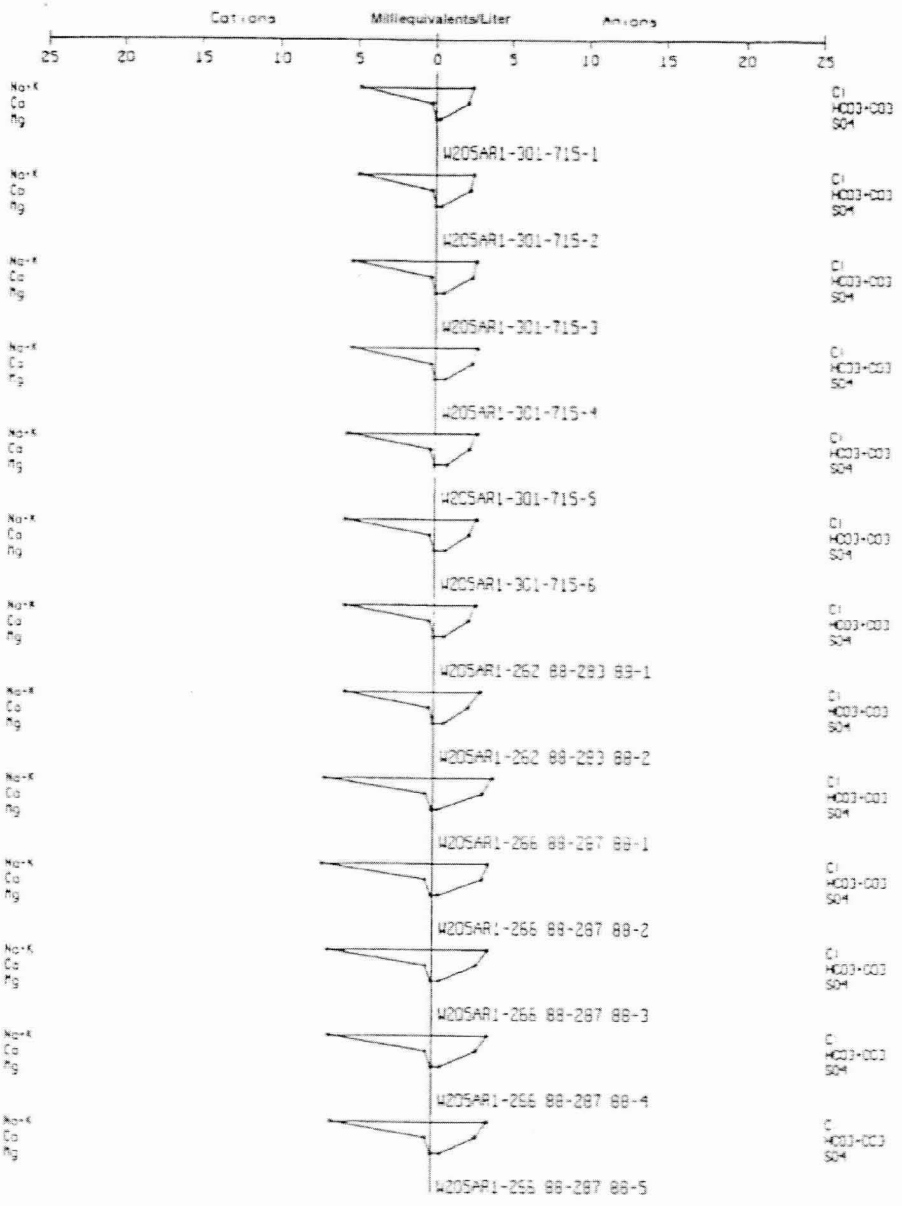

Harding Lawson Associates
Engineering and
Environmental Services

Stiff Plots Presented in the Order of Collection for 1997 Packer Test Wells
North Carolina Low-Level Radioactive
Waste Disposal Facility Project
Wake County, North Carolina

FIGURE
H-9c

DRAWN	JOB NUMBER	APPROVED	DATE	REVISED DATE
LDZ	36595,301	RAH	9/97	

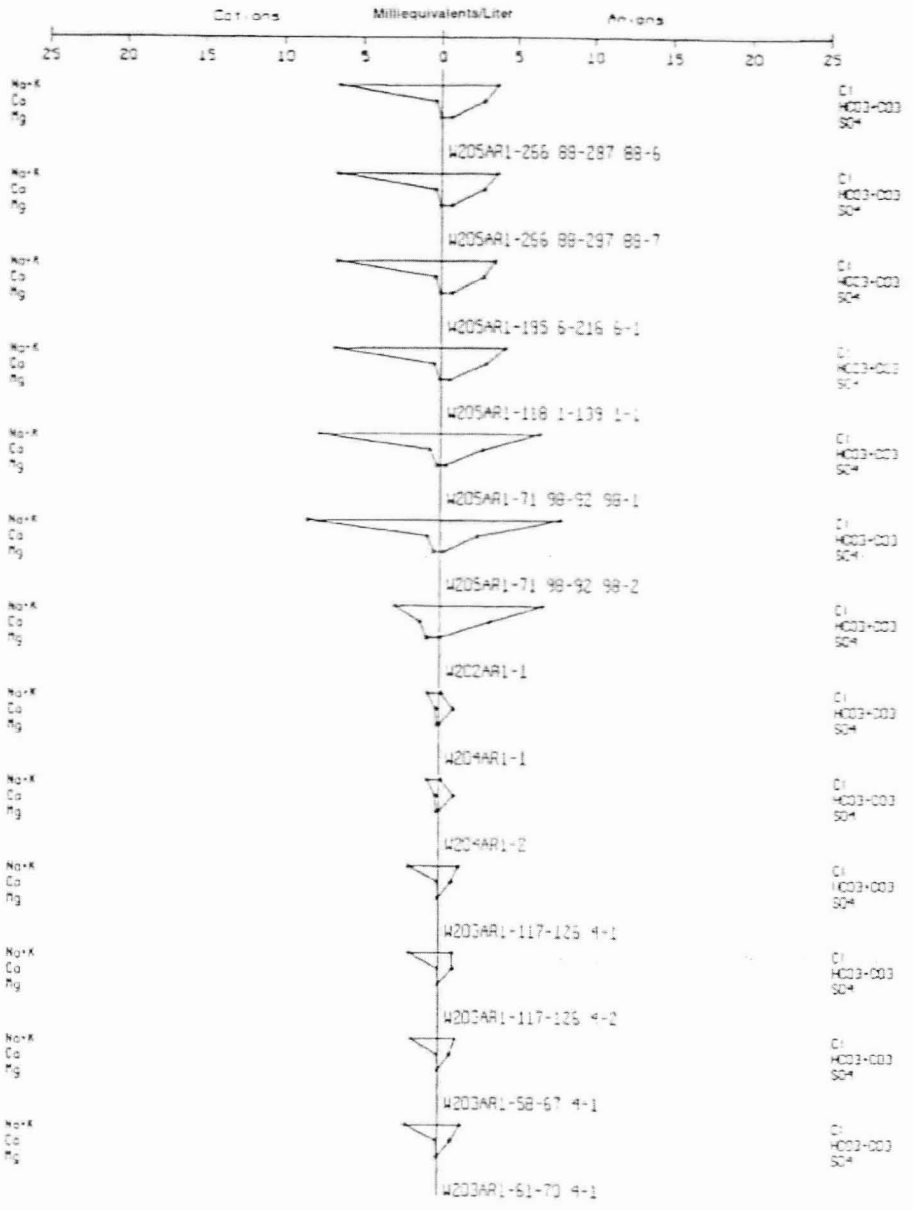

Harding Lawson Associates
Engineering and
Environmental Services

Stiff Plots Presented in the Order of Collection for 1997 Packer Test Wells
North Carolina Low-Level Radioactive
Waste Disposal Facility Project
Wake County, North Carolina

FIGURE
H-9d

DRAWN	JOB NUMBER	APPROVED	DATE	REVISED DATE
LDZ	36595,301	RAH	9/97	

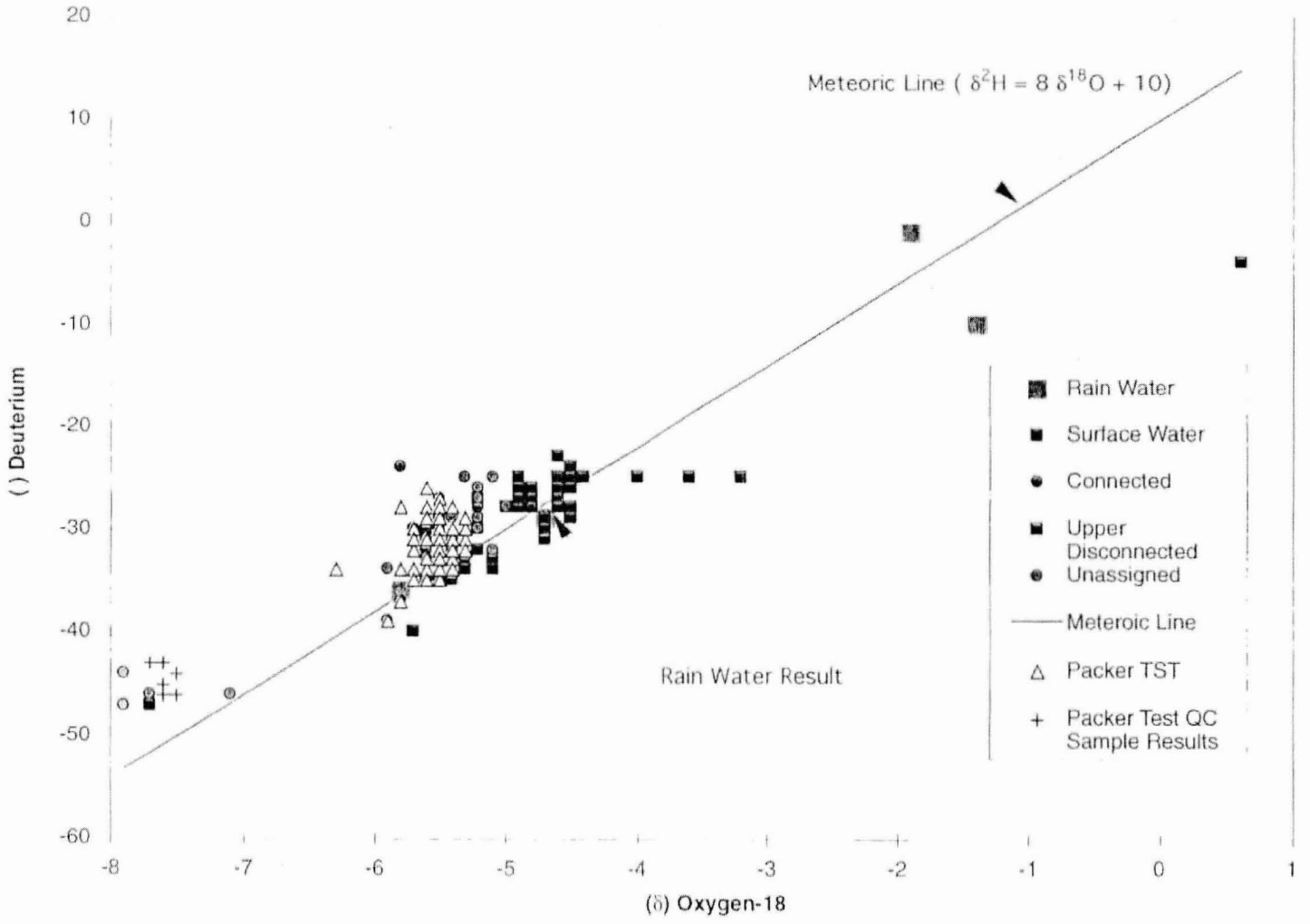

NCLL_4x 9/25/97 GEA

Harding Lawson Associates
Engineering and Environmental Services

Oxygen-18/Deuterium Results for 1997 Packer Test Wells Versus Other Samples Collected at the Site
North Carolina Low-Level Radioactive Waste Disposal Facility Project
Wake County, North Carolina

FIGURE
H-10

DRAWN	JOB NUMBER	APPROVED	DATE	REVISED DATE
LDZ	36595.301	RAH	9/97	

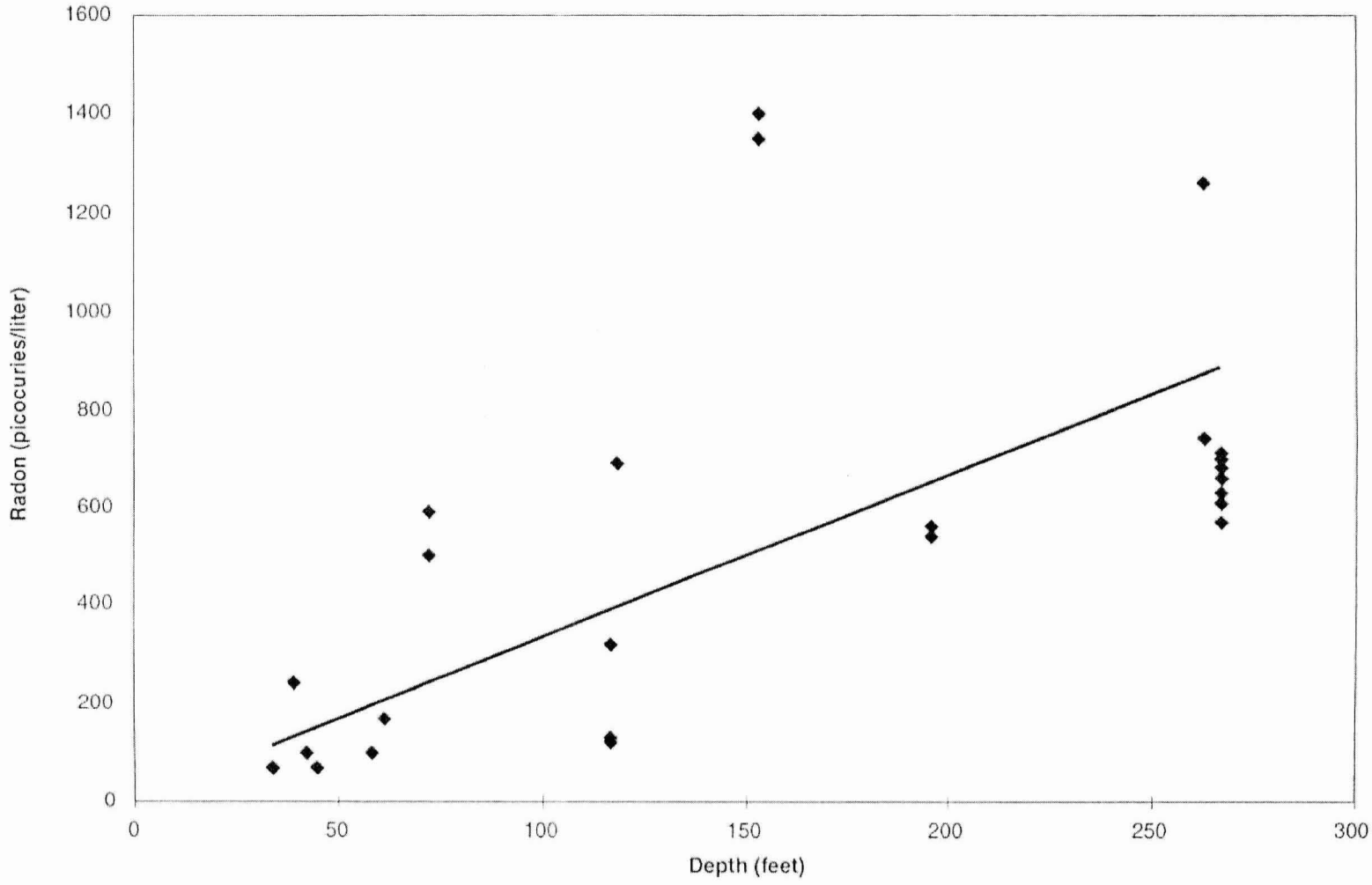

NCLL_4 9/22/97 GEA

Harding Lawson Associates
Engineering and
Environmental Services

Radon Concentrations for 1997 Packer Test Sample Results Versus Depth
North Carolina Low-Level Radioactive
Waste Disposal Facility Project
Wake County, North Carolina

FIGURE
H-11

DRAWN	JOB NUMBER	APPROVED	DATE	REVISED DATE
LDZ	36595,301	RAH	9/97	

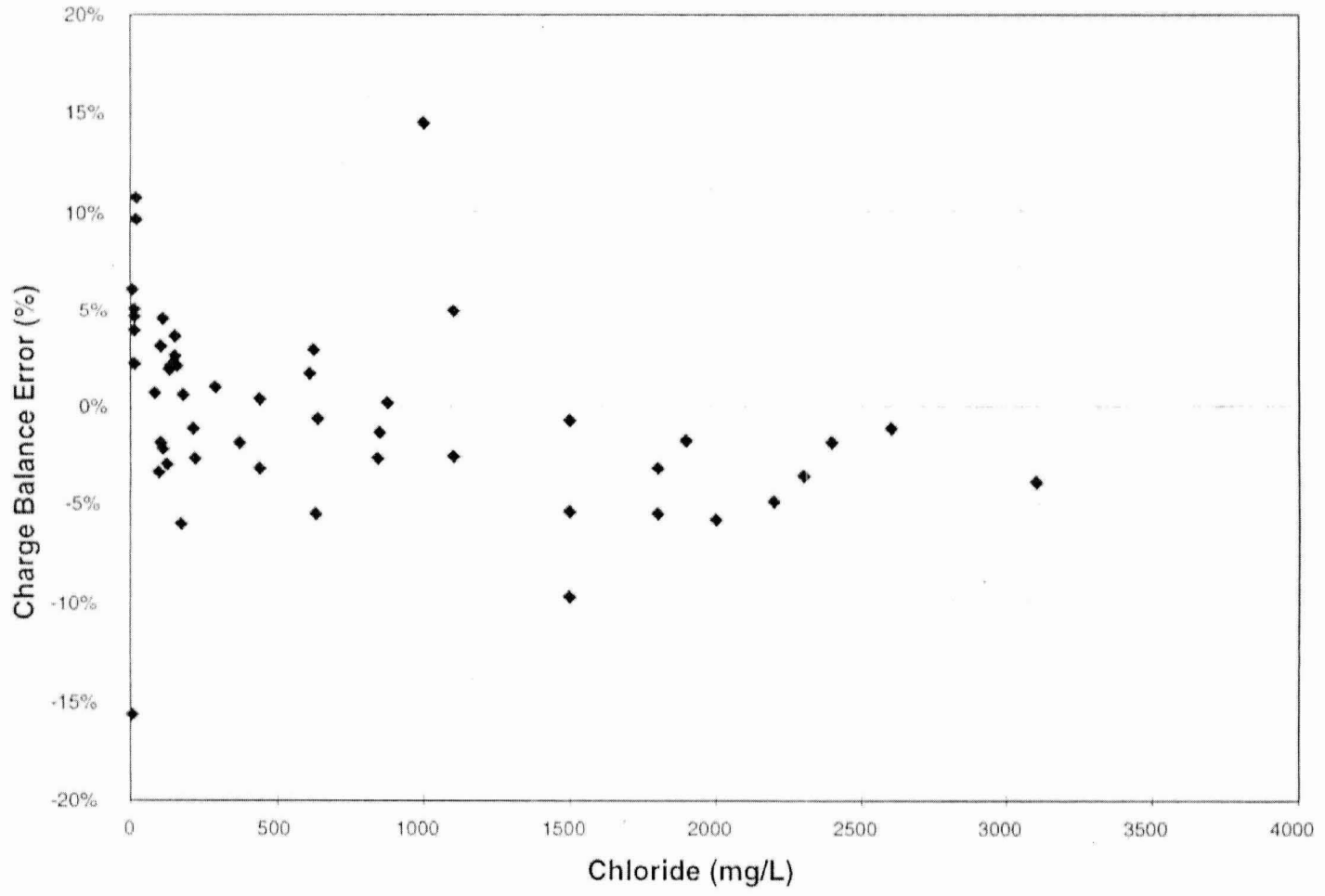

NCLL 4m 92297 GEA

Harding Lawson Associates
Engineering and
Environmental Services

Charge Balance Errors Versus Chloride for 1993 and 1995 Ground Water
North Carolina Low-Level Radioactive
Waste Disposal Facility Project
Wake County, North Carolina

FIGURE
H-12

DRAWN	JOB NUMBER	APPROVED	DATE	REVISED DATE
LDZ	36595,301	RAH	9/97	

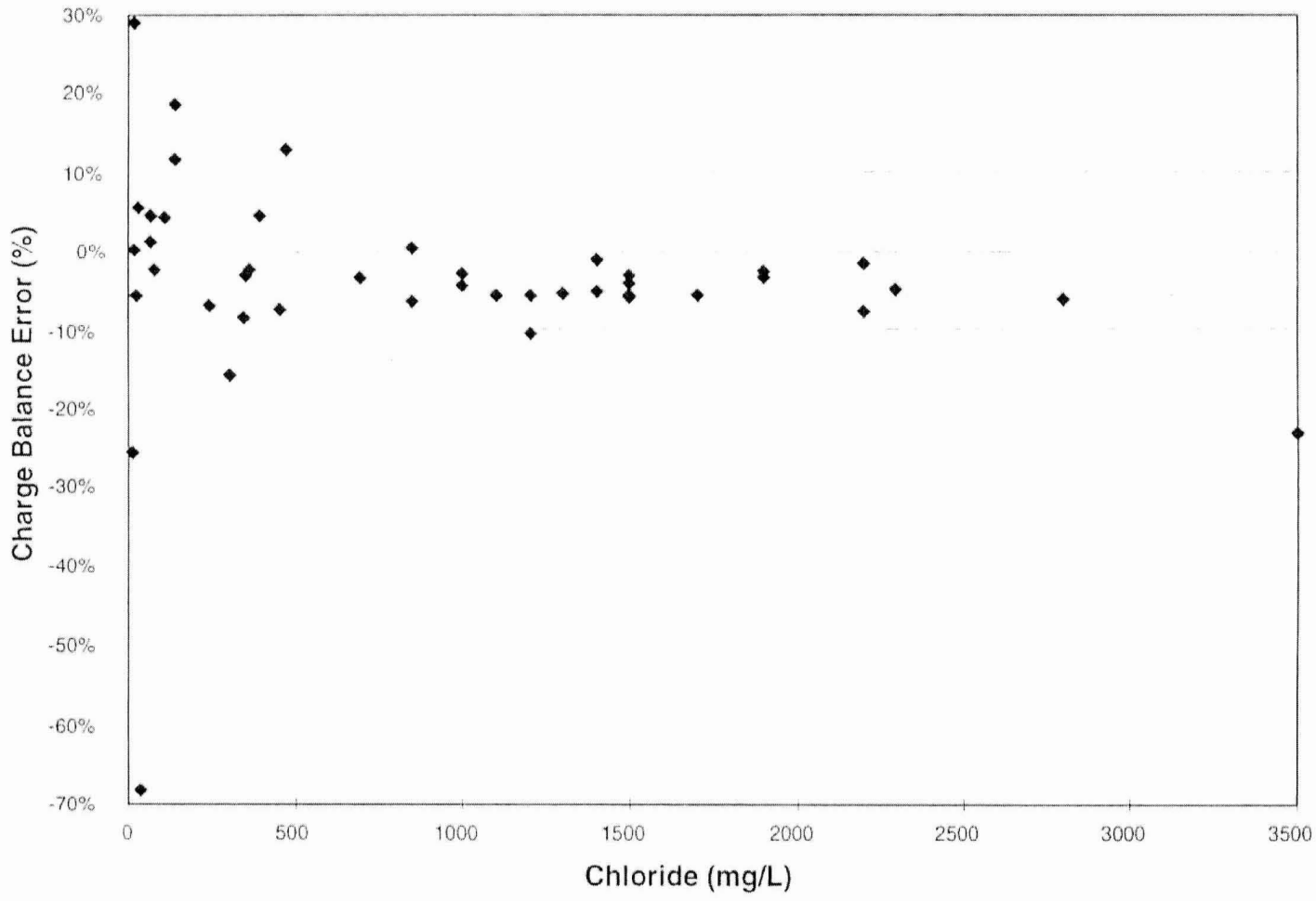

Harding Lawson Associates
Engineering and
Environmental Services

Charge Balance Errors Versus Chloride for 1995 Drainage Stud Results
North Carolina Low-Level Radioactive
Waste Disposal Facility Project
Wake County, North Carolina

FIGURE
H-13

DRAWN	JOB NUMBER	APPROVED	DATE	REVISED DATE
LDZ	36595,301	RAH	9/97	

NCLL_4b 9/22/97 GEA

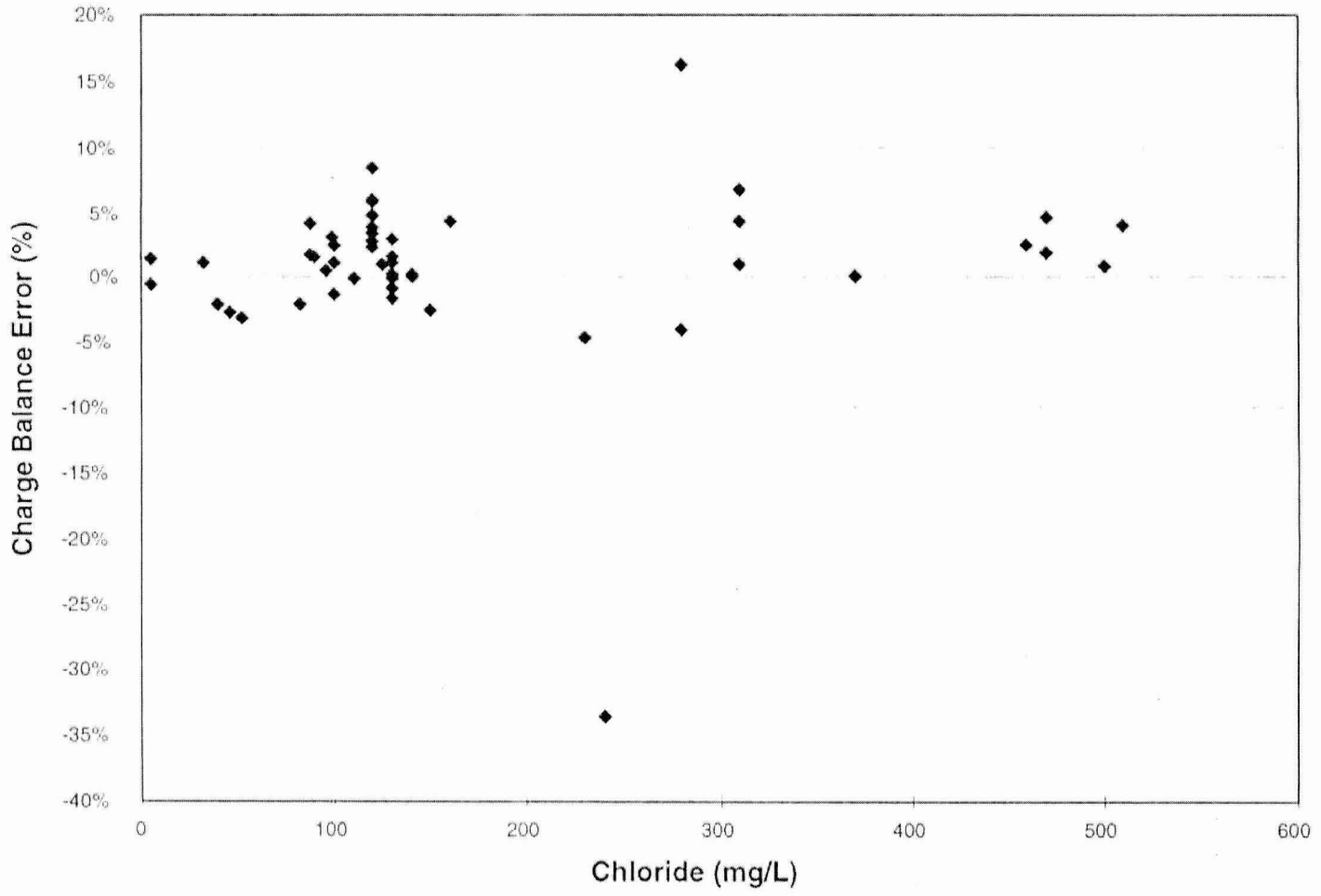

Harding Lawson Associates
Engineering and
Environmental Services

Charge Balance Errors Versus Chloride for 1997 Packer Test Results
North Carolina Low-Level Radioactive
Waste Disposal Facility Project
Wake County, North Carolina

FIGURE
H-14

DRAWN	JOB NUMBER	APPROVED	DATE	REVISED DATE
LDZ	36595,301	RAH	9/97	

NCLL_fo 9/22/97 GEA

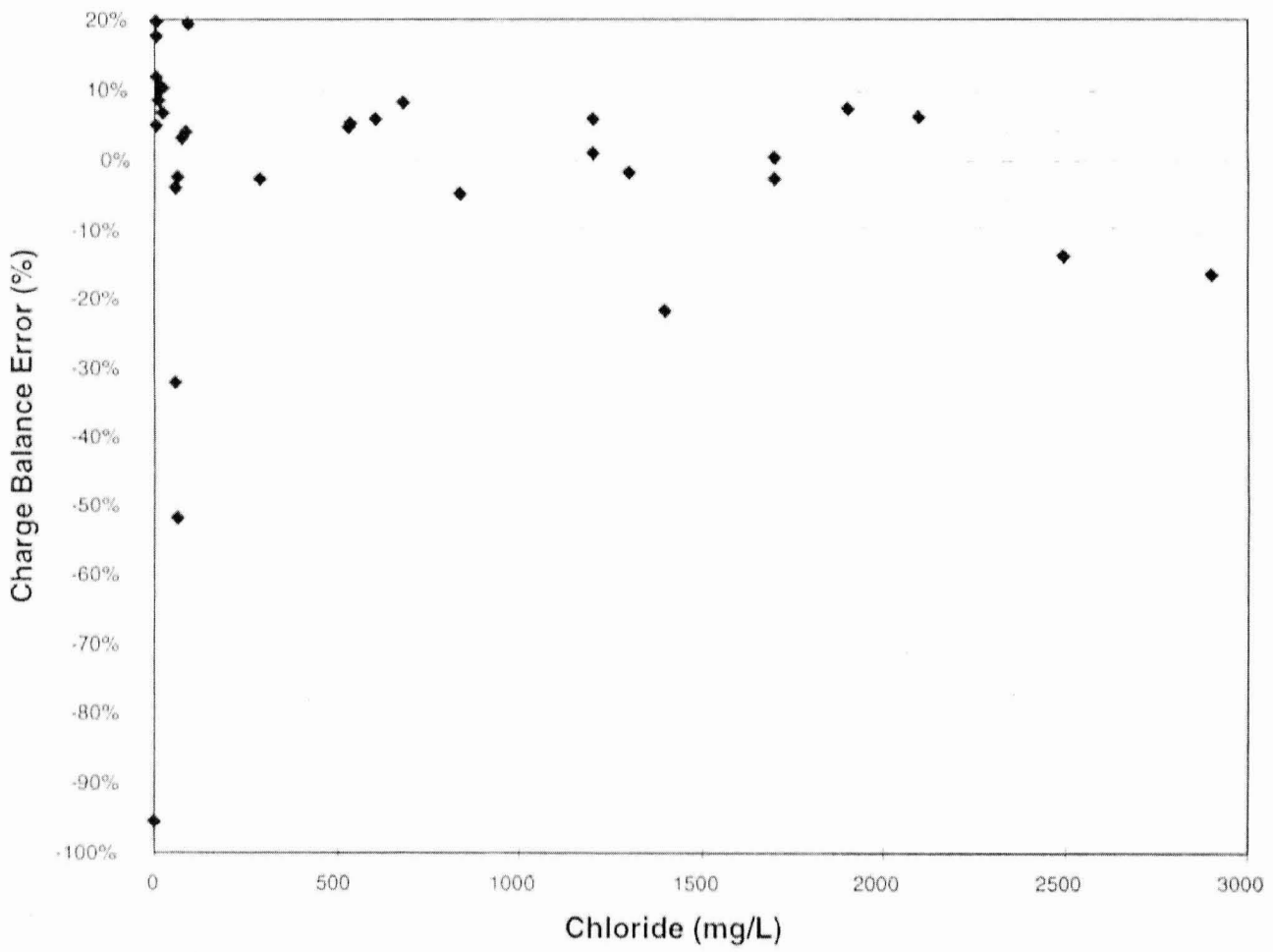

NCLL_4b 9/22/97 GE4

Harding Lawson Associates
Engineering and
Environmental Services

Charge Balance Errors Versus Chloride for 1997 Ground Water Results
North Carolina Low-Level Radioactive
Waste Disposal Facility Project
Wake County, North Carolina

FIGURE
H-15

DRAWN	JOB NUMBER	APPROVED	DATE	REVISED DATE
LDZ	36595,301	RAH	9/97	

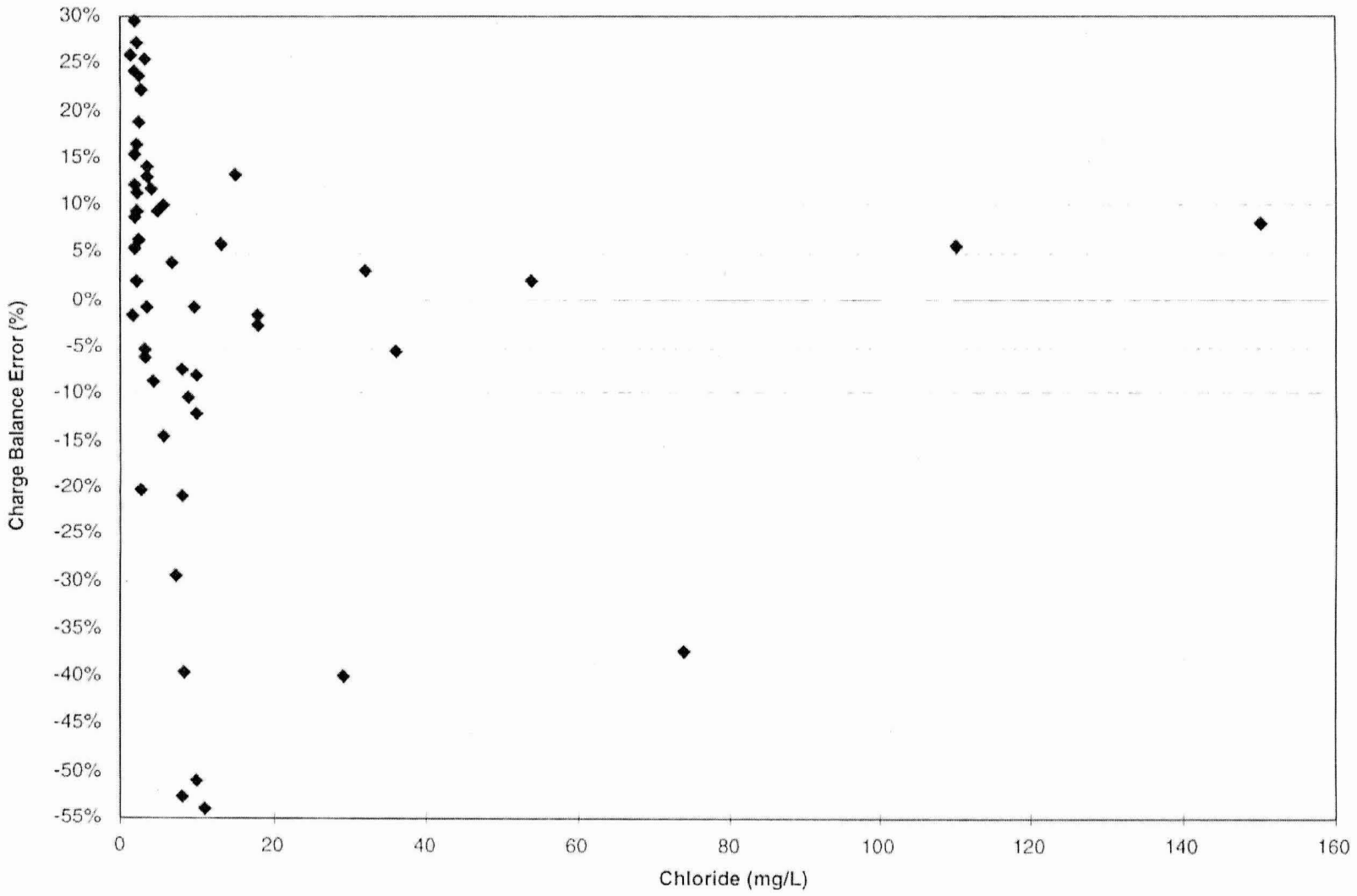

Harding Lawson Associates
Engineering and
Environmental Services

Charge Balance Errors Versus Chloride for 1997 Surface Water Results
North Carolina Low-Level Radioactive
Waste Disposal Facility Project
Wake County, North Carolina

FIGURE
H-16

DRAWN	JOB NUMBER	APPROVED	DATE	REVISED DATE
LDZ	36595,301	RAH	9/97	

Appendix I

Seismic Data

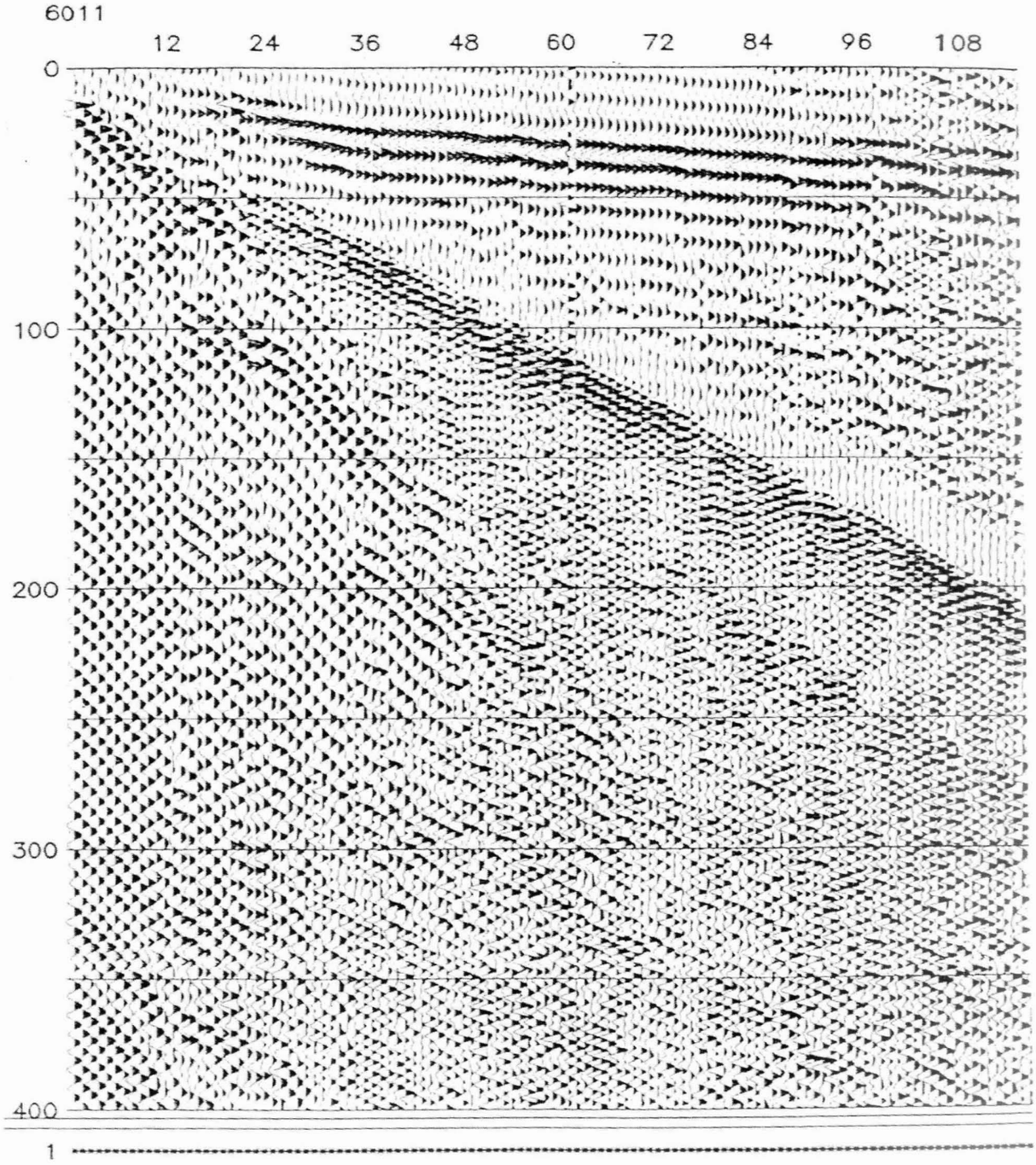

Figure I-1 Shotpoint 1. Line 1 Raw field gather, no processing applied other than vibroseis sweep correlation.

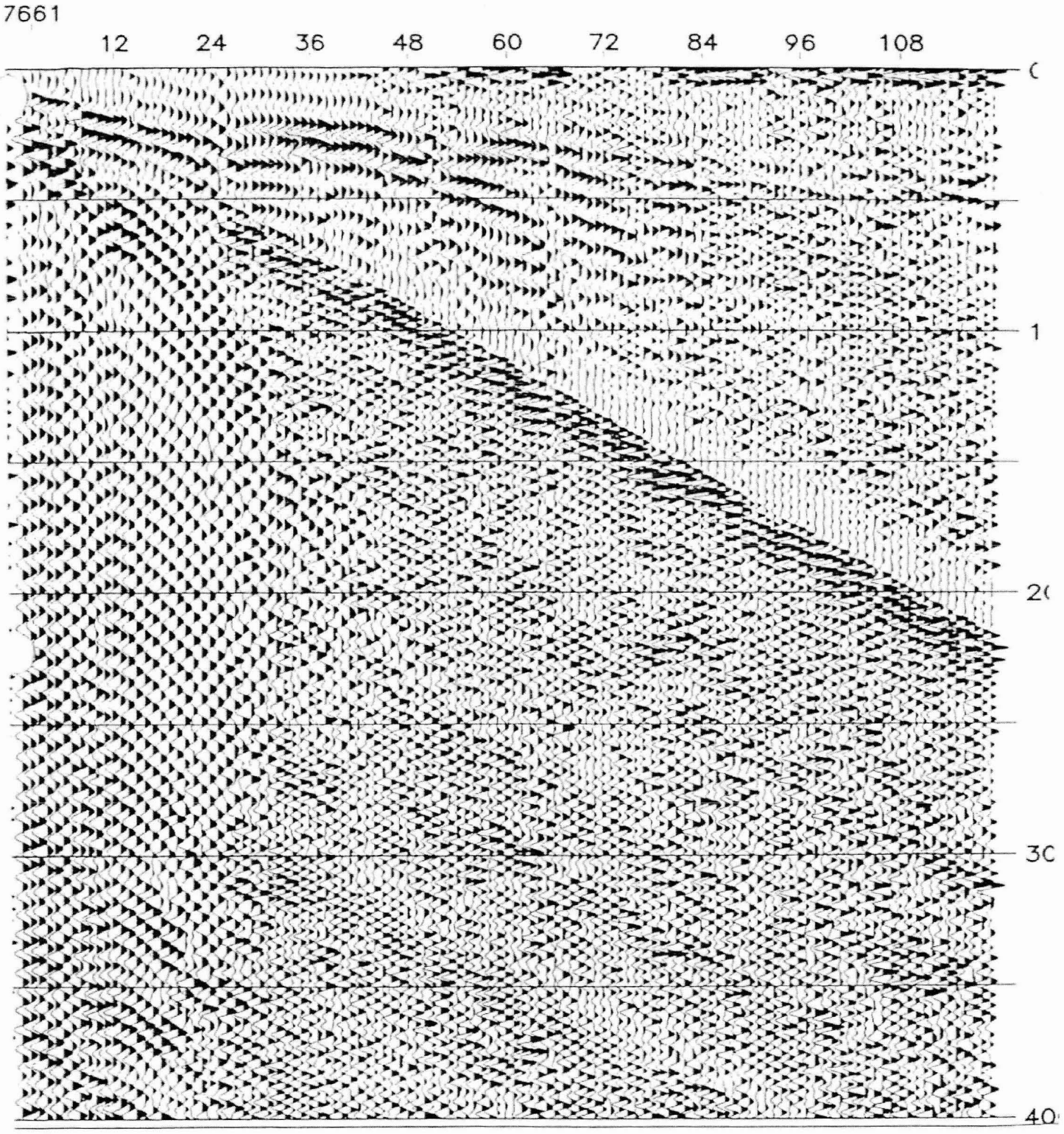

Figure I-2 Shotpoint 305. Line 1 Raw field gather, no processing applied other than vibroseis sweep correlation.

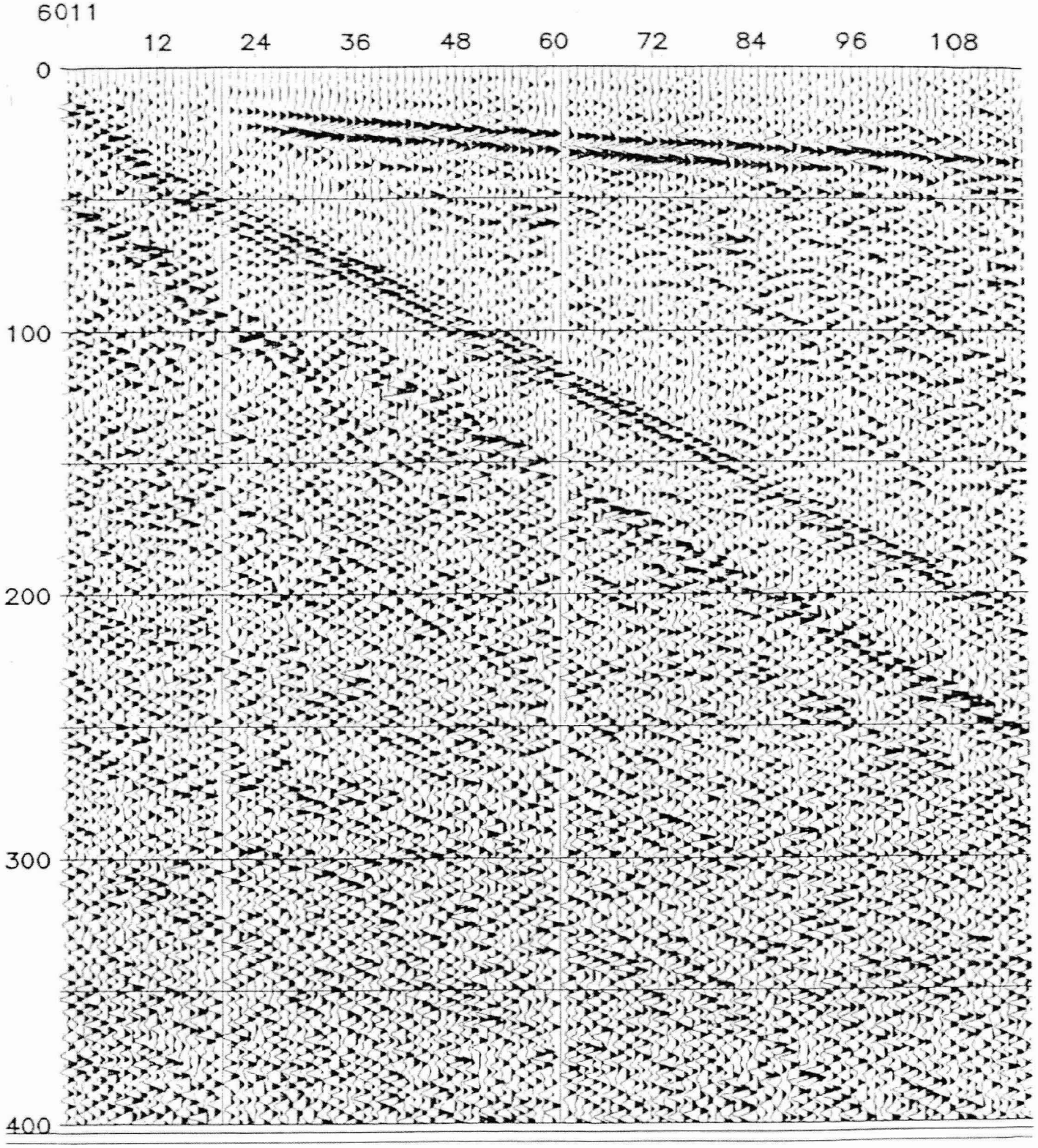

Figure I-3 Shotpoint 1. Line 1. Deconvolution and spectral whitening added to previous processing.

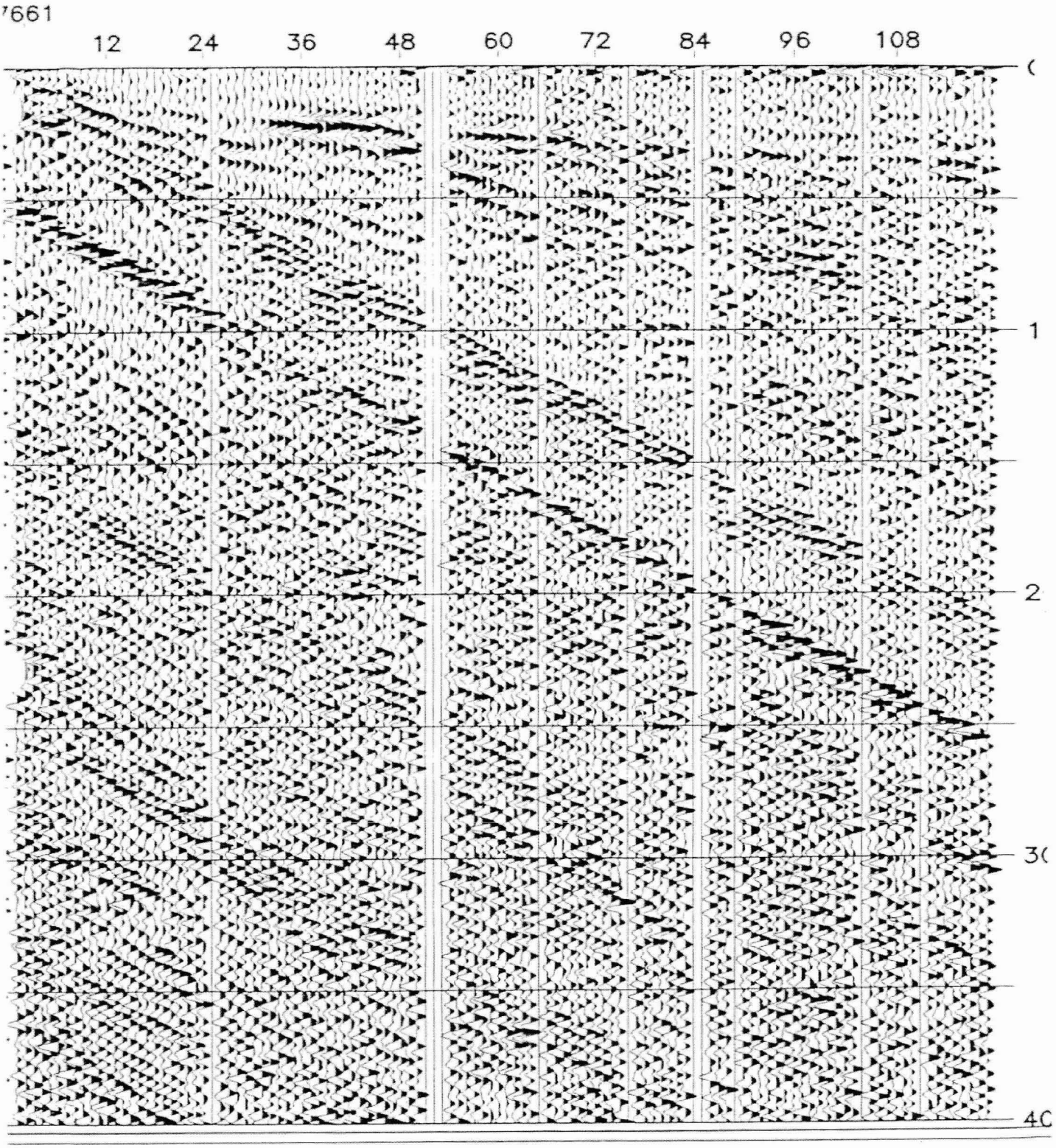

Figure I-4 Shotpoint 305. Line 1. Deconvolution and spectral whitening added to previous processing.

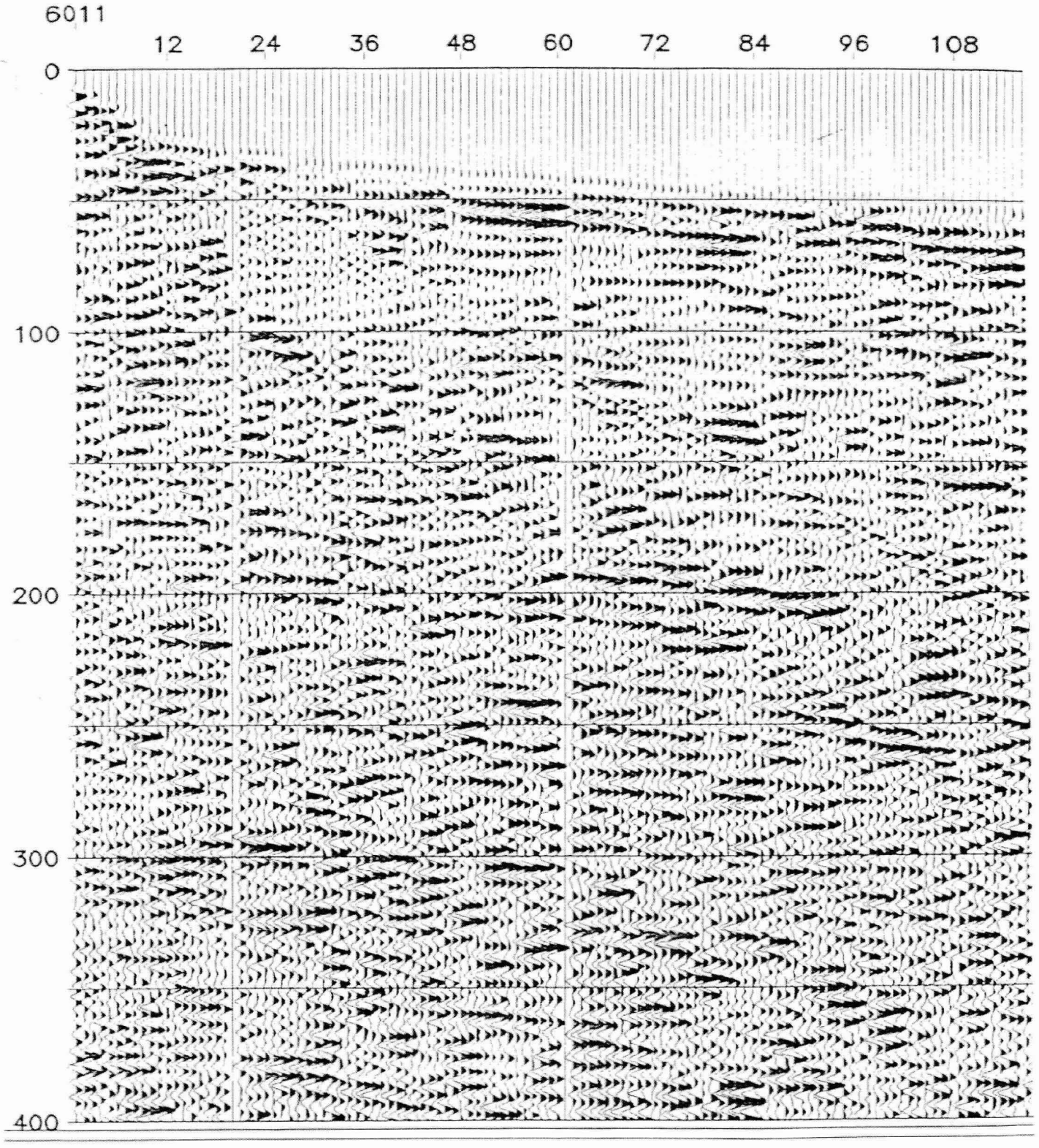

Figure I-5 Shotpoint 1. Line 1. First arrival muting and f-k filtering added to previous processing.

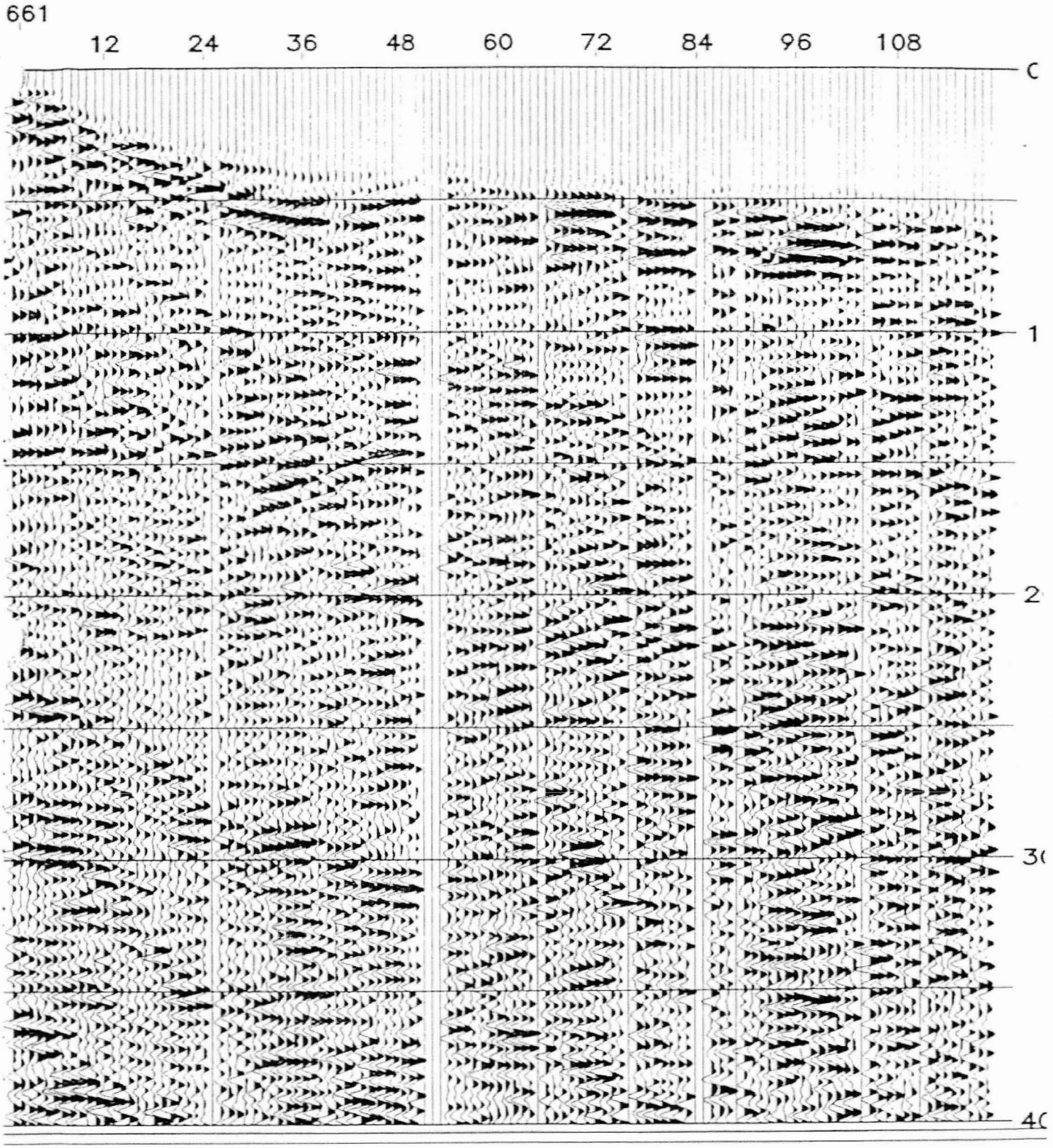

Figure I-6 Shotpoint 305. Line 1. First arrival muting and f-k filtering added to previous processing.

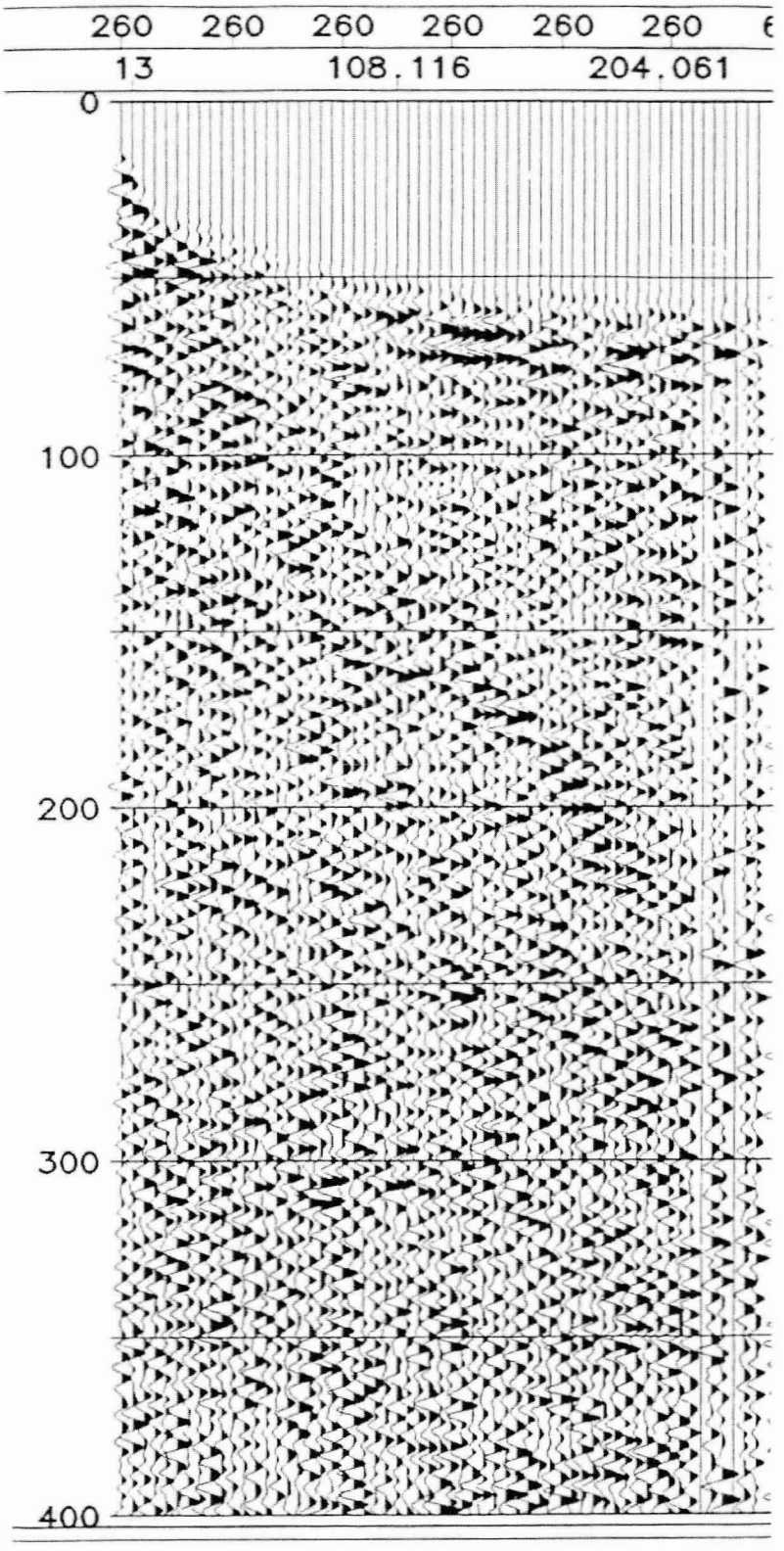

Figure I-7 CDP gather 260, shotpoint 130. Line 1. Gather and normal moveout added to previous processing.

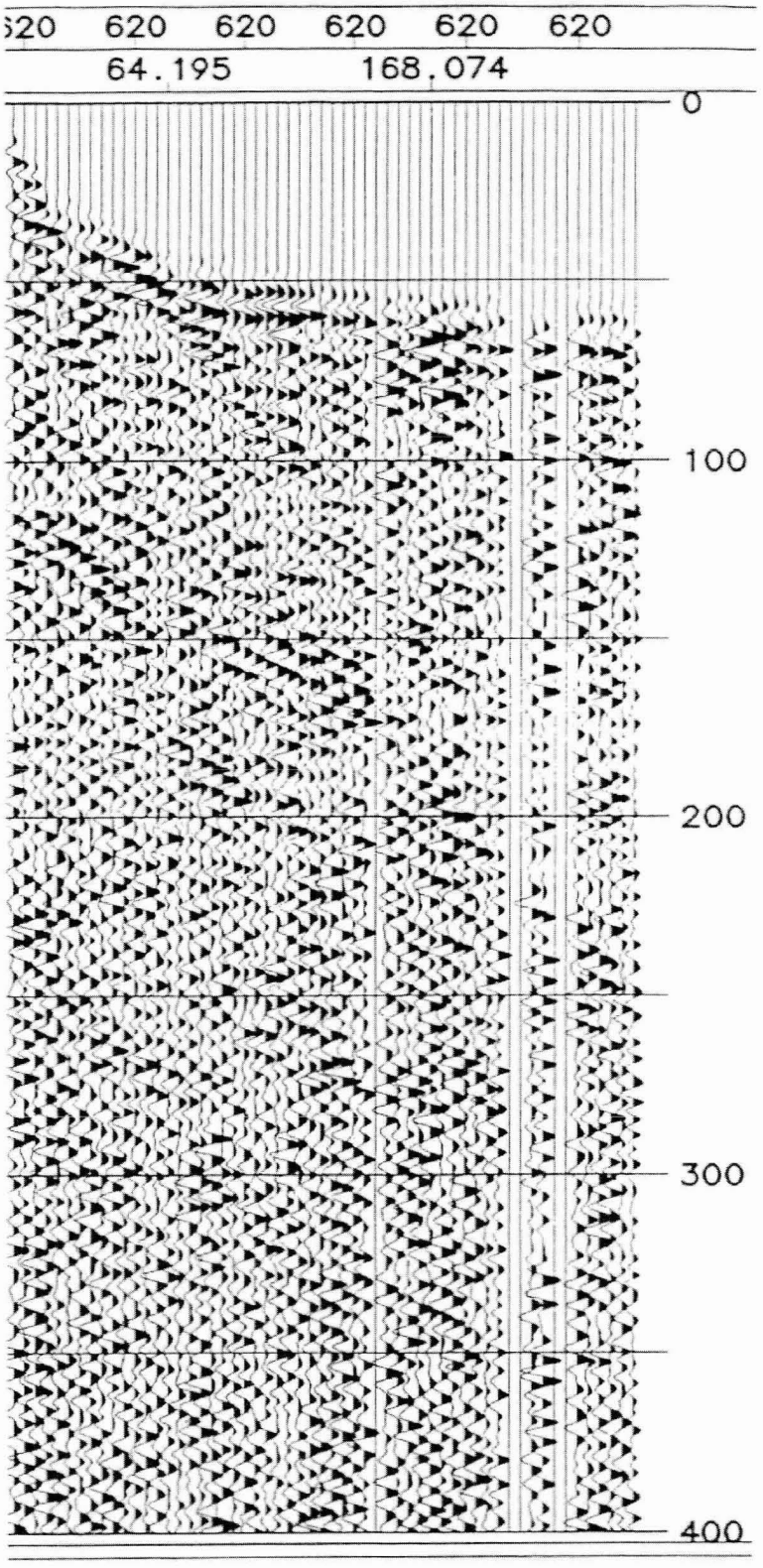

Figure I-8 CDP gather 620, shotpoint 310. Line 1. Gather and normal moveout added to previous processing.

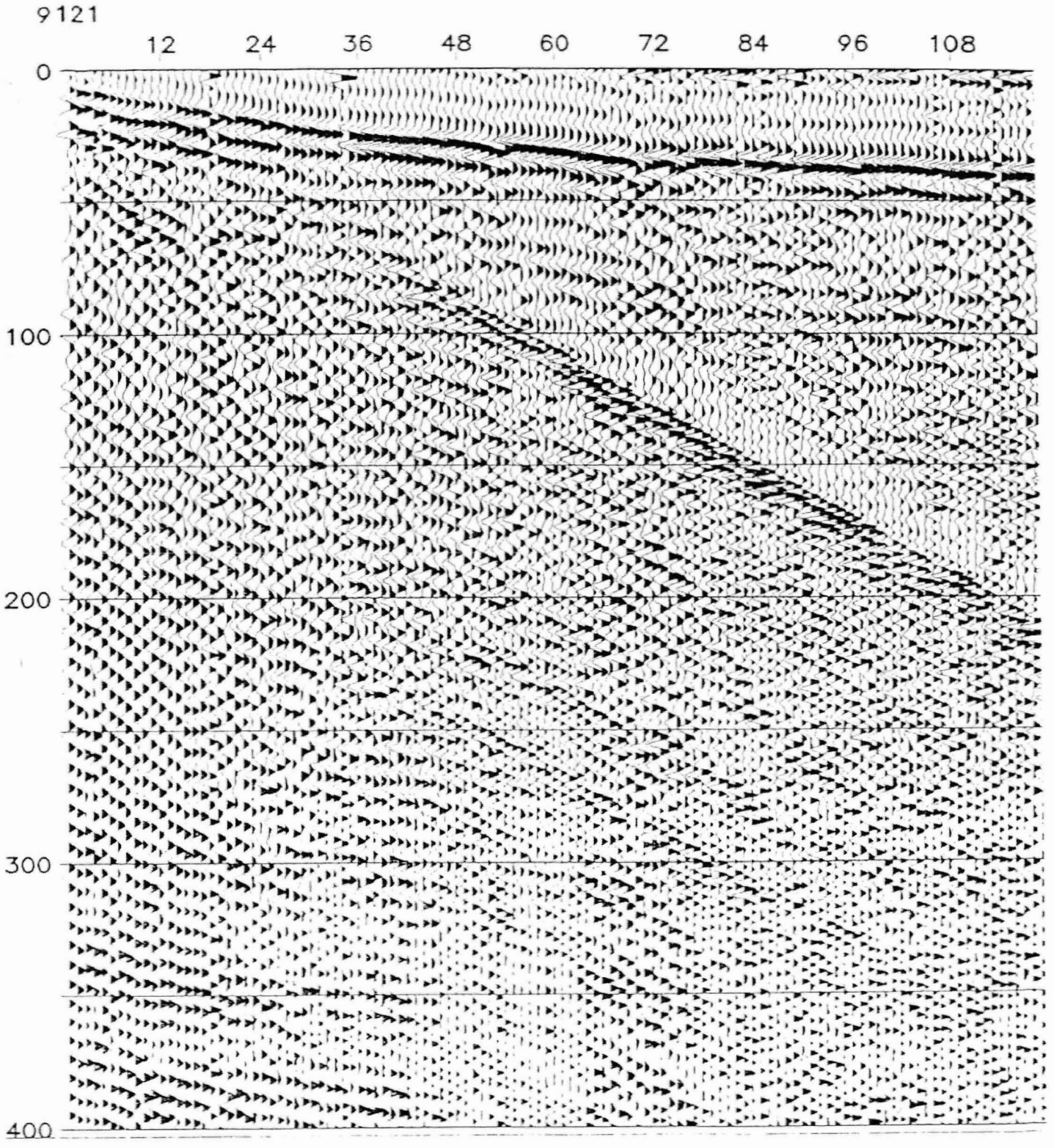

Figure I-9 Shotpoint 1057. Line 2. Raw field gather, no processing applied other than vibroseis sweep correlation.

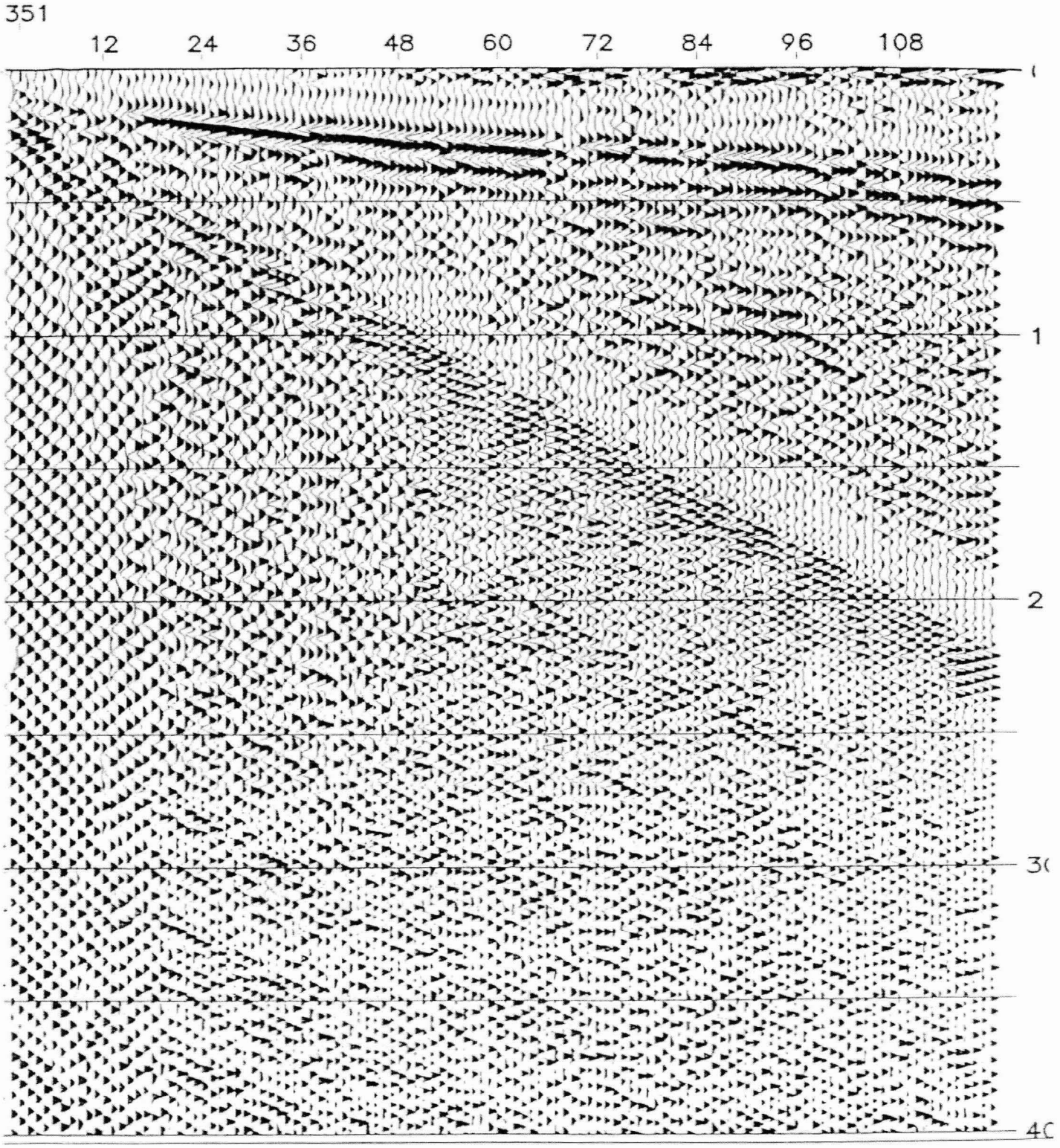

Figure I-10 Shotpoint 1115. Line 2. Raw field gather, no processing applied other than vibroseis sweep correlation.

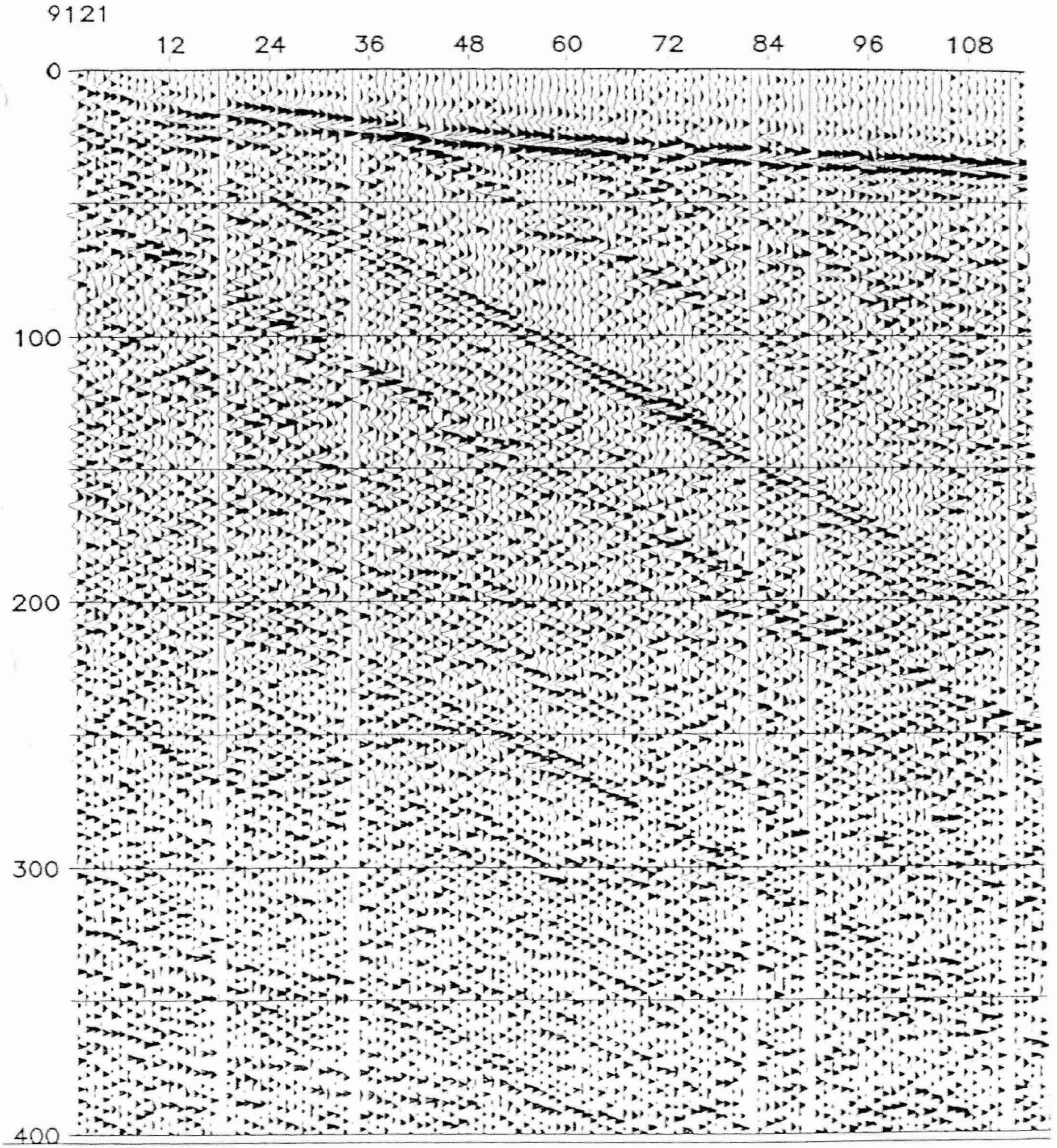

Figure I-11 Shotpoint 1057. Line 2. Devconvolution and spectral whitening added to previous processing.

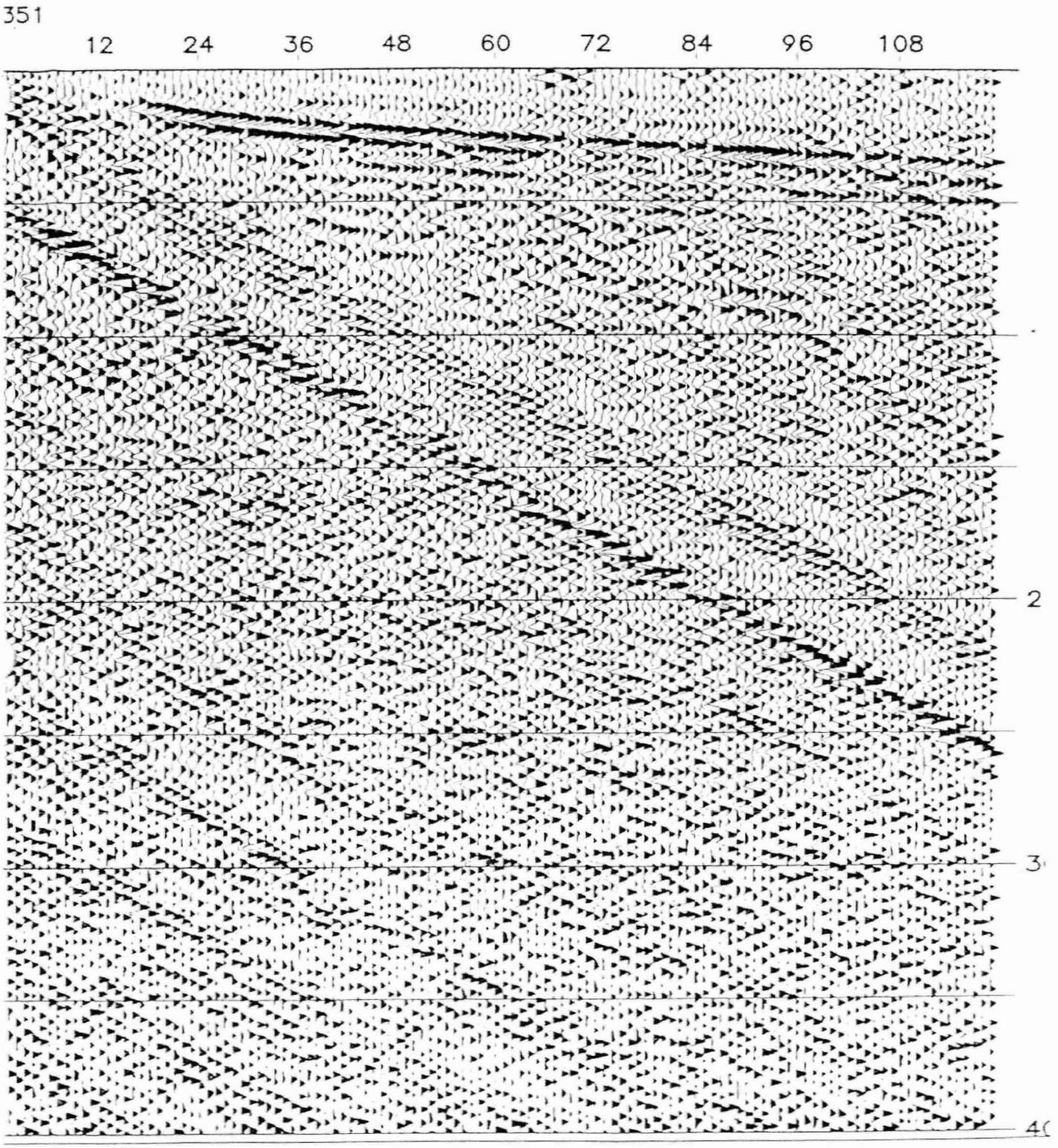

Figure I-12 Shotpoint 1115. Line 2. Devconvolution and spectral whitening added to previous processing.

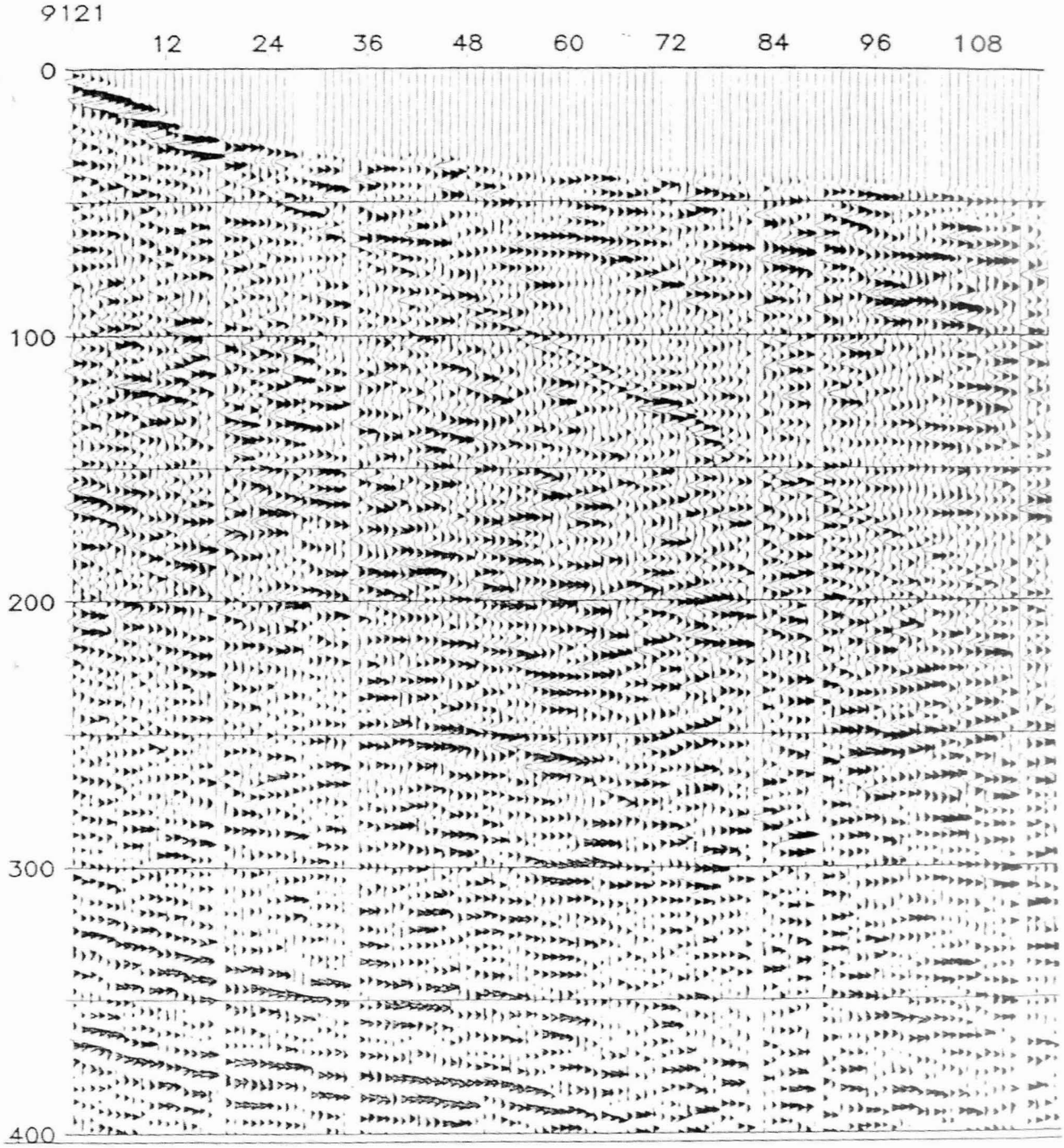

Figure I-13 Shotpoint 1057. Line 2. First arrival muting and f-k filtering added to previous processing.

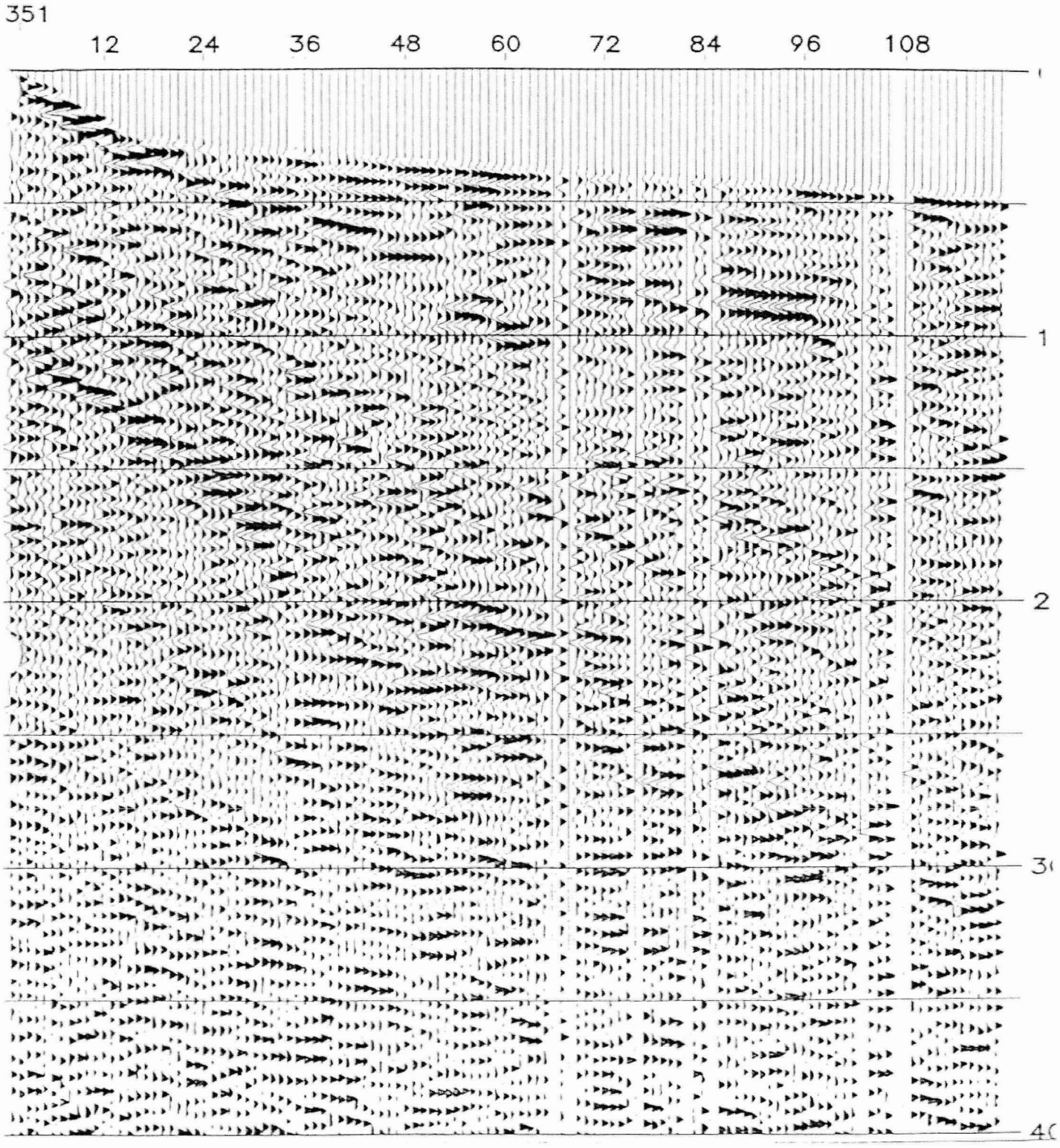

Figure I-14 Shotpoint 1115. Line 2. First arrival muting and f-k filtering added to previous processing.

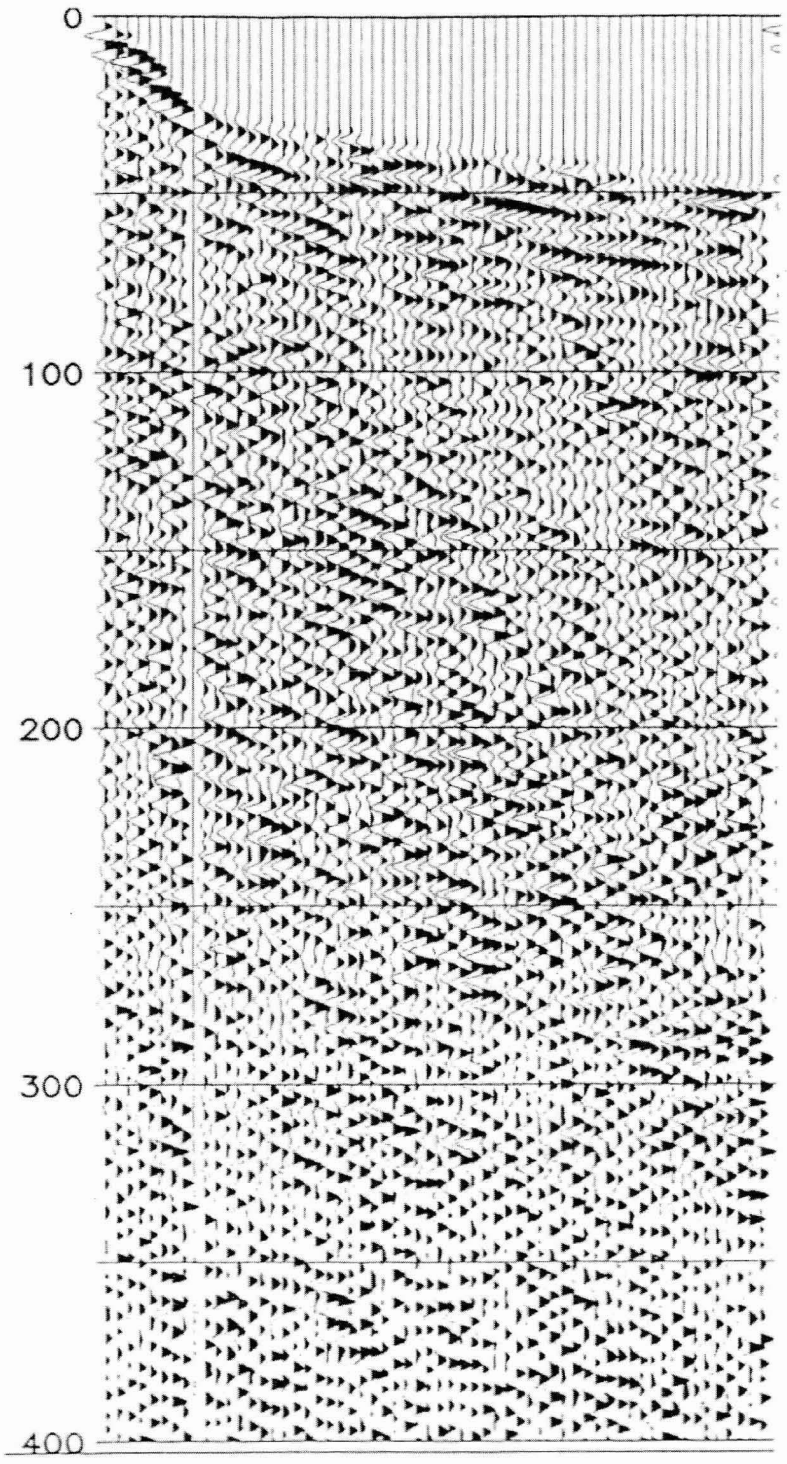

Figure I-15 CDP gather 2135, shotpoint 1067.5. Line 2. Gather and normal moveout added to previous processing.

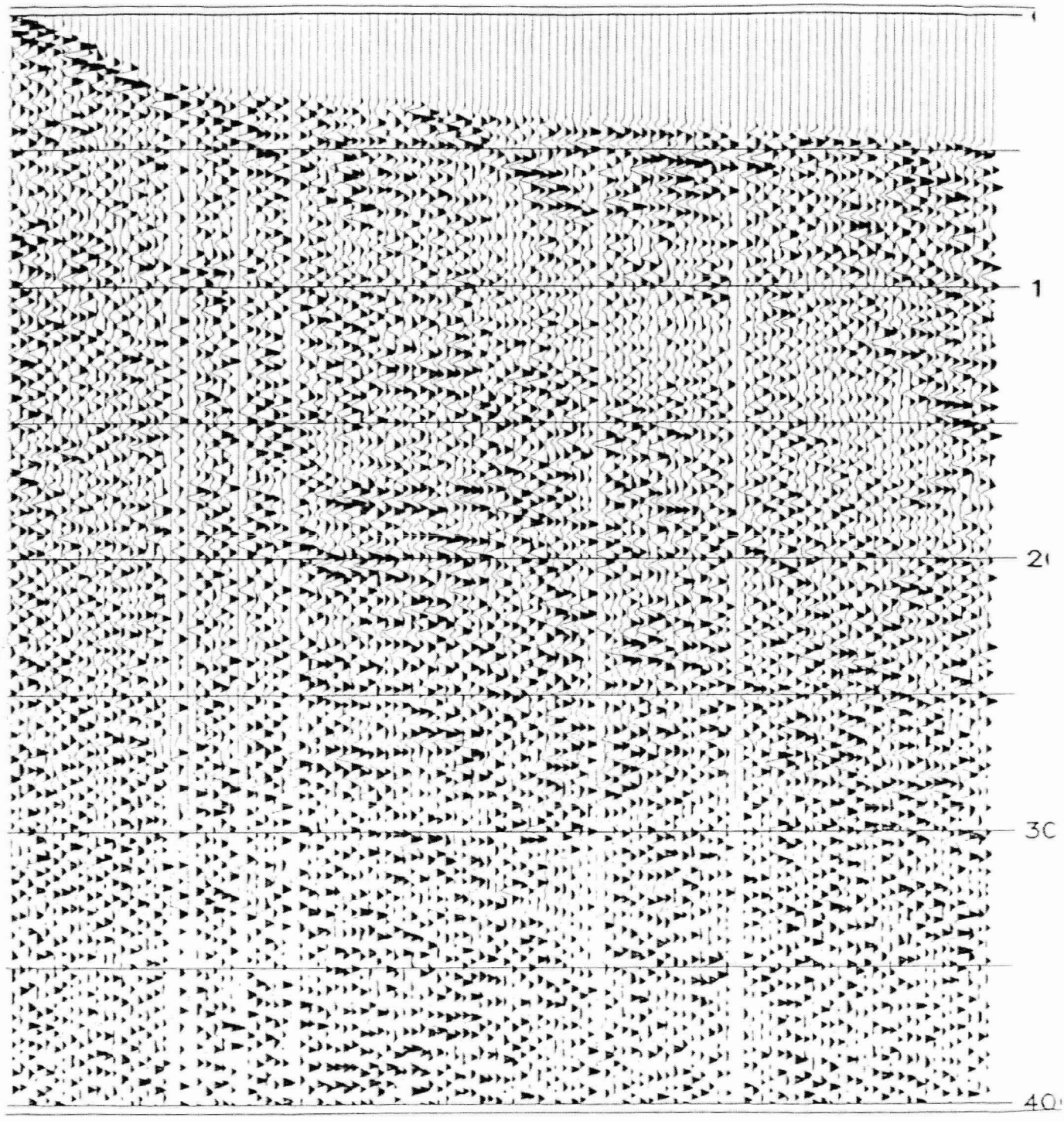

Figure I-16 CDP gather 2370, shotpoint 1185. Line 2. Gather and normal moveout added to previous processing.